The Effect of DHT Treatment on Changes in Amino Acid Transport Occurring in Aged Muscle

Submitted with corrections: 15, May 2018

Oskar Wendowski

PhD Thesis

UEA School of Medicine (MED)

Abstract

The hypothesis that age related muscle dysfunction is a result of diminished anabolic stimuli resulting in impaired amino acid uptake was tested as follows. Small muscle fibre bundles isolated from the extensor digitorum longus and the soleus of young, mature and elderly mice were used to investigated the effects of age and dihydrotestosterone (DHT) treatment on the expression and function of SNAT2 and LAT2. C2C12 muscle cells were cultured and tested for both SNAT2 and LAT2 function with DHT and various inhibitors.

At all ages investigated, amino acid uptake was significantly higher in slow-twitch fibres than in the fast-twitch fibres. Ageing led to a decrease in amino acid uptake and protein synthesis in both fibre types. The decline was greater in the fast-twitch than in the slow-twitch fibres and was accompanied by a reduction in the expression of both SNAT 2 and LAT2 proteins. Mirroring the uptake results the decrease in SNAT 2 protein was greater in the fast-twitch fibres than in the slow-twitch fibres. The rends seen in SNAT2 uptake and expression were also seen with fluorescence imaging of muscle sections. Ageing had no effect on mRNA levels of LAT2, but has shown a significant reduction in SNAT2.

Treating the muscle fibre bundles with physiological concentrations of DHT significantly increased amino acid uptake and SNAT2/LAT2 protein expression in the fast twitch fibres of all elderly group mice. There was a trend toward increased uptake and expression in response to DHT treatment in all groups. Chloroquine and flutamide treatment abolished the increased amino acid uptake induced by DHT treatment. Blocking SNAT2 in C2C12 cells with MeAIB resulted in decreased LAT2 response in starvation conditions, suggesting the role of these as transceptors. It is proposed that reduced anabolic stimuli in ageing leads to impairment of SNAT2/LAT2 recruitment leading to sarcopenia.

List of Publications

Journal Publications

Wendowski, O., Zoe Radshaw, Gabriel Mutungi. (2016). "Dihydrotestosterone treatment rescues the decline in protein synthesis as a result of sarcopenia in isolated mouse skeletal muscle fibres." J Cachexia Sarcopenia Muscle.

('15-'16 impact factor: 7.883)

Poster Presentations

"Dihydrotestosterone (DHT) rescues the age-dependent decline in protein synthesis in mouse fast-twitch skeletal muscle fibres." Wendowski Oskar, Mutungi Gabriel September 11-13th 2014. European Muscle Conference 2014 Salzburg Australia.

"Effect of Dihydrotestosterone Treatment on Young and Elderly Mice Skeletal Muscle" O. Wendowski. April 4-5th 2016. Experimental Biology 2016 Sand Diego, California. B572 767.1

"Dihydrotestosterone treatment rescues the decline in protein synthesis as a result of sarcopenia in isolated mouse skeletal muscle fibres." March 5th 2015. Faculty of Health and Medicine Postgraduate Conference. University of East Anglia.

Oral Presentations

"Sarcopenia is caused by a failure in protein synthesis and can be reversed by dihydrotestosterone" February 26th 2015 University of East Anglia. Queens Building 1.03.

List of Abbreviations

5aR – 5 alpha- reducatase

AA- amino Acid

AKT- protein Kinase B

CQ- chloroquine

DHT- dihydrotestosterone

EDL- extensor digitorum longus muscle

ERK- extracellular Signal-regulated Kinase

EWGSOP- European Worker Group On Sarcopenia

FLU- flutamide

GH- growth Hormone

HBSS- hanks' Balanced Salt Solution

IGF- insulin like Growth Hormone

IP- immunoprecipitation

JNK- C-JUN, N-terminal kinase

LAT- large-Neutral Amino Acid Transporter

mTOR- mechanistic target of rapamycin

MeAIB- methylaminoisobutyric acid

PI3K- phosphatidylinositol-4,5-bisphosphate 3-kinase

PKA- protein Kinase A

PKB- protein Kinase B

qPCR- quantitative polymerase chain reaction

SDS- sodium Lueryl Sulphate

SNAT- sodium-coupled Neutral Amino Acid Transporter

SOL- soleus muscle

T- testosterone

TA- tibialis anterior muscle

WB- western blot

Chapter 1: Introduction

1.1 Skeletal Muscle Physiology

Skeletal muscle forms the bulk of body weight (around 40-50% of body mass in young adult males). It is also the main store of proteins in the body (Rooyackers and Nair, 1997). In addition to its main physiological functions of postural support and control of movement, skeletal muscle is also vital to the maintenance of body shape, structure and composition.

General muscle structure is shown on figure 1.1. Skeletal muscle is composed of muscle fibres, further divided into sarcomeres, which are the smallest contractile units in skeletal muscle. These combine to form bundles called fascicles. The fascicles form the whole of the muscle, which is surrounded by a sheath called the epimysium on the outside of the muscle and the perimysium, which surrounds the fascicles on the inside. The muscle membrane underneath the epimysium is called the sarcolemma, which is composed of the plasma membrane of the muscle cell and a layer of polysaccharide. The muscle fibres fuses at the sarcolemma with the basement membrane with the help of transmembrane receptors on the sarcolemma. At lengthwise ends of the fibres, the distal ends of the sarcolemma fuse into tendons, which further attach to bones. Each muscle cell is composed of a tubular network of myofibrils. The myofibrils are further made up of repeating units called sarcomeres, each of which is composed of myofilaments. These myofilaments can be further categorised into thin and thick filaments, which interact and move over one another during contraction as described below (Boulpaep, 2012).

Muscle tissue is specialised to perform the main function of generating force. Huxley et al. first described the sliding filament theory of muscle contraction in 1954 which has proven to be accurate (Huxley and Niedergerke, 1954). Contraction is initiated by the motor neuron and signalled by the neurotransmitter Acetylcholine, which is released at the neuromuscular junction and depolarises skeletal muscle cells. This in turn causes release of calcium ions from the skeletal cells sarcoplasmic reticulum. Calcium ions

bind to the protein troponin, resulting in a conformational change and the movement of tropomyosin. This exposes a myosin binding site on actin filaments.

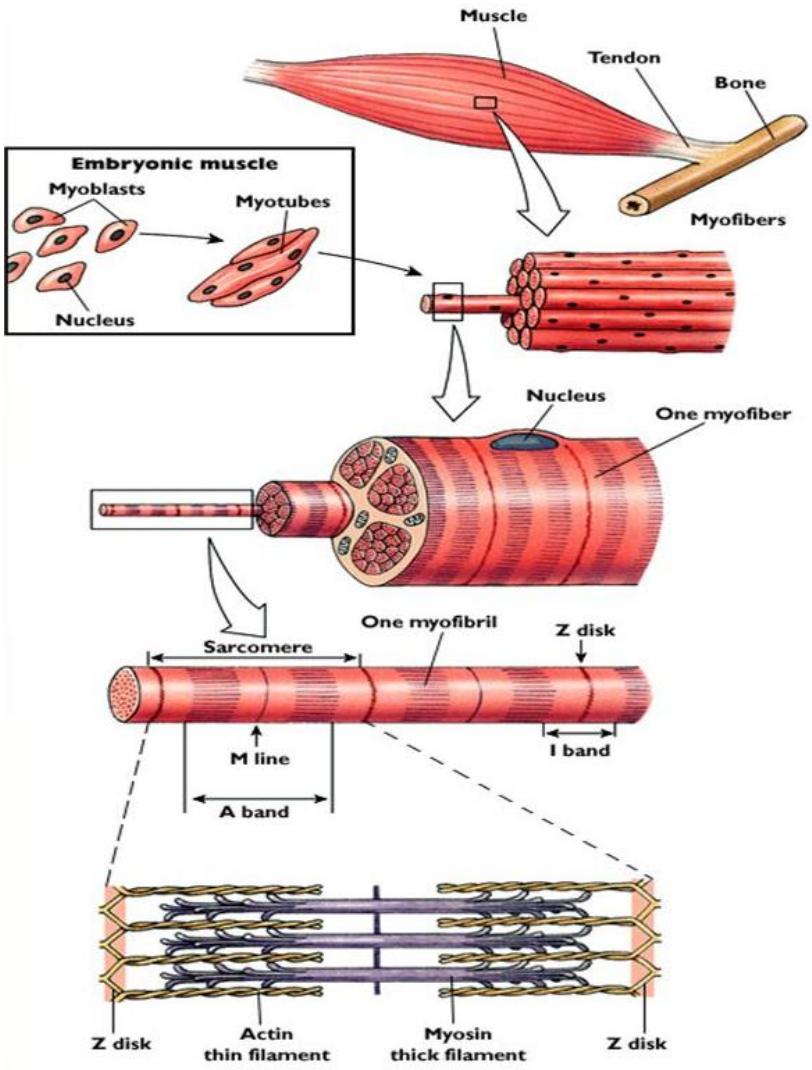

Figure 1.1 Illustration showing the structure of skeletal muscle. Notice that all muscle units are arranged in parallel, allowing for the generation of force through shortening of the sarcomeres. Myoblasts are progenitor cells which differentiate into functional myotubes (Randall et al., 1997).

Myosin binds to the active site and changes confirmation, which slides the filament forward. This is known as the power stroke of contraction, which is repeated over and over during a contraction event. The thin filaments in skeletal muscle slide over the thick filaments, thus generating tension in line with each sarcomere. The force generated pulls on the tendon, and if the force opposing the contraction is less than that being generated, movement results.

Muscle fibre phenotype has more recently been considered as being closer to a continuum rather than rigidly characterised into two or three groups (Pette and Staron, 2000). However, the classical terminology is still a useful heuristic to group fibre types into three general categories based on their physical characteristics and isoforms of myosin expressed. This allows for easier classification of muscle groups.

IIn humans, there have been four different muscle fibre types identified. In mice skeletal muscle theseare type 2B, 2D, 2A which contain the “fast” isoforms of myosin: MHC-2b, MHC-2d and MHC-2a respectively. Slow fibres contain MHC-1 and are donated as type 1 under this classification. In humans the 2D isoform is not present. This classification stems from the different isoforms speed of force production caused by the different isoform power stroke kinetics (Neunhauserer et al., 2011). This order can be expressed in decreasing kinetic action as: MHC-IIb>MHC-IId> MHC-IIa>>MHC-I. It is also important to note that hybrid fibres are abundant in mammals, which can express varying MHC isoforms, as well as post translational modifications that can alter kinetic function (Stephenson, 2001).

Because of the complexity of fibre typing, it is simpler to look at the two extremes in muscle fibre types or a more classic view of fast vs slow. Type 1 oxidative are known as the classic “slow” fibres, and as their name suggest the metabolism in these fibres is centred around oxidative phosphorylation. This is the most efficient form of metabolism, yielding between 30 and 36 ATP per molecule of glucose (Korzeniewski, 1998). An example of this is seen in aerobic exercise, as oxygen is necessary as an electron acceptor that drives the cycle. Type 2B are the classic fast twitch fibres, characterised by high force production and reliance on glycolysis, which generates 2

ATP from one glucose. Type 2A oxidative fibres fall in between the two classical extremes.

As illustrated on the table below the two extremes of classical slow and fast muscle fibre types:

Table 1: Muscle Fibre Types

	SLOW OXIDATIVE	FAST GLYCOLYTIC
TWITCH SPEED	SLOW	FAST
RESISTANCE TO FATIGUE	HIGH	LOW
BLOOD SUPPLY	HIGH	LOW
ATPase ACTIVITY	LOW	HIGH
GLYCOGEN	LOW	HIGH
TWITCH FORCE	LOW	HIGH
COLOUR	RED	LIGHT PINK

While skeletal muscle is vital to normal functioning and movement, there are numerous conditions that involve the atrophy of muscle. Skeletal muscle mass is maintained by a fine balance between protein synthesis and breakdown (Balagopal et al., 1997). Therefore, a decrease in skeletal muscle mass, such as that seen during ageing, must reflect an imbalance between these two processes, resulting in net nitrogen loss. Although several studies have previously reported a 30-40% reduction in mixed protein synthesis with age (Volpi et al., 2001, Toth et al., 2005), the direct anabolic effects of certain amino acids and endocrine factors are still intact in the elderly (Volpi et al., 1999). These findings have suggested that conditions of muscle wasting may be caused by failure in the transport of amino acids into and out of skeletal muscle fibre themselves.

1.2 Satellite Cells

Another closely associated cell type called myosatellite cells lie between the sarcolemma and basement membrane of muscle fibres. Satellite cells are multipotent cells found on the mature skeletal muscle. Normally they are present in a quiescent state. Upon activation, they are able to proliferate as skeletal myoblasts, which have the ability to differentiate into functional skeletal muscle cells or back into satellite cells which acts to replenish the satellite cell pool of a fibre (Kadi et al., 2005, Birbrair and Delbono, 2015). Satellite cells are able to act as a source of nuclei to muscle fibres, which otherwise have no other mechanism to repair damaged nuclei. These cells have the capability to either form brand new myotubes or fuse with existing fibres (Kadi et al., 2004).

Satellite cells are crucial for the repair and regeneration of damaged muscle. It has been found that elderly patients have a reduced pool of satellite cells which is a proposed factor in the onset and severity of age related muscular dysfunction (Joanisse et al., 2017). Their exact role in ageing has been a popular field of recent research.

Satellite cells play a vital role in the regeneration and maintenance of healthy skeletal muscle fibres. Satellite cells respond to trauma and damage in skeletal muscle. (Seale et al., 2003) Because of their ability to replicate as well as differentiate into functional muscle fibres, the satellite cell pool as a whole does not become depleted. Fig 1.2 Illustrates the typical response of skeletal muscle to injury and specifically the role of satellite cells in the regenerative process.

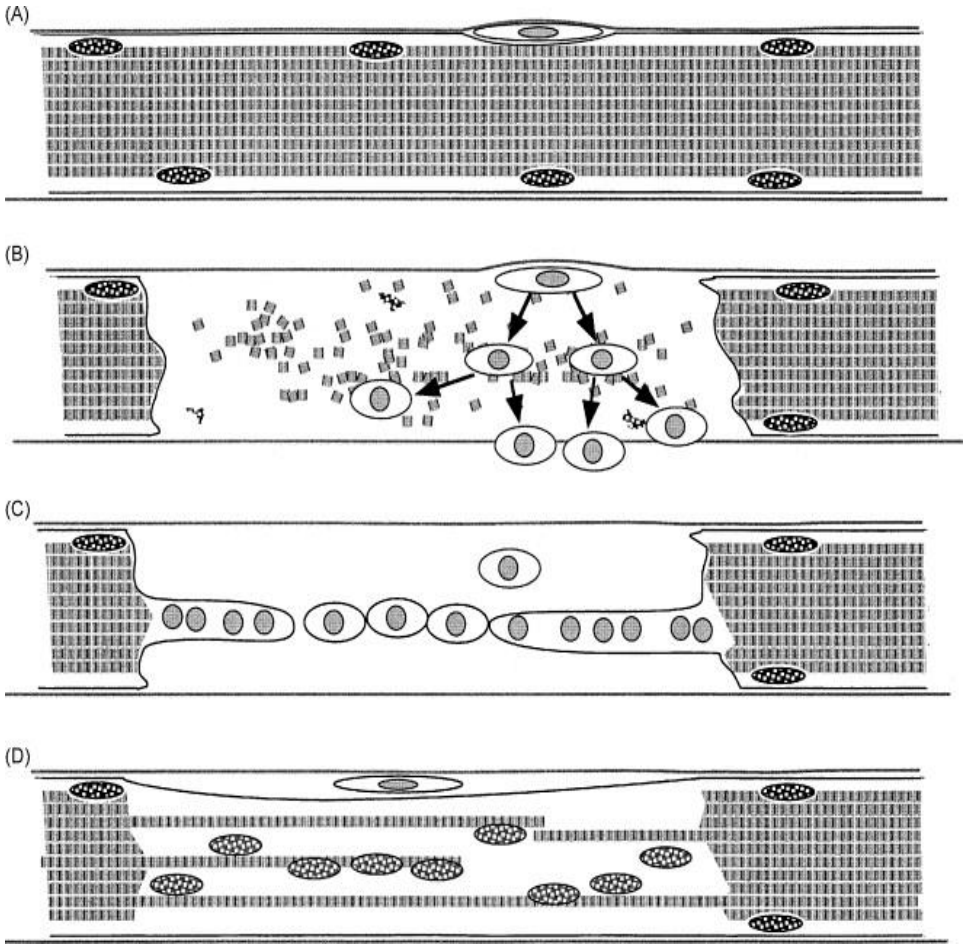

Figure 1.2 Diagram of muscle satellite cell mediated response to injury. (A) shows a single satellite cell in a muscle fibre with numerous nuclei. (B) In response to injury the satellite cells proliferate. (C) Most these proliferated cells differentiate into active myofibers. (D) A proportion of these cells become quiescent and return to their original location between the sarcolemma and basement membrane of the muscle fibres. Image from: (Morgan and Partridge, 2003).

However, it is not clear whether the satellite cell response changes with ageing. A higher rate of apoptosis in satellite cells has been discovered in elderly populations, most likely a result of impaired vascularisation (Wang et al., 2014). However, it is possible that this reduction is acting to retain proportionality of satellite cells to functional fibres, which also reduce in size with age. No proportional change has been found in the rat soleus in terms of satellite cell to fibre ratio (Brooks et al., 2009). It is proposed that it may be the function and response to stimuli that is impaired in satellite cells rather than their number (Hikida, 2011). Reduction in MAPK signalling, leading to impaired skeletal muscle cell self-renewal has been shown in ageing, possibly playing a smaller part in sarcopenic muscle dysfunction (Bernet et al., 2014).

1.3 Amino Acid Transporters

Amino acids enter and leave cells through highly specialised proteins known as amino acid transporters that are located on the cell membrane. The intracellular concentration of most amino acids in animal cells is normally higher than the extracellular amino acid concentration, meaning amino acids undergo active transport across plasma membranes against a gradient (Hyde et al., 2003). The sodium/potassium ATPase plays a vital role in many of the amino acid transporters. It is the most frequently expressed transporter, moving three molecules of sodium out of the cell in exchange for moving 2 molecules of potassium into the cell per one ATP. Many amino acid transporters, such as the system A transporters of the Slc38 family use the sodium gradient created to transfer amino acids into the cell via secondary active transport (Lingrel et al., 1994).

These amino acid transporters play an important role in protein turnover by providing the building blocks necessary for protein synthesis (Volpi et al., 1999). A larger number of different amino acid transporters are present in all mammalian cells (Wagner et al., 2001). The focus of this thesis is particularly on two, the sodium-coupled neutral amino acid transporter, SNAT2 (Mackenzie and Erickson, 2004) and the sodium-independent L-type amino acid transporter LAT2. These two have been consistently found in significant quantities in skeletal muscle (Palacin et al., 1998).

1.3.1 SNAT2

SNAT2 (Small Neutral Amino Acid Transporter) is a system A amino acid transporter first discovered in 1965 (Christensen et al., 1965) that belongs to the SLC38 gene family mentioned before. It mediates the sodium-coupled transport of small neutral amino acids such as glycineand alanine into muscle fibres. It transports one molecule of Na^+ and one substrate amino acid into the cell. The substrate amino acid is preferentially a small neutral amino acid such as glycine. Larger neutral amino acids on the other hand are very poor substrates (Lopez et al., 2006). SNAT2 is widely expressed throughout the body, found in the brain, adipose tissue, liver, intestine, lung, kidney, and importantly, skeletal muscle (Mackenzie and Erickson, 2004). In fact, out of the Slc38 gene family of transporters, it is the only one consistently found at measurable expression levels in skeletal muscle (Hyde et al., 2001). SNAT2 like the other members of its family of transporters shares the ability to transport a non metabolisable substrate known as methyl-aminoisobutyrate (MeAIB), a unique ability which also allows for the quantification of transport through these transporters.

Structurally, SNAT2 is composed of 506 amino acids with a molecular weight of 56kDa. It spans the membrane with 11 transmembrane helices and contains a single disulphide bridge (Chen et al., 2016). See figure 1.3.1 for a diagram of SNAT2 structure. It has been discovered through hydropathy analysis that the transporter contains an intracellular N-terminus and also containing an extracellular C-terminus. This C-terminus does not play a role in amino acid substrate binding, but it does play a role in pH sensing and the transport of Na+ into the cell (Zhang et al., 2011). SNAT2 shares a characteristic disulphide bride on its third extracellular loop with other members of the SNAT family of transporters. The exact function of this bond is unknown, but it is likely involved in translocation of the protein to the plasma membrane (Chen et al., 2016).

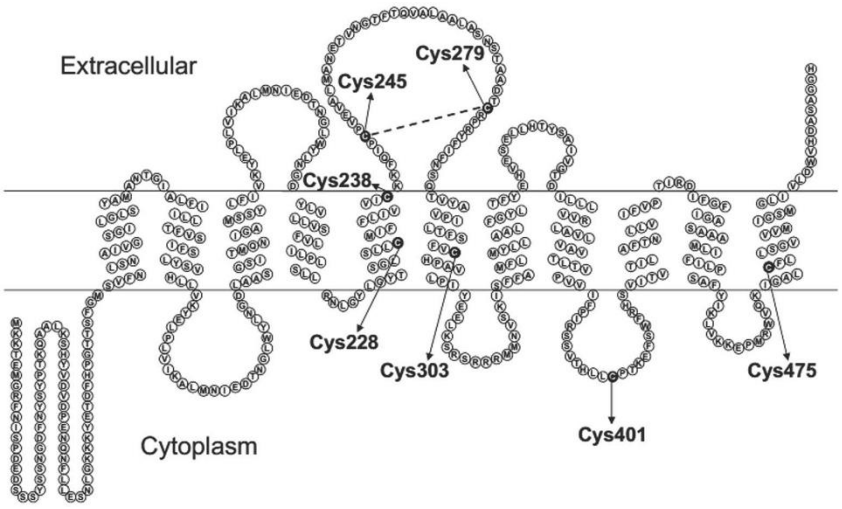

Figure 1.3.1 A model of SNAT2 showing general structure of the transporter. There are 11 transmembrane helixes and a characteristic disulphide bond between Cys245 and Cys279. image from (Chen et al., 2016).

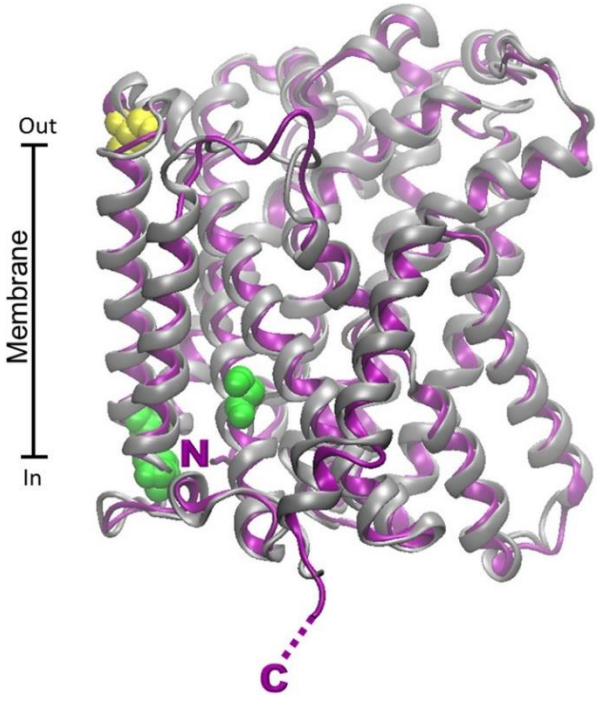

Figure 1.3.2 Homology structural model comparing rat LAT2 with human (purple) LAT2 92% homogenous. Green sites represent possible PKA and PKC phosphorylation sites derived from Scan-Prosite software. Image from (Pochini et al., 2014).

Another characteristic feature of SNAT2, like all system A transporters is the phenomena of *transinhibition*. In other words, the accumulation of a system A substrate inside the cell acting to inhibit the transporter itself (Bracy et al., 1986). This is due to the accumulation of substrate inside the cytoplasm of the cell and can be achieved with only one amino acid. The dual role of some transporters to modulate their own expression, is likely achieved through initiation of signalling cascades such as MAPK (Pinilla et al., 2011). This ability of transporters to act as *transceptors* and governing their own expression in response to changing nutrient availability has been documented in many cell types (Kriel et al., 2011).

A well-documented phenomenon of SNAT2 is its adaptive regulation in response to amino acid deprivation (Hyde et al., 2001). Evidence suggests that the acute phase of this response, which happens during minutes rather than hours, is due to recruitment of SNAT2 from an internal pool localised in intracellular compartments (Hyde et al., 2002). The exact mechanism involved in mediating the adaptive response of SNAT2 is not known. However, the PI3K and JNK pathways seem to be likely targets, as the inhibition of both respectively blunts the adaptive response (Hyde et al., 2007). ERK phosphorylation was also increased in amino acid deprivation. However, it is unclear if this pathway plays a role as its inhibition did not decrease the adaptive response.

The addition of the amino acids L-Gln, L-Ala, L-Tyr as well as MeAIB also blunts the adaptive response (Hyde et al., 2007). The effectiveness of MeAIB in this case is notable, because as it is not metabolisable once within the cell, it suggests that the presence or movement of a substrate at SNAT2 is sufficient to blunt the adaptive response. This suggests that SNAT2 may in fact be a “transceptor”, playing a vital role in controlling amino acid uptake in response to changing extracellular amino acid levels.

SNAT2 has shown to be sensitive to changes in pH. The activity of SNAT2 is reduced as the pH drops below physiological 7.4 (Munoz et al., 1992, Chaudhry et al., 2002, Baird et al., 2006). This sensitivity has shown to be mediated through the protonation of a histidine residue (Baird et al., 2006). This property can be used to validate uptake

studies and means that maintenance of a physiological pH is critical for accurate assays, which needs to be incorporated into the experimental design.

There are three main triggers for the modulation of SNAT2 activity. These are osmotic shock, amino acid deprivation and hormonal stimulation such as insulin (Kashiwagi et al., 2009). ERK and JNK pathways are proposed to be active in upregulating *de novo* synthesis of SNAT2 via transcription along with the classical genomic pathway of AR binding. Both pathways appear to be in play during amino acid starvation, while only ERK is active in DHT induced acute upregulation of SNAT2 activity (Kashiwagi et al., 2009, Hamdi and Mutungi, 2010).

It has been shown that SNAT2 activity is directly controlled by hormones. Insulin has been shown to increase SNAT2 activity without increasing synthesis of new SNAT2. The proposed mechanism of this involves the exocytosis and endocytosis of SNAT2 from intracellular compartments (Hyde et al., 2002). In this way, SNAT2 activity is thought to be able to adapt quickly to meet the amino acid demands of the cell.

Amino acid deprivation and osmotic shock have also been shown to upregulate SNAT2 function, working through different pathways. It has been shown that AA starvation induced upregulation is blunted by PI3K and JNK inhibitors, while osmotic shock induced upregulation is blunted by mTOR inhibitors but not vice versa (Kashiwagi et al., 2009). Catechol amines have been shown to also upregulate System A activity in human liver parenchymal cells and rat hepatocyte, however this action seems to be mediated by transcription as it is completely inhibited by actinomycin D and cycloheximide (McGivan and Pastor-Anglada, 1994). The past work by Hamdi and Mutungi show that DHT also has a profound effect on regulating SNAT2 activity (Hamdi and Mutungi, 2010). However, anabolic steroids such as testosterone and its active metabolite, Dihydrotestosterone have not been extensively studied in regard to their effects on SNAT2 in aged animals (Hamdi and Mutungi, 2011). We theorise that a baseline anabolic signal is necessary for the proper functioning of these amino acid transporters.

Regardless of whether the stimulation is hormonal, amino acid deprivation or osmotic shock, the efficacy of SNAT2 does not change in response to any form of stimulation.

This is proven by an observed increased V_{max} (maximal transport) rather than K_m (Franchi-Gazzola et al., 2006, Gaccioli et al., 2006, Kashiwagi et al., 2009). This means that the upregulation in SNAT2 transport can be solely accounted for by the quantity of functioning SNAT2 transporter on the plasma membrane. This makes quantification of SNAT2 function relatively easy, the transport of a given substrate being proportional to the expression of SNAT2 protein.

1.3.2 LAT2

LAT2 is a system L amino acid transporter of the Slc7 gene family. It is a relatively recently identified membrane transporter (Pineda et al., 1999). It cannot use a sodium gradient to drive transport but rather exchanges small neutral amino acids for the larger branched-chain amino acids such as leucine and histidine which are essential for protein synthesis in skeletal muscle (Hamdi and Mutungi, 2011). This is called tertiary active transport and it relies on the presence of sodium coupled amino acid transporters such as SNAT2. LAT2 has overlapping specificity in transporting smaller amino acids, thus being able to utilise the gradient created by SNAT2 to transport in the larger amino acids (Verrey, 2003).

Structurally LAT2 is composed of a light chain which makes a functional heterodimer with aheavy chain, together acting as a transmembrane glycoprotein (Ikotun et al., 2013). As illustrated in 1.3.2 Pochini et al. (2014) have used Scan-Prosite protein modelling software to map homogeneity of rodent LAT2 showing 92% overlap with the human LAT2. This analysis has also identified two potential phosphorylation domains of PKC and PKB, possibly hinting at a transceptor function of LAT2. More research needs to be done to elucidate the function and validity of these sites.

Because LAT2 is responsible for the transport of large branched chain amino acids, it plays a vital role in regulating protein synthesis and plays a role in disease. LAT2 has been found to be upregulated in cancer cells and high expression levels of LAT2 are correlated with poor outcomes (Fuchs and Bode, 2005). This has led some to believe that LAT2 is a suitable target for cancer therapy or diagnosis (Sakata et al., 2009). LAT2 has been proposed as a biomarker of advanced malignancy of prostate and brain tumours (Nawashiro et al., 2006, Sakata et al., 2009).

1.3.3 Relationship Between SNAT2 and LAT2

There is strong evidence that the System A and System L transporters are coupled, relying on each other to maintain the intracellular amino acid pool (Meier et al., 2002, Ramadan et al., 2007). SNAT2 transports small neutral amino acids into the cell alongside sodium in 1:1 ratio. This drives the internal small AA pool that enables LAT2 to transport large neutral amino acids into the cell in exchange for transporting one small neutral AA out of the cell in a 1:1 ratio (Hyde et al., 2007). This possible relationship is illustrated in figure 1.3.3. To date, little is known about the effects of age on the number and function of these amino acid transporters in mammalian skeletal muscle fibres. It is also yet uncertain whether the coupling between SNAT2 and LAT2 is affected by ageing. When considering the interplay between SNAT2 and LAT2 transporters, it is important to note the difference in substrate specificity. Below is a table illustrating the amino acid substrates of the SLC family of transporters.

Table 2: Specificity of SNAT and LAT family of transporters

SYSTEM	**PROTEIN**	**GENE**	**AA SUBSTRATES**
A	SNAT1	SLC38A1	Me-AIB, Gly, Ala, Ser, Cys, Gln, Asn, His, Met, Thr, Pro, Tyr, Val
A	SNAT2	SLC38A2	Me-AIB, Gly, Pro, Ala, Ser, Cys, Gln, Asn, His, Met
A	SNAT3	SLC38A3	His, Lys, Me-AIB, Ala, Cys
A	SNAT4	SCL38A4	Gly, Pro, Ala, Ser, Cys, Asn, Met, His, Lys, Arg
L	LAT1	SLC7A5	Leu, Iso, Val, His, Met, Leu, Ile, Val, Phe, Tyr, Trp, Gln
L	LAT2	SLC7A8	Leu, Iso, Val,

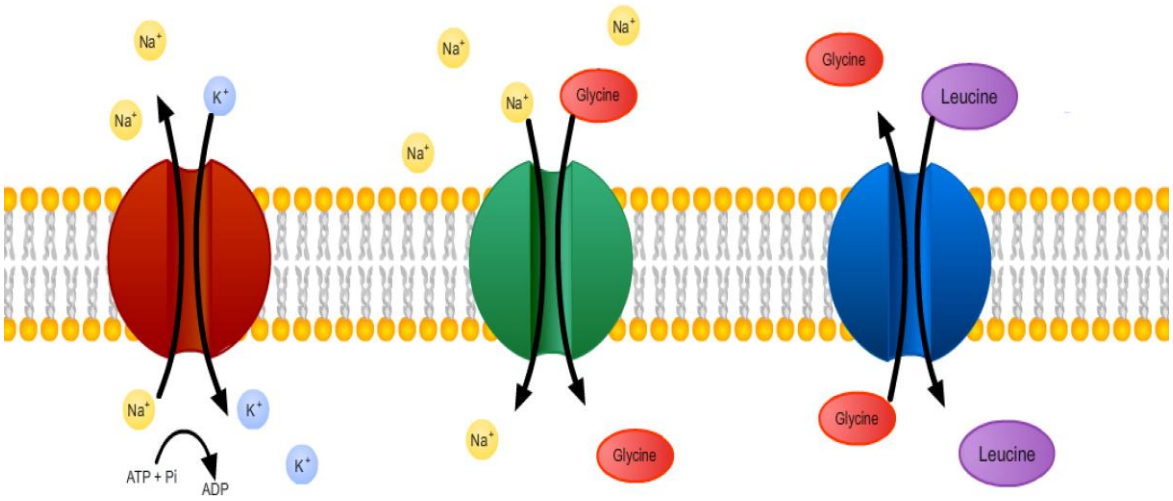

Figure 1.3.3 Diagram of SNAT2 (green) and LAT2 (blue) transporters. SNAT2 is driven on a sodium gradient, established by the Na^+/K^+ ATPase (red). SNAT2 transports 1 molecule of Na^+ per 1 small amino acid such as glycine into the cell. LAT2 in turn utilises the gradient of small amino acids to exchange one of these for a larger amino acid such as leucine. In this way SNAT2 maintains the function of LAT2, which in turn supplies the cell with larger, bulky side chain containing amino acids ensuring the cell has the complete array necessary for protein synthesis. Image produced using Adobe Flash.

1.4 Vesicular Trafficking

One of the earliest and most studied examples of vesicular involvement in membrane transporter recruitment is that of GLUT4 trafficking. GLUT4 or glucose transporter 4, is a membrane bound transporter of glucose. It belongs to the SLC family of solute carrier proteins, of which SNAT2 is a member. GLUT4 is known to be upregulated by insulin, which triggers a recruitment of already formed GLUT4 from an intracellular vesicular pool (Leto and Saltiel, 2012). Insulin binding at the membrane insulin receptor sets of a cascade involving PI3K, Akt/Pkb, and Rab10 (Sano et al., 2007).

The exact system of GLUT4 vesicular storage is unclear as of yet. However, it appears that the bulk of unrecruited GLUT4 resides in GLUT4 specific vesicles. These can either fuse with the plasma membrane directly or fuse with endosomes, which then in turn fuse with the plasma membrane (Chen and Lippincott-Schwartz, 2013). The vesicular sorting protein, Sortilin plays a role in trafficking of GLUT4 into stationary pools for later use (Hatakeyama and Kanzaki, 2011). This response is rapid and profound, resulting in up to a 30-fold increase in functional transporter on the plasma membrane (Muretta et al., 2008).

The effects of GLUT4 recruitment can be seen in under 30 minutes, underlying the rapid timeline of the recruitment process in the case of this transporter. The signalling between different GLUT4 pools is also tightly controlled. RABs are small GTPases involved in membrane trafficking. It has been shown that RAB14 ferries GLUT4 into special storage vesicles, while RAB10 in conjunction with its activating protein AS160 is responsible for the accumulation of these storage vesicles at the plasma membrane (Sadacca et al., 2013). These storage vesicles accumulate at the highest concentrations on T-tubules in skeletal muscle. Interestingly, in vivo studies of insulin mediated GLUT4 recruitment showed that there is very little actual movement of vesicles throughout the cell. Rather, the nuclei serve as a main storage site for GLUT4 while secondary smaller vesicles deplete stored transporter in response to hormonal stimuli (Lauritzen et al., 2008).

Comparatively little work has been done in elucidating the mechanism of recruitment of SNAT2 or LAT2 but we can speculate that a similar level of complexity and feedback is involved in their recruitment and trafficking. Hyde et al. (2007) has shown evidence for a vesicular pool model of LAT, but this has been in response to insulin rather than anabolic signalling. Figure 1.4 illustrates the function and localisation of GLUT4 transporters. More work is needed to elucidate the underlying mechanisms of these two amino acid transporters, which are vital to the function of skeletal muscle.

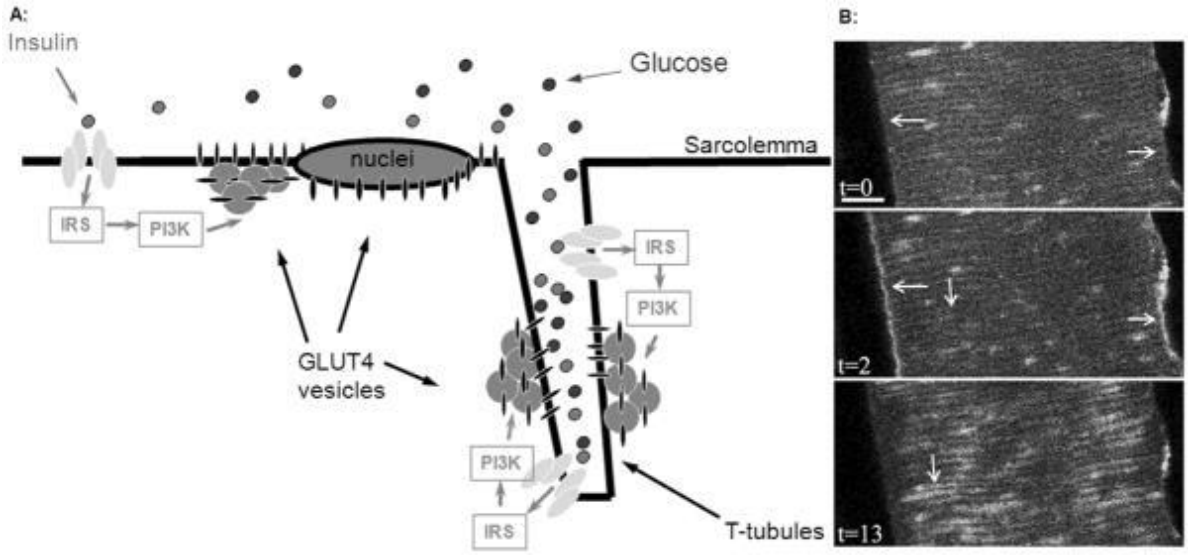

Figure 1.4 Diagram of GLUT4 trafficking system. GLUT4 vesicles are located predominantly around the nuclei and t-tubules. These release transporters locally to fuse into the plasma membrane. Signalling in GLUT4 recruitment is mediated by PI3K and predominantly stimulated by insulin binding with the insulin receptor (IRS). Adapted from: (Lauritzen et al., 2008).

1.5 Anabolic Steroids

Sex steroids are vital regulators of body shape, structure and composition in mammals (Bhasin and Buckwalter, 2001). For example, treating adult female rats (Exner et al., 1973), hypogonadal men (Bhasin et al., 1997) and elderly men with low testosterone concentrations (Ferrando et al., 2002) with testosterone or any of its numerous synthetic derivatives has been shown to increase lean body mass. This suggests that sex steroids are essential for the normal maintenance of skeletal mass and may be instrumental in the treatment of sarcopenic muscle dysfunction.

Anabolic steroids as therapeutic interventions have been used and are still employed for numerous clinical purposes. The most prevalent is the treatment of hypogonadism, or physiologically low levels of androgens, as hormonal replacement therapy in males. Testosterone has also been shown as a beneficial treatment as an add on to female hormone replacement therapy, showing a protective effect against breast cancer (Glaser and Dimitrakakis, 2015). They were and still are used for the treatment of anaemias, most commonly aplastic anaemia (Basaria and Dobs, 2001). Patients with wasting conditions, such as HIV often respond well to these drugs which preserve lean body mass and increase appetite(Grunfeld et al., 2006).

Testosterone, is often regarded as the principal male hormone. Produced mainly (95%) by the Leydig cells of the male testes, it then undergoes many metabolic changes. (Brooks, 1975) Figure 1.5.1 shows the metabolic pathways testosterone undergoes to produce the active DHT metabolite. The concentration of free testosterone in plasma decreases with age in both men and women (Mooradian and Korenman, 2006). Testosterone supplementation has been shown to increase lean body mass, as well as also increasing the number of nuclei per muscle fibre (Eriksson et al., 2005). Long term administration with anabolic steroids causes morphological changes in human skeletal muscle even after stopping treatment, the most long lasting being increased nuclei density (Yu et al., 2014).

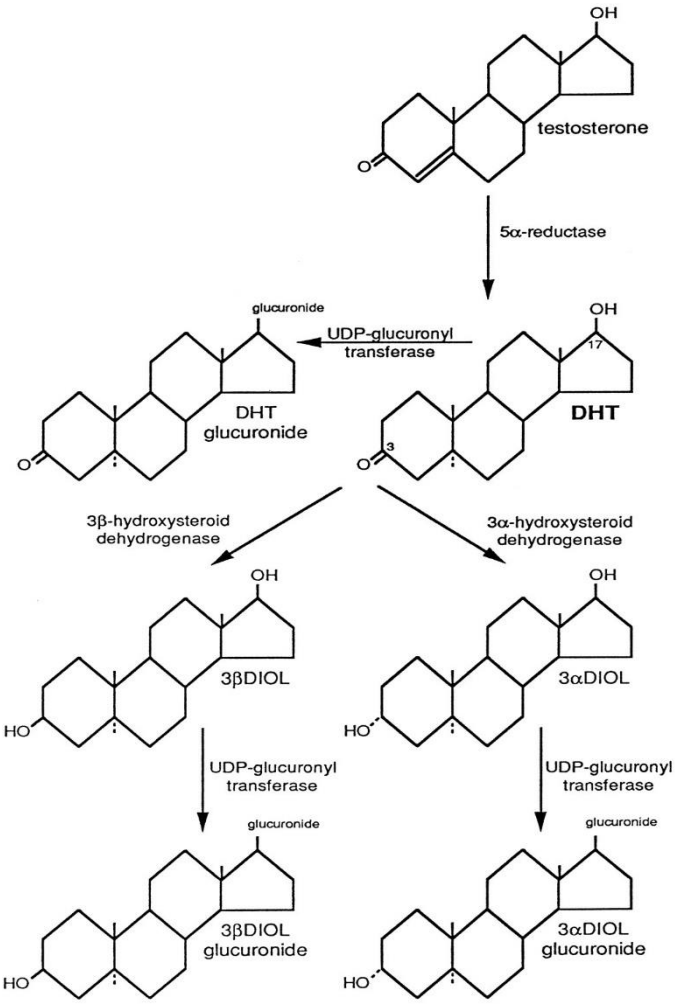

Figure 1.5.1 DHT metabolism in the liver. 5α-reductase converts Testosterone into the much more potent DHT. 3α-hydroxysteroid dehydrogenase converts DHT into the much less active 3α-diol derivative. Both enzymes are expressed in peripheral tissue, indirectly controlling the extent of anabolic activity. UDP-glucoronyl transferase is predominantly found in the liver. Adapted from (Pirog and Collins, 1999).

Testosterone however, is not the most potent sex steroid in the body (Gruenewald and Matsumoto, 2003). Instead, in certain target tissues such as the skin, prostate and brain, it is irreversibly metabolised to dihydrotestosterone (DHT) by the enzyme 5alpha (α)-reductase (Bruchovsky and Wilson, 1968). This metabolite of testosterone, has proven itself to be a much more potent androgen. It has been shown that it takes roughly 10 times the amount of testosterone to elicit the same increase in transcription as seen with DHT administration (Grino et al., 1990). This is due to the binding kinetics of DHT to the androgen receptor (Saartok et al., 1984). Recent studies from our laboratory have shown that DHT but not testosterone increases maximal isometric force and amino acid transport in fast-twitch muscles (Hamdi and Mutungi, 2010, Hamdi and Mutungi, 2011, Wendowski et al., 2016). However, whether skeletal muscle expresses 5α-reductase necessary for the conversion into DHT has not been conclusively shown. It is also unclear whether DHT can reverse the effects of age on protein synthesis in skeletal muscle, as there is little work done using DHT treatment on elderly populations.

1.5.1 Steroid Mode of Action

Steroid hormones are classically thought to act by travelling through the plasma membrane to activate a cytoplasmic androgen receptor (AR). The AR is a protein of 110 kDa in size, consisting of 919 amino acids in 12 α-helices and 2 β-sheets (Rochette-Egly, 2003).

The AR is normally bound to other chaperone proteins which prevent enzymatic damage, one of which is heat shock protein 90 (Pratt and Kinch, 2003, Pratt and Toft, 2003). The binding of androgens to the AR causes a conformational change, which leads to detachment of chaperone proteins and exposes a nuclear localisation domain causing the AR-androgen complex to translocate into the nucleus (Gelmann, 2002). This complex then acts on transcription factors on specific DNA elements in target genes, resulting in either the activation or suppression of transcription. The DNA binding domain of this complex then interacts with hormone responsive elements on target genes, which can either lead to activation or repression of these genes (Losel and Wehling, 2003).

The genomic effect of anabolic steroids peaks several hours after administration (Cato et al., 1988). After this increase in transcription, it is necessary to translate the mRNA into proteins, which then must be processed before they are usable and cause an observable physiological effect in the cell. It was because of this, that steroids were ordinarily thought to work on a timeframe of days rather than hours. This from herein will be referred to as the genomic action of anabolic steroid hormones.

However, we now know that steroid actions are not limited to this pathway. In addition to the classical idea of androgen binding to nuclear receptors, androgens have been proven to elicit their effects on tissue through non-genomic pathways (Dubois et al., 2012). This will be herein referred to as the *non-genomic* action of steroid hormones. Both anabolic steroids and corticosteroids have shown to elicit measurable effects after an hour of administration. The most studied non genomic action of steroids is the acute rise in calcium concentration, which is seen in response to not only androgens (Gorczynska and Handelsman, 1995, Benten et al., 1999) but in fact all classes of steroids (Lieberherr et al., 1993, Audy et al., 1996, Benten et al., 1997). An experiment by Wunderlich et al (2002), showed that in murine macrophages lacking intracellular AR testosterone was able to ellicit an intracellular calcium concentration increase. This was also accomplished with a testosterone and BSA conjugate, which cannot cross the plasma membrane. This suggests that the androgen receptor at work is associated with the membrane and able to bind molecules outside the cell. In addition to binding to a membrane associated AR receptor other proposed non-genomic modes of action of androgens involve acting directly or indirectly on G-protein receptors or intracellular kinases (Foradori et al., 2008, Dent et al., 2012).

1.5.3 Signalling Kinases

There is evidence from the work in our lab on skeletal muscle that some of the non-genomic actions of androgens are mediated, at least in part by EGFR phosphorylation and further EGF signalling through the ERK1/2 pathway (Hamdi and Mutungi, 2010, Hamdi and Mutungi, 2011). More recently, DHT was found to potentiate the action of EGF in lung fibroblasts leading to significant increases in ERK signalling (Lee et al., 2014). It is unclear however, whether this effect involves the initial binding of an AR

element, as work with prostate cells has shown androgen receptor blockers to completely abolish this effect, while in the previous work by Hamdi et al. it has not shown total inhibition (Oliver et al., 2013). Interestingly, work by both groups has shown this effect to be specific to Dihydrotestosterone. Testosterone administration alone failed to induce these effects (Zhou et al., 2015b).

The SRC family of kinases has also been found to be involved in acute DHT signalling. Both SRC and epithelial growth factor receptor (EGFR) are phosphorylated in response to DHT (Lee et al., 2014).

Although the exact nature of non-genomic binding of androgens remains to be elucidated, the data from our lab strongly suggests the involvement of the EGFR. It is unknown whether androgens are capable of direct binding to the EGFR domain or a proximal androgen sensitive domain. DHT has been shown to greatly *potentiate* the effect of EGF, but does not elicit an action in the absence of EGF (Lee et al., 2014). This suggests that an AR domain is interacting with the EGFR to co-activate the MAPK/ERK signalling cascade. There is evidence of this interaction between AR and the EGFR, showing that androgen binding has direct effects on the magnitude of signalling in response to EGF (Bonaccorsi et al., 2004). It has recently been shown that baseline EGF levels are necessary not only for development, but also for the maintenance of healthy ageing muscle by controlling protein homeostasis (Rongo, 2011).

Mitogen activated protein kinases are the correct term for ERKs (extracellular signal-regulated kinases). The pathway is initiated with the phosphorylation of the EGFR receptor. The process continues with GRB2 containing a SH2 domain that then binds at phospotyrosine residues on the activated EGFR. This then binds to guanine nucleotide exchange factor SOS. GRB2-SOS is activated by phosphorylated EGFR, then going on to remove a molecule of GDP from Ras kinases. Ras goes on to activate RAF kinase cascade, which causes a phosphorylation and activation of MEK1/2 and MAPK (McCubrey et al., 2007).

RAS-RAF-MEK-ERK-MAPK signalling is instrumental in maintenance of protein synthesis and healthy muscle function. It is also a potential drug target for the treatment of malignancy (McCubrey et al., 2007, Sebolt-Leopold, 2008). As this pathway controls

cell growth, it is often upregulated in cancer cells and this upregulation serves as a sign of worsened prognosis (Hew et al., 2016).

1.5.4 Impact of Ageing

It is well documented in human and animal models that endogenous testosterone production decreases with age (Harman et al., 2001, Feldman et al., 2002, Chen et al., 2015a). This is observed as a gradual decline from around the age of 25, followed by a sharp decline in serum testosterone in old age. This is most likely due to lesions formation in Leydig cells of the testes resulting in decreased output of anabolic hormone (Midzak et al., 2009). This reduction of testosterone predisposes both males (Matsumoto, 2002) and females (Carcaillon et al., 2012) to greater risk of falls resulting in disability, reduced independence and overall lower standard of living. This can be otherwise characterised as sarcopenia.

1.6 Sarcopenia

Sarcopenia, stemming from the Greek *sarco* meaning flesh and *penia* meaning poverty refers to skeletal muscle wasting due to old age, is a condition that is characterised by the progressive and gradual (at a rate 1-5% per annum depending on age) decline in skeletal muscle mass, strength and function (Frontera et al., 1991). In humans we observe a gradual but slow decrease in muscle mass from around the age of 30 (Ryall et al., 2008). While statistically significant, this loss does not normally lead to any functional decline until much further into old age. At an average age of just over 70, the prevalence of sarcopenia was found to be 36.5% (Brown et al., 2016).

Sarcopenia manifests itself predominantly in the elderly population and leads to inactivity, increased susceptibility to falls and eventually to the loss of independent living (Morley et al., 2001). Falls especially, are a major health concern because they lead to hospitalisation and increased mortality in the elderly. This of course means a significant financial burden on the NHS. However, despite its profound socioeconomic implications, the exact causes and mechanisms underlying sarcopenia are still poorly understood at present. In addition to causing movement related debilitation, the onset of sarcopenia has also been linked with a decline in cognition associated with dementia and Alzheimer's disease (Mori et al., 2016).

Several groups have attempted to define sarcopenia in humans. The most robust consensus definition today is approved by the European Working Group on Sarcopenia EWGSOP (Cruz-Jentoft et al., 2010b). It is defined in its severe form as a measured muscle mass of over 2 standard deviations below the average in young adults of same sex and ethnicity, an abnormally low gait speed, and low muscular strength measured by resistance exercise. See Fig 1.7 for a proposed EWGSOP diagnosis algorithm (Cruz-Jentoft et al., 2010a).

There is no definitive treatment protocol that has proven to be effective for sarcopenic muscle dysfunction. Testosterone has been used successfully, but also causes a number of side effects, including prostate growth and alopecia(Wakabayashi and Sakuma, 2014). Growth hormone (GH) seems to be ineffective for increasing muscle

strength, likely due to a reduction in mRNA levels of GH receptor in elderly populations (Sakuma and Yamaguchi, 2012). Myostatin blockers and SARMS (selective androgen receptor modulators) remain an appealing option, but study of these compounds in treating sarcopenia is still limited and stricter guidelines need to be established for running drug treatment studies for sarcopenia (Reginster et al., 2016). There is scarce data on the use of DHT rather than testosterone in elderly models.

As stated above, the reduction in testosterone seen with ageing has been widely linked to sarcopenia. This occurs in males as well as females (Carcaillon et al., 2012). This reduction is not only linked to dysfunction in skeletal muscle. It is also implicated in osteoporosis, leading to impaired bone density and higher incidences of fractures (Fink et al., 2006). The combination of increased risk of falls due to fast twitch fibre loss coupled with the decrease in bone density is especially perilous in elderly populations.

Genetic variations among individuals also play an important role in determining the magnitude of anabolic stimuli available to skeletal muscle. For instance, variants on the SHBG and X chromosome are strongly associated with low concentrations (<300ng/dl) of testosterone in man (Ohlsson et al., 2011). These mutations are also implicated with an increased risk of developing sarcopenia in older age.

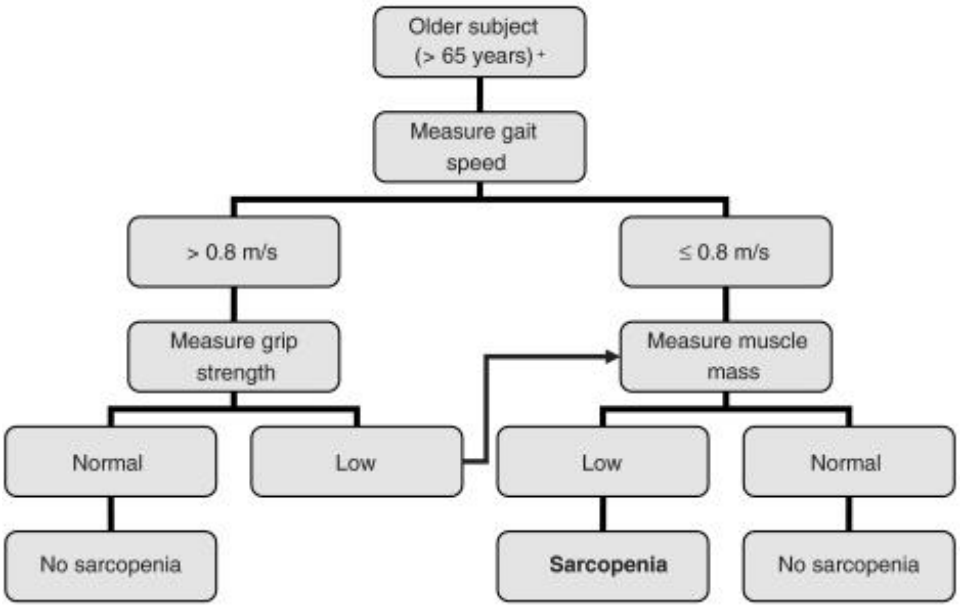

Figure 1.7 Accepted algorithm of sarcopenia diagnosis is based on a combination of functional tests and muscle mass. Adapted from: (Cruz-Jentoft et al., 2010a).

1.7 Thesis Aims

The aims of the thesis are:

Aim one: To assess the effects of normal ageing on total and relative muscle weights of the soleus and EDL, and the expression and transport of the sodium-coupled neutral amino- amino acid transporter SNAT2 and the sodium-independent L-type amino-acid transporter LAT2, and quantify protein incorporation. To also quantify the extent of change in AA transport with ageing and to relate these findings to the onset of sarcopenia.

Aim Two: To assess whether treatment with DHT can be an effective intervention for the reversal of SNAT2 and LAT2 related muscle dysfunction associated with ageing. To propose a likely mechanism for the DHT response.

Aim Three: To study the relationship between SNAT2 and LAT2 in mice skeletal muscle. To artificially increase the quantity of functional SNAT2 as well as to block it, then subsequently measure the effects of this intervention on LAT2 activity. Relate findings to the ability to modulate LAT2 activity through SNAT2.

Chapter 2: Materials and Methods

2.1 Buffers

AMPS: 100mg Ammonium Persulphate in 1mL distilled water. TE buffer 10 mM Tris-Cl, 1 mM EDTA, adjusted to pH 7.5.

Differentiation Media: MEM stock, 30mg/ml L-Glutamine (Invitogen, UK 11880-028) 1% Streptomycin/1% Penicillin (Invitogen UK 15140-122), 2% Horse Serum (Thermo-Fisher UK SR0035C).

Elution solution: 1.0M Tris buffer with sodium chloride, EDTA; adjusted to pH 7.4.

GTE buffer: 50 mM Glucose, 25 mM Tris-Cl, 10 mM EDTA, adjusted to pH 8.

HBSS: Hanks Balanced Solution (Invitogen UK 24020).

IP wash buffer: Wash 10mM Tris; adjust to pH 7.4, 1mM EDTA , 1mM EGTA; pH 8.0 150mM NaCl , 1% Triton X-100, 0.2mM sodium orthovanadate, Protease inhibitor cocktail.

Laemmli buffer: 1 mL Glycerol, 1g SDS 10%, 6.25 mL Tris HCl 0.5M pH 6.8, 2.5 mL β-mercaptoethanol, 1 mL Bromophenol 0.5%, made up with 10 mL of distilled water.

Mild Stripping Buffer: 1 liter 15 g glycine 1 g SDS 10 ml Tween20 adjusted to pH 2.2.

NP40 Lysis Buffer: 150mM NaCL, 50mM Trsibase, 1.5mM $MgCl_2$ 10% Glycerol, 1% NP-40, 1mM EDTA, pH calibrated to 7.5 with HCl.

PBS 10X: 40g NaCl,1g KCl, 13.4 g Na_2HPO_4-$7H_2O$, 1.2 g H_2O, pH adjusted to 7.4, made up to 500ml with distilled water.

Ringer Solution: 109mM NaCl, 5mM KCl, 1mM $MgCl_2$, 4mM $CaCl_2$, 24mM $NaHCO_3$, 1 $NaHPO_4$, 10 sodium pyruvate plus 200 mg l^{-1} bovine calf serum; and its pH was maintained at 7.42 by constantly bubbling it with 95% O_2 and 5% CO_2.

RIPA buffer: 150 mM sodium chloride, 1.0% NP-40, 0.5% sodium deoxycholate, 0.1% SDS, 50 mM Tris, then made up to pH 8.0 with HCl.

Running Buffer 10x: 30.3g Trisbase, 144g Glycine, 10g SDS, pH calibrated at 8.3 and made up to 1000mL.

SDS lysis solution: 0.2 M NaOH, 1% SDS.

Standard Culture Media (DMEM): (DMEM) 4500 mg/L glucose, Invitogen DMEM stock, 30mg/ml L-Glutamine (Invitogen, UK 11880-028), 10% FBS (Invitogen, UK 16000044) 1% Streptomycin/1% Penicillin (Invitogen UK 15140-122).

TBST 10X: 250mM Trisbase, 1.4M NaCl, 30mM KCl.

Transfection Media: DMEM, Lipofectamine 3000 (Therfmo Fisher, USA) 75µL/ well.

Transfer Buffer: 28.8 g glycine, 6.04g Trisbase, 200mL methanol, made up to 2L with water.

Tris Buffer 8.8: 1.5M Trisbase, adjusted pH to 8.8 with HCl.

Trisbase 6.8: 0.5M Trisbase, adjusted to pH of 6.8 with HCl.

Wash buffer: 10mM Tris; adjusted to pH 7.4, 1mM EDTA, 1mM EGTA; pH 8.0, 150mM NaCl, 1% Triton X-100, 0.2mM sodium orthovanadate.

Western Blot Running Gel 10%: 5.0ml Acrylamide 40%, 9.69mL distilled water, 5.0mL Tris HCl 8.8, 200uL 10% SDS, 100uL 10% AMPS, 10uL TEMED.

Western Blot Stacking Gel 4%: 1.0mL Acrylamide 40%, 6.4mL Distilled water, 2.5mL Tris HCl 6.8, 100uL 10% SDS, 50uL 10% AMPS, 10uL TEMED .

2.2 Isolation of small skeletal muscle fibre bundles

2.2.1 Animal Husbandry

The mice cohort used for these experiments consisted of CD-1 female mice of specified ages. The mice were maintained at the DMU (Disease Modelling Unit), University of East Anglia. They were kept at a maximum of 4 mice per cage and exposed to 12hrs of daylight and 12hrs of darkness. The mice were fed a diet of standard rodent chow and water *ad libitum*.

CD-1 mice strain was chosen due to the minimal incidence of genetic complications and genotype diversity comparable to a normal murine population (Aldinger et al., 2009). Relatively short lifespan of CD-1 mice makes them suitable for ageing studies. The mice were regularly inspected for signs of disease or stress and recorded weights matched those of healthy CD-1 populations at given ages (Percy and Jonas, 1971). No animals with signs of illness were used for data collection.

2.2.2 Fine Dissection

All the experiments reported were performed at room temperature (~20°C) using small skeletal muscle fibre bundles isolated from the extensor digitorium longus (EDL, a fast-twitch muscle in adult mice) and the soleus (Sol, a predominantly slow-twitch muscle in adult mice) of young (~100 days old), middle aged (300-400 days old) and elderly (>700 days) female CD-1 mice. Animals were killed by the Schedule 1 method of cervical dislocation as recommended by the Home Office and compliant with The Animal Scientific Procedures Act of 1986. For summary of the legislation see Drummond. (Drummond, 2009). Additionally, the experiments conformed to the University of East Anglia Animal Welfare and the Ethical Review Board guidelines on animal treatment. Approval for the project was sought from the AWERB and approved for the use of licensed procedures to be performed by licensed individuals. However, during the project, the mice were not subjected to any procedures and were sacrificed, after which muscle tissues were extracted. The number of animals used was minimised to the lowest level possible whilst still allowing for significance testing.

Dissections were done as promptly as possible. SOL was isolated as a whole muscle, while the EDL was split into its three constituent bundles to isolate the most predominantly fast twitch bundle (medial bundle). Care was taken to ensure the fibres

were intact and responsive to electrical stimulation for the duration of the experimental runs. Fibres were tested for contractility after isolation using low voltage stimulation, repeated every 2 seconds prior to start of the experiment.

2.2.3 Experimental Procedure

During the experiments, the muscles and muscle fibre bundles were bathed in mammalian Ringer's solution continuously bubbled with 95% O2 and 5% CO2 gas to maintain a physiological pH of 7.4 or 80% 02 and 20% CO2 to achieve an acidic pH of 6.8. Ringers solution was based on prior formulations by Mutungi and Ranatunga (2000), (for composition see materials) and its pH was maintained at 7.42 by constant bubbling.

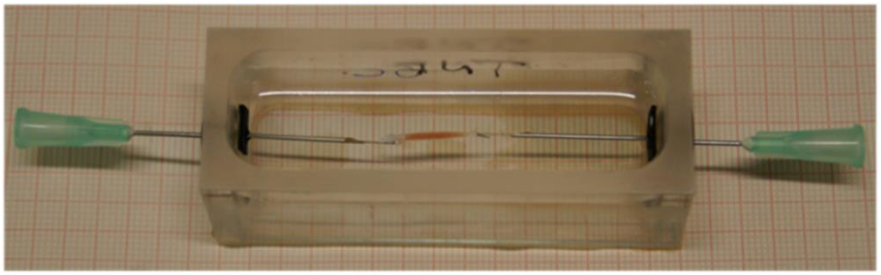

Figure 2.2.1 Example of the tissue baths used for uptake testing. Hooks rotate freely to allow access to muscle. Ringer's solution submerges tissue fully and is constantly bubbled with CO2 to maintain physiological pH.

Two types of muscle chambers, one with a total volume of 5 ml and 25 ml, (25mL shown in figure 2.2.1) were used for the determination of amino acid uptake and muscle tissue treatments. The fibre bundles were continuously perfused with the standard mammalian Ringer solution to ensure muscle tissue viability. For the duration of uptake experiments the muscle fibres were mounted horizontally in between stainless-steel hooks in the specially designed muscle chambers.

2.3 SDS-PAGE analysis

2.3.1 Experimental Setup

SDS-PAGE was used to investigate the acute effects of DHT on the expression of AA transporters. In an effort to reduce variability and destruction of aged mice, one set of EDL and SOL from each mouse was subjected to control and the other set was treated with DHT. Tissue from a minimum of 3 different mice was used in each individual experimental cohort to achieve n≥3.

Group 1 (controls) was treated with 107.9µM ethanol in Ringers solution (the vehicle used to dissolve DHT) for 1hr. Group 2 (experiment) was treated with 2.17nM of DHT for the 1hr plus 107.9µM ethanol in Ringers solution.

At the end of the treatments, the bundles were snap frozen in liquid nitrogen and pulverized in eppendorf with plastic tissue grinder (Fisher Scientific, UK), then placed in 100µl of NP40 buffer (see buffers 2.1.1) containing 10mg/10mL protease (Roche, Switzerland) and 100µl/10mL phosphatase inhibitors (Calbiochem, Nottingham). These were then further agitated with rotary tissue grinder to homogenise.

2.3.2 Sample Preparation

Crude membrane fraction was isolated from lysate using NP-40 buffer cellular membrane fractionation by centrifugation at 15000g for 10min at room temperature, washing three times with PBS and then resuspension of resulting pellets in 100µL of NP-40 buffer as first described by Holden et al. (2009) (Perez et al., 2013). The lysates from the resuspension step contained the desired crude membrane fraction and kept for use in further experiments. Samples were then stored at -80°C or used immediately.

Protein concentration was determined by preparation of 5µL of each lysate with 100µL of Bradford reagent (Sigma-Aldrich, Dorset UK) The Bradford reagent is a dilution of Coomassie brilliant blue G-250 dye (CBBG). This was then compared alongside a calibration curve of varying concentrations of Bovine Serum Albumin (BSA) to perform a Quick Bradford Assay (Bradford, 1976). Concentrations of BSA used were 0,1,5,10 and 20µL using a 1mg/mL BSA stock. The reagents were dissolved in double distilled water in 1mL disposable cuvettes and then inverted three times to ensure thorough

mixing. A spectrophotometer (Helios Y, Fisher Scientific, UK) was used to read absorbance of samples at a wavelength of 595nm. The Quick Bradford technique provided an accurate and fast method of quantifying lysate protein concentrations. 10µg of total protein (as calculated from results of Quick Bradford analysis on extracted lysates) was pipetted into empty eppendorfs. Each of these were then mixed with 5µL 2x Laemmli buffer containing 10% β-mercaptoethanol (see buffers 2.1.1). Samples were boiled at 100°C for 2 minutes prior to centrifugation for 30 sec at 13,000rpm and loaded into each well of a 12% SDS-PAGE gel. Finally, 1µL of protein ladder was (ab116028, Abcam, USA) added to the first well of every gel.

2.3.3 Casting and Running Gels

Gels were produced according to the following formula:

Table 3: SDS-PAGE Gel Composition

Ingredient	12% Running Gel	4% Stacking Gel
ddH_20	9.69mL	6.4mL
Acrylamide 40%	5mL	1mL
Trisbase (pH 8.8)	5mL	0
10% SDS	200µL	100µL
AMPS	100µL	50µL
TEMED	15µL	10µL
Trisbase (pH6.8)	0	2.5mL
Total Volume	20mL	10mL

12% gels were found to be most suitable for running both SNAT2 and LAT2 proteins. Gels were inspected for conformity and well formation. These were either used after casting or refrigerated at 4-8°C and used within 14 days. Samples were separated by standard gel-electrophoresis using Mini-Protean Tetra-Cell (BioRad Laboratories, Hemel Hempstead) and ran in transfer buffer (see buffers 2.1.1) at 90V for 3-4hrs until proteins ran to close proximity of the bottom of the gel.

Precut PVDF membranes were soaked in methanol for 10 minutes. The finished gels were then placed onto the PVDF membranes and placed in a Trans-Blot Semi-Dry Transfer Cell, (BioRad Laboratories, Hemel Hempstead) These were then transferred onto the PVDF membranes by running the semi dry transfer system for 40 minutes, at

250V and 0.2 Amperes. After completion, membranes were placed in TBST (see buffers 2.1.1) and refrigerated at 4-8°C for storage.

The membranes were blocked for non-specific antibody binding using 5% milk in TBST for 10 min. They were then analysed for the expression of SNAT2 (rabbit polyclonal; Santa Cruz Biotechnology, Santa Cruz, Ca, USA) or LAT2 (rabbit polyclonal; Abcam, Cambridge, UK). Primary antibodies were incubated at a 1:500 dilution for a minimum of 2hrs (SNAT2) or overnight at 4°C (LAT2) under rocking. Anti-rabbit secondary antibodies conjugated to horse radish peroxidase (HRP) were used at a 1:2500 dilution and incubated for 1hr at room temperature.

Membranes were washed in TBST (see materials twice and then left under rocking for 10min, this was then repeated three times. Finally, they were visualized using SuperSignal WestPico chemiluminescence substrate (Perbio Science UK Ltd, Cramlington and Northumberland, UK) and exposure was done on ChemiDoc XRS+ (Bio-Rad, Watford,UK).

The following day, the membranes were stripped with mild stripping buffer for 20min under rocking (see buffers 2.1.1) and re-probed with a pan-actin antibody (Mouse monoclonal, Abcam, Cambridge, UK). Actin antibody was used at a 1:2000 dilution and incubated for 1hr at room temperature. Secondary HRP conjugated antibody (Goat anti-mouse, Abcam, Cambridge, UK) was used at dilution of 1:5000 for 1hr at room temperature. All the blots were run in duplicates and each experiment was performed a minimum of three times, each using proteins from a different animal.

Table 4: Antibodies used in Western Blotting

Antibody Target	Dilution	Supplier Code	Supplier
SNAT2 (Rabbit Polyclonal)	1:500 (WB)	sc-67081	Santa Cruz Biotechnology, Santa Cruz, Ca, USA
LAT2 (Rabbit Polyclonal)	1:500 (WB)	ab123893	Abcam, Cambridge, UK
Secondary antibody (Goat Anti-Rabbit IgG HRP conjugated)	1:2500 (WB)	ab6721	Abcam, Cambridge, UK
Anti Actin (Mouse Monoclonal)	1:2000 (WB)	ab3280	Abcam, Cambridge, UK
Secondary Antibody (Goat Anti-Mouse IgG HRP conjugated)	1:5000 (WB)	ab97040	Abcam, Cambridge, UK

2.4 Reverse transcription quantitative polymerase chain reaction (RT-qPCR)

2.4.1 Sample Preparation

Total RNA extraction from fast-twitch and slow-twitch muscle fibre bundles was performed using TRIzol® reagent according to the manufacturer's instructions (Lifetechnologies, Paisley, UK). The muscle samples were snap frozen in liquid nitrogen, then pulverised and mixed with 100µl ice cold TRIzol. The mixture was centrifuged at 12,000g for 10min at 4°C and the supernatant was transferred into a new tube. It was mixed with chloroform and incubated for 3 minutes at room temperature before it was centrifuged at 12,000g for 15 min at 4°C. The aqueous phase was separated, mixed with isopropanol then left to incubate at room temperature for a duration of 10min. It was centrifuged at 12,000g for 10 at 4°C and the precipitated RNA was purified from contaminants using an RNeasy Mini Kit (Qiagen, Manchester, UK) and dissolved in RNAse-free water and stored for further use. The quantity and quality of the RNA extracted was determined spectrophotometrically using a Nanodrop 2000 spectrophotometer (Thermo Fisher, Massachusetts U.S.A.). 1µg of RNA was reverse transcribed using Quantitect Reverse Trancriptase to generate cDNA following the manufacturer's standard protocol (Qiagen 2009). SYBR green Readymix (Sigma-Aldrich, Irvine UK) was used for cDNA amplification, setup as follows:

Table 5: PCR Experimental Composition

Component	Experimental	No Template Controls	No RT Control
SYBR Green qPCR Readymix (2x)	10µL	10µL	10µL
Forward Primer (10µM stock)	0.4 µL	0.4 µL	0.4 µL
Reverse Primer (10µM stock)	0.4 µL	0.4 µL	0.4 µL
Template cDNA	5.0 µL	-------	5.0 µL (reverse transcriptase replaced with H_2O)
PCR Grade H_2O	4.2 µL	9.2 µL	4.2 µL
Total Volume	20 µL	20 µL	20 µL

2.4.2 Experimental Runs

To test for DNA contamination, a no template control was used for each experimental run consisting of PCR grade H_2O in place of cDNA template. A no reverse transcriptase control was used by omitting the reverse transcriptase in the cDNA generation step. Only experimental samples that resulted in no significant amplified products in the two corresponding negative controls were used.

The PCR consisted of the following steps:

Table 6: PCR Protocol Summary

Step	Temperature	Time	Times completed
Initial Denaturation	94°C	2 min	1
Denaturation	94°C	15 sec	35
Aneal and extension	55°C	1 min	35

The primers used were as follows:

SNAT2:
Forward: 5’ ATCGTGGTGATTTGCAAGAA 3’
Reverse: 5’ GTCTGCGGTGCTATTGAATG 3’
LAT2
Forward: 5’ GCCCTCACCTTCTCCAACTA 3’
Reverse: 5’ CCATGTGAGGAGCAACAAAC 3’
S29 (housekeeping gene standard)
Forward 5’ CGGAAATACGGCCTCAATATG 3’
Reverse 5’ CAACCAACAAGTTTATGCAACCA 3’

PCR equipment used for experimental protocol was the 7500 Real-Time PCR System (Applied Biosystems, Grand Island, NY). All the experiments were performed in triplicate and were completed a minimum of 3 times, each with a different animal. S29 was used as the housekeeping gene for standardization. Melting curves were recorded and samples with peaks suggesting additional amplified entities were discarded (Fig. 2.4). Representative melt curves as shown on following page.

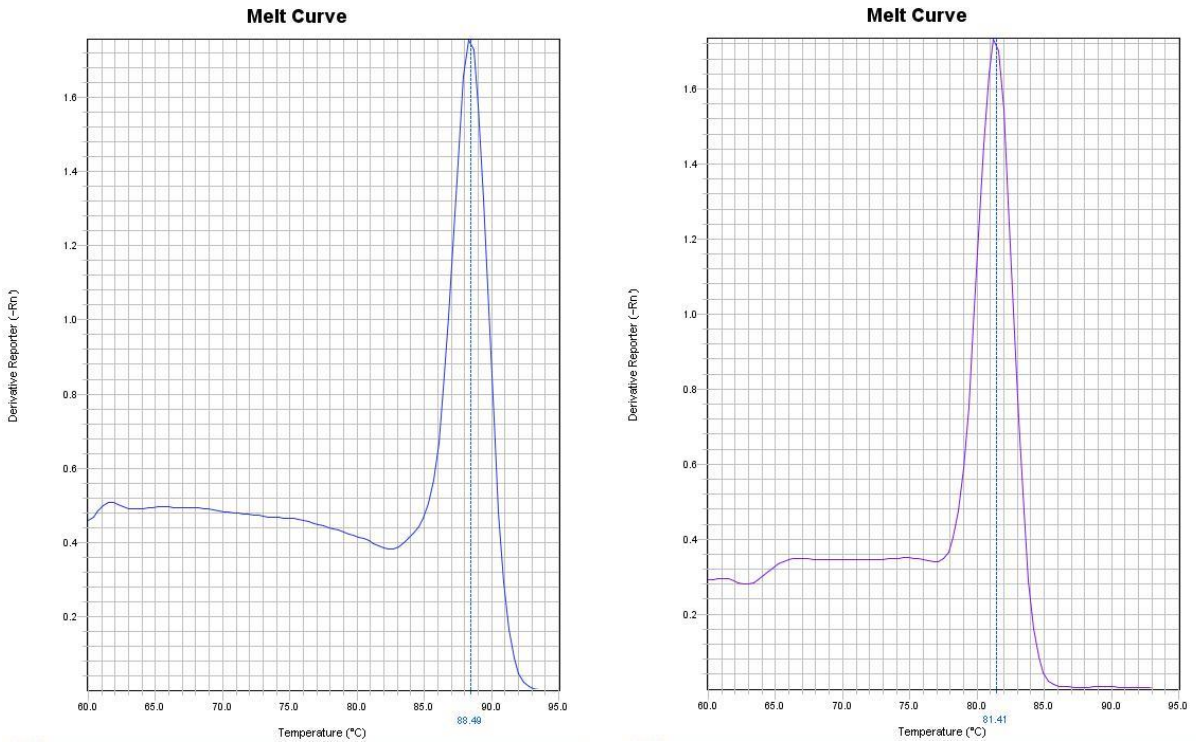

igure 2.4 S29 and SNAT2 melting curves. Graphs showing representative melting curves of S29 (LEFT) and SNAT2 (RIGHT). There is no evidence of any secondary products being produced during the amplification.

2.5 Cell Culture

2.5.1 General Cell Maintenance

The cell line C2C12 is an immortal line of mouse skeletal myoblasts originally derived from the satellite cells of a C3H mouse donor after an injury of the animals thigh (Yaffe and Saxel, 1977). Cells used for all experiments were at passage 5 or below.

C2C12 cells were kept in T25 culture flasks (Fisher Scientific, Loughborough, Leicestershire) at a temperature of 37°C and 95% O_2, 5% CO2. Standard medium used was DMEM (Invitogen UK 11880-028) with added 10% fetal bovine serum, supplemented with 2mM L-glutamine and 1% streptomycin (Sigma-Aldrich, Poole, UK). Cells were routinely monitored in order to not allow them to reach higher than ~80% confluence at which point they were split into additional flasks. Cells were detached from flasks using trypsin as follows:

C2C12 cells were examined to ensure they did not exhibit signs of distress or contamination. Trypsin, HBSS and DMEM were prewarmed to 37˚C, culture media was removed from the flasks. Cells were rinsed with HBSS (Ca^{+2} and Mg^{+2} free) and trypsin solution was used to dislodge any firmly adherent cells. Trypsin solution was added to submerge the bottom of the flask and swirled gently. After 2-3 minutes 2 volumes of DMEM was added to inactivate the trypsin. Resulting cell suspension was spun at 500xg for 5 minutes and the cells were re-plated and DMEM replaced.

2.5.2 Differentiation into Myotubes

For differentiation into myotubes, myoblast cells were re-plated and allowed to grow for 3 days. At this point, the media was changed to MEM with 2% horse serum supplemented with 2mM L-glutamine and 1% streptomycin, (Invitogen UK 21090-022) and incubated overnight for 12hrs then changed to fresh MEM with 2% horse serum, 2mM L-glutamine, and 1% streptomycin. This procedure initiates differentiation of the myoblasts into myotubes (Lawson and Purslow, 2000). Myotubes were inspected after 3 days for differentiation and good health then used for experiments before they were allowed to reach confluence.

2.5.3 DHT treatment

Myoblasts were cultured in full media at 37°C until 70-80% confluence. Myotubes were used 3 days after differentiation. DHT was used at 2.17nM (physiological) or 4nM

(supraphysiological). 107.9µM ethanol was used as DHT vehicle and added to DHT-free controls. Experiments were run at 37°C in DMEM (myoblasts) or MEM (myotubes) in the presence or absence of DHT and in the presence of either 2mML C_{14}Isoleucine or 68.3µM C_{14}MeAIB.

T25 Flasks were kept in a sealed and heated container maintained at 37°C and bubbled with 95/5% O_2/CO_2 to maintain physiological pH. The experiment was completed over the course of 1hr to mirror skeletal muscle experiment conditions. At the end of the 1hr experimental run, flasks were then washed three times with ice cold PBS and cells removed off using cell culture scrapers and PBS. These were then put into 5mL glass tubes, then centrifuged at 500 rpm to remove PBS. The pellet was resuspended in 100µL of NP40 buffer and put on ice for 20min to encourage cell lysis. These were then pulverised using a rotary eppendorf grinder until pellet was homogenised and then spun at 13000g for 10min. Resulting pellet was discarded and the total cell lysate used for scintillation counting.

2.5.4 Treatment with antagonists

Myoblasts were cultured in full media at 37°C until 70% confluence before start of experiments. Myotubes were used 3 days after differentiation. Cells were pretreated with antagonists for 1hr prior to starting experiment. Chloroquine was used at a concentration of 40µM, Flutamide at 3µM, SP600125 at 10µM and Wortmannin at 200nM (see antagonists 2.1.3). Experiments were all run at 37°C in DMEM (myoblasts) MEM (myotubes) in the presence or absence of antagonists and in presence of either 2mM C_{14}Isoleucine (for LAT2 transport) or 68.3µM C_{14}MeAIB (for SNAT2 transport). Flasks were kept in a sealed and heated container bubbled with O_2/CO_2 mixture to maintain physiological pH. Experiment was run over the course of 1hr. Flasks were then washed three times with ice cold PBS and scraped to remove cells. These were then centrifuged at 500 rpm to remove PBS and then lysed in NP40 buffer as described aboce (refere to section) .

2.5.5 C2C12 cell starvation and SNAT2 blockade

Myoblasts were cultured in full media at 37°C until 70-80% confluence before start of experiments. For starvation cohorts, cells were placed in HBSS for 3hr prior to start of experiments. Experiments were then run at 37°C in HBSS. SNAT2 was blocked using

saturating concentrations of 5mM and 10mM of MeAIB. as described by Hundal et al. (Hundal et al., 1994). 5mM was found to be the concentration necessary for saturable block of SNAT2. (see Chapter 5.) Cells were preincubated with saturating concentrations of MeAIB (as determined to be >5nM) for 1hr prior to start of experiments. Flasks were kept in a sealed and heated container bubbled with O_2/CO_2 to maintain physiological pH. Experiment was ran over the course of 1hr. After 1hr, flasks were then washed three times with ice cold PBS and scraped to remove cells. These were then centrifuged at 500 rpm to remove PBS. These were then pulverised in NP40 buffer and centrifuged at 13500 rpm, pellet was discarded and total cell lysate used for scintillation counting as before.

2.6 Radio-Isotope Techniques

2.6.1 LAT2 transport in Muscle

Muscle tissues of various ages were treated with the standard Ringer's solution containing 107.9µM ethanol plus 2mM C_{14} isoleucine containing a radioactivity level of 3.46µCi/mL. (PerkinElmer, Buckinghamshire, UK) for 1hr to assess LAT2 transport. Isoleucine was used because it alone does not increase protein synthesis, unlike Leucine (Anthony et al., 2000).

The DHT treatment group was treated with the Ringer's solution containing 2.17nM 4,5α-dihydrotestosterone (DHT) (Sigma, Gillingham, Dorset, UK), 107.9µM ethanol, plus the C_{14} isoleucine for the same duration (1hr). During this time, the muscles were held in muscle chambers at 22°C, with constant bubbling to maintain physiological pH. At the end of the 1hr experiment, the fibre bundles were washed three times with ice cold PBS and the excess PBS was blotted on tissue paper. The bundles were immediately snap frozen in liquid nitrogen, pulverised and mixed with NP40 buffer containing 10mg/10mL protease (04693116001 Roche, Basel, Switzerland) and 100µl/10mL phosphatase inhibitors (524625 Calbiochem, Nottingham). The mixture was centrifuged at 13,000g for 10min and the supernatant was collected and used for scintillation counting.

2.6.2 Protein Incorporation in Muscle

When assessing protein incorporation, 2mM C_{14} isoleucine was used as with LAT2 transport protocol above. The supernatant was further processed by mixed with ice-cold 10% TCA. It was then left standing on ice for 1-2hrs before the mixture was centrifuged at 13,000g for 10 minutes and the supernatant discarded. The resulting pellet was washed three times with ice cold acetone and re-dissolved in 200µL of KOH then quantified for incorporated C_{14} isoleucine.

2.6.3 SNAT2 Transport in Muscle

To determine the effects of ageing and DHT treatment on SNAT2 amino acid uptake by the muscle fibre bundles, steps were repeated exactly as described before with the exception that the radioactive tracer was replaced by 68.3µM C_{14} α-methylaminoisobutyric acid containing a radioactivity level of 0.8µCi/mL . (PerkinElmer, Buckinghamshire, UK) ran for 1hr as before. All samples probing for

SNAT2 transport were measure for raw AA uptake only, therefore there was no TCA precipitation step.

2.6.4 Treatment of Chloroquine and Flutamide on Muscle

All steps were followed as before. Groups were split into: control, chloroquine and DHT treated, flutamide, flutamide and DHT and DHT treatment alone. Muscles were pre-treated with 40µM chlorquine or 3µM flutamide for one hour, then treated again with 40µM chloroquine or 3µM flutamide for the duration of the one-hour experiment within their respective groups. DHT was administered at the usual concentration of 2.17nM and ethanol was administered as vehicle control. Tissues were pulverised in liquid nitrogen and placed in NP40 buffer as usual. For amino acid uptake, the ground tissue lysate was tested directly. Liquid scintillation counting was used to quantify Ille-C_{14} and MeAIB-C_{14} quantities.

2.6.5 SNAT2 and LAT2 transport in C2C12 Cells

C2C12 radio-isotope treatments mirrored those of muscle drug interventions. 68.3µM C_{14} α-methylaminoisobutyric acid and 2mM C_{14} isoleucine were used mixed in cell media for the quantification of SNAT2 and LAT2 transport respectively. Radio-isotopes were only added at the start of 1hr experimental runs, they were not used in pretreatment.

2.6.6 Scintillation Counting

The amount of proteins in each lysate was first determined using the quick Bradford assay (Bradford, 1976) and the level of radioactivity in the mixture was determined using a liquid scintillation counter (Tri-Carb 2250 CA, Canberra-Packard). Ecoscint A (National Diagnostics, UK) was used as scintillation liquid, using 100µL of lysate per 2mL of scintillation fluid. The scintillant and lysate solution was thoroughly mixed and allowed to stand overnight to quench. The next day the samples were examined using scintillation counter, with a count time of 2.5hrs per sample tube to allow for variance in C_{14} activity. Samples were kept away from light at all times. Each experiment was run a minimum of three times, using different cell colony each time.

Table 7: Summary of Drugs and Radio-Isotopes Used

Ingredient	Concentration	Supplier Num.	Supplier
Absolute Ethanol	107.9µM	NC9602322	Fisher Scientific, Loughborough, Leicestershire
Dihydro-Testosterone (5α-Androstan-17β-ol-3-one)	4nM	A8380-1G	Sigma-Aldrich, Gillingham, Dorset
Chloroquine	40µM	C6628-25G	Sigma-Aldrich, Gillingham, Dorset
Flutamide	3µM	F9397-1G	Sigma-Aldrich, Gillingham, Dorset
MeAIB-C_{14}	68.3µM (0.8µCi/ml)	NEC671050UC	PerkinElmer, Buckinghamshire, UK
Isoleucine-C_{14}	2mM (3.46µCi/ml)	NEC278E050UC	PerkinElmer, Buckinghamshire, UK
MeAIB	0.5,5,10mM	M2383-250MG	Sigma-Aldrich, Gillingham, Dorset
SP600125 (JNK inhibitor)	10µM	S5567-10MG	Sigma-Aldrich, Gillingham, Dorset
Wartmannin	200nM	S5567-10MG	Sigma-Aldrich, Gillingham, Dorset

2.7 Expression Vector

2.7.1 Plasmid Design and Sourcing

SnapGene (GLS Biotech, USA) program was used to create plasmid sequence including a SNAT2 encoding insert. The pcDNA™3.1/CT-GFP (Genscript, USA) plasmid vector backbone was bought directly from Genescript using the SnapGene sequence. (see appendix A for vector structure) The plasmid contains a GFP tag useful for identification in fluorescence imaging and inserts conferring ampicillin and neomycin resistance.

2.7.2 Plasmid Identification

A restriction digest was performed on the expression vector to verify its identity following protocol from (Addgene, Cambridge USA). Reaction was prepared in 1.5mL Eppendorfs using 1 µg DNA, 1 µL each of restriction enzymes kpn1 (Sigma-Aldrich, UK R1258 and nhe1 (Sigma-Aldrich, UK R5634) 3 µL 10x Digestion Buffer and 25µL dH2O. Restriction digest was performed around the site of SNAT2 insert (omitting GFP tag) to assess for correct insert size.

This was then ran on 1% agarose gel containing 0.3µg/mL EtBr at 120V in 1% TAE/EtBr and seperated using standard gel electrophoresis. This was then visualized using UV light imaging. An expected band at around 1001 base pairs was observed, showing the presence of SNAT2 and secondary band at 5138 base pairs was observed, accounting for plasmid backbone.

A molecular sequence was provided by Genscript for conformation. A sample of the plasmid was sent to an independent analytical laboratory (Source Bioscience, Notthingham UK) to verify the molecular sequence.

2.7.3 Plasmid Amplification

The expression vector was amplified in DH5α Ecoli cells using protocol from (ABM, USA). Briefly, Ecoli cells were thawed on ice, 1µL of plasmid at a concentration of 10 ng/µl was added per aliquot and left on ice for 30 minutes. These were then heat shocked for 45 seconds at 42°C, then placed back ice for 2 minutes. 150µL of sterile Lysogeny broth (see materials) was added and incubated for 1 hr at 37°C. Cells were plated and left overnight in incubator in LB broth at 37°C 95% O_2/ 5%CO_2 and sufficient humidity.

2.7.4 Plasmid Isolation

Best colonies, as assessed by fluorescence imaging were chosen for vector purification. ABM Mini-Prep Kit (ABM, Vancuver Canada) was used for plasmid isolation Successful SNAT2 expressing cell colony was chosen and inoculated with LB broth. This was shaken at 37°C overnight. 1.5 mL of cells were centrifuged at 13000 RPM for 1 minute. The supernatant was discarded. The cell pellet was resuspended in 100 uL of GTE buffer by vortex (see buffers 2.1.1). Solution was lysed by adding 200µl ABM Buffer 2 and inverting tube 5 times, then keeping at room temperature for 1 min. 350µl of ABM Buffer 3 was then added and tube inverted repeatedly as before. This was spun at 13,000 RPM for 1 minute. Supernatant was transferred to filtered spin column, centrifuged at 10,000 RPM for 2 min and resulting solution discarded. The filter was then washed with 750µl of wash solution, centrifuged and the resulting solution discarded once again. This wash step was repeated 2 more times. 50µl of elution buffer was added and the columns spun at 13,000 RPM for 2 min.

The DNA was quantified using spectrophotometer at an absorbance of 260nm. Purified DNA was kept at -20°C for later use.

2.8 Fluorescence Imaging

Tissue was dissected from mice of varying ages as outlined above. Isolated EDL and Soleus were put on ice to prevent protease degradation. These were placed on aluminium foil disc and dipped in isopentane which has been lowered in temperature by submersion in liquid nitrogen. In this way tissue damage from formation of ice crystals was minimised. Samples were kept at -80°C until ready for use.

Samples were mounted on stainless steel discs and kept vertical using pre cooled OTC mounting solution. Care was taken to ensure tissue did not thaw before being placed in the cooled cryostat. Cutting was performed at -20°C. Sections were cut at a thickness of 10µm and placed onto gelatin coated glass slides and air dried.

For fluorescent staining, slides were incubated in humidifier at all times to prevent evaporation. Slides were incubated in 40% methanol for 30 seconds at 20°C. Sections were then incubated in 4% paraformaldehyde for 10 minutes at 20°C. These were then washed three times with PBS and blocked for 1hr with 5% goat or 1% horse serum to minimise nonspecific binding.

Primary antibodies (SNAT2 H-60 Sc-166366 mouse monoclonal, Santa Cruz, USA) were incubated in 2% goat serum overnight at 4°C at dilution of 1:250. This was then washed three times with PBS under rocking for 10 minutes per washing. These were then incubated with secondary at a concentration of 2 µg/ml (A-11032 Alexa Flour 594; anti-mouse; Thermo Fisher, USA) for 1hr at room temperature.

These were then washed 3 times with PBS as before. Fluoroshield DAPI containing mountant (Sigma-Aldrich, Gillingham, Dorset) was used to affix the slide covers. Slides were kept at 4°C until ready to view.

Slides were examined for fluorescence using Carl Zeiss Axio Imager using Axio Vision software. Alexa 594 channel was used to image SNAT2, while DAPI 354 channel was used to image DAPI. DAPI channel was exposed for 20ms while SNAT2 was exposed for 500ms. Resulting images were not altered and ImageJ (Scion/NIH) was used to quantify signal at the plasma membrane.

2.9 Immunoprecipitation

2.9.1 Setup

Upon delivery, the beads were incubated with 1ml of PBS to allow beads to swell up. These were centrifuged and the supernatant discarded. 1ml of PBS/0.1% BSA was added as blocking agent, mixed for 1h on a rotator and then rinsed twice with PBS. 1mL aliquots of bead slurry were then stored at 4-8°C until ready for use.

2.9.2 Immunoprecipitation

Immunoprecipitation was used following Abcam IP protocol using Protein A Sepharose beads. The beads were first crosslinked with SNAT2 antibody. First, 100µL of slurry from stock bottle was transferred to a microcentrifuge tube. To this, the SNAT2 polyclonal (Santa Cruz Biotechnology, Santa Cruz, Ca, USA) antibody was added at a final concentration of 2µG/100µL. This was then incubated on a rotator at 4°C for 4h. This was centrifuged for 5min at 3000rpm then washed with PBS buffer twice. 30uL of tissue lysate in NP40 buffer was transferred into the microcentrifuge per 100uL pre made bead slurry. This was incubated overnight at 4°C on rotator. The beads were then centrifuged as before and washed using wash buffer three times.

2.9.3 Elution

The beads were eluted using a SDS elution method. They were heated with 50uL of SDS buffer for 10min at 50C. The beads were then placed in 750uL centrifugal microfilters and spun at 10,000g for 5 minutes and supernatant kept. For the second elution, 50uL of SDS buffer was added with addition of 100mM DTT. The samples were boiled for 5min and centrifuged as above. Both elutes were kept and analysed by Western Blotting.

2.10 Statistical Analysis

Control and individual treatment/intervention groups were organised as nominal data, while their corresponding respective quantifications were organised on an interval scale. 95% Confidence interval was used and a minimum n value of 3 for any statistical analysis. Significance was defined as $p<0.05$.

Analysis was performed using SPSS software version 20. Analysis of variance was performed on all data sets (ANOVA) followed by Bonferroni *post hoc* test. Type of ANOVA used varied on each dataset. Two-way ANOVA was used for studying significance with two independent variables such as testing of effects of age and muscle type on AA transporter expression and transport. (chapters 3 and 4) One-way ANOVA was used for datasets containing only one independent variable, such as myoblast and myotube experiments in chapters 4 and 5. Type of variance tests used are specified in figure legends.

2.11 Image Creation

Image J (scion/NIH) was used for Western Blot and fluorescence image quantification. Background was always accounted for by reducing intensity of entire blot by the intensity of a clear portion of the blot. For Western Blot analysis the intensity of the bands of interest were normalised to the corresponding actin intensity and the data presented are the mean of the blots performed.

Fluorescence images were quantified for plasma membrane intensity by a method proven in plasma membrane quantification of human embryonic kidney cells (Leterrier et al., 2004). This was done by manually drawing around the outer ages of the cells, selecting the area within. This intensity was calculated as whole cell intensity. Erode command was used to subtract selection area away from edges by 5 pixels. This was calculated to be cytoplasmic intensity. Whole cell – cytoplasmic intensity was determined to calculate plasma membrane intensity. This was done individually to eliminate overlap between cells.

All Illustrative images were produced using Adobe Flash CS5.

2.12 Experimental Limitations

Various experimental limitations were identified during these experiments. These include but are not limited to:

- Relatively small sample sizes of animals due to high cost and availability of aged animals.
- Experimental runs of DHT uptake on skeletal muscle was performed at 22°C not physiological temperature.
- 107.9µM of ethanol had to be included in all DHT and control experiments (due to poor solubility of DHT).
- Uptake quantification was observable only at the endpoint of experiments.
- Transfection rate of SNAT2 plasmid was 10-20%.
- Limited choice of inhibitors and agonists due to high cost of radioactive isotopes.

Chapter 3: Effects of ageing on mice skeletal muscle

3.1 Aim

3.2 Results

3.2.1 Effect of ageing on muscle weight.

3.2.2 Effect of age on SNAT2 and LAT2 transporter protein expression.

3.2.3 Effect of ageing on amino acid transport into muscle

3.2.4 Effect of ageing on incorporation of amino acids into muscle protein.

3.2.5 Effect of ageing on SNAT2 and LAT2 mRNA expression

3.3 Discussion

3.1 Aim

The aim of chapter 3 is to determine the effects of ageing on mice skeletal muscle. The parameters investigated were muscle weight, SNAT2/LAT2 expression and transport, and protein synthesis. This data allowed for the quantification of the effect of ageing on mice and would serve as a baseline for further experiments.

3.2 Results

3.2.1 Effect of ageing on muscle weight.

Firstly, we investigated the effects of ageing on skeletal muscle mass alone. Initially three age groups were tested: 100 day old mice representing post pubescent young mice, 300 day old "mature" mice representing fully mature mice, and mice over 700 days old, representing an elderly group. These mice ages were chosen based on previous work in mice development and ageing (Banerjee et al., 2014). The first experiment recorded the total weight of the isolated extensor digitorum longus (EDL) and soleus (SOL) muscles in each age group. Total muscle mass was chosen because it is the predominant determinant of force production in mice (Bonetto et al., 2015), and a reduction of total muscle mass is the primary observation in sarcopenia. Fig. 3.1A shows that ageing led to a marked decline in the total weight of the EDL and SOL muscle. EDL weight fell by ~50% with an approximate ~25% fall for SOL.

An accumulation of body fat relative to muscle mass is known as sarcopenic obesity (Lee and Park, 2015) which correlates with reduced prognosis and increased chance of disability when compared with muscle loss alone (Zoico et al., 2004). Sarcopenic obesity was assessed from the ratio of the muscle weight to the whole weight of the animal to account for increase in fat mass proportional to lean mass (Fig 3.1B). In figure 3.1B the weight of the muscle is expressed as a percentage of total body weight. The weight of the muscle dropped from ~1.4% of body weight in young mice to between 0.4% and 0.6% body weight for the EDL, and soleus muscles in elderly mice, respectively. The elderly mice therefore showed a marked decline in proportional lean mass when compared to young and mature mice. This was effect was greater in fast twitch EDL muscle.

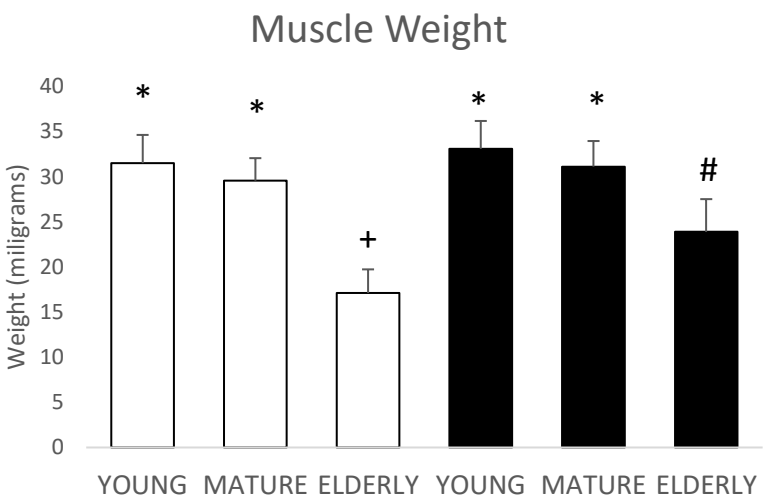

Figure 3.1A. Effect of age on muscle weight in mice. Fast twitch extensor digitorum longus (EDL) and slow twitch soleus (SOL) muscles were isolated from mice at the indicated ages and weighed. Young mice were ~100 day old, mature mice ~300 days old and elderly mice were over 700 days old. EDL white bars SOL black bars). No significant difference was found between muscle weights of young and mature cohorts (* to * $p>0.05$) Elderly muscle weights were significantly lower in both EDL and SOL groups as compared to both young and mature mice (+ to * $p<0.01$ and # to * $p<0.05$). 2-Way ANOVA used, n=12.

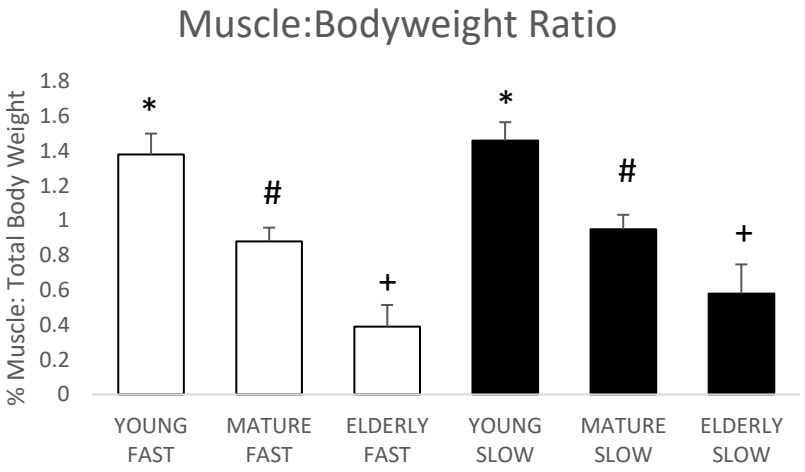

Figure 3.1B Effect of age on sarcopenic obesity in mice. Fast twitch extensor digitorum longus (EDL) and slow twitch soleus (SOL) muscles were isolated from mice at the indicated ages. Young mice were ~100 day old, mature mice ~300 days old and elderly mice were over 700 days old. EDL white bars SOL black bars. The weight of each muscle was calculated as a percentage of the total weight of the animal. each respective age group showed significant difference between age groups (difference between # + and * $p<0.05$). There was no significant difference between muscle types (**, ##, ++ $p>0.05$). 2-Way ANOVA used, n=12.

Interestingly, there was no statistical difference in terms of total muscle weight between young and mature mice. This is in line with observable onset of sarcopenic muscle loss in humans and rhesus monkeys (Colman et al., 2005). However, figure 3.1B shows that the percentage of muscle weight relative to total body weight decreased with age in a linear fashion in both fast extensor EDL and slow SOL with the young, mature and elderly groups all showing statistically significant differences ($p<0.05$) between each other. This is likely explained by a gradual accumulation of adipose tissue in our mice cohorts and is evidence of the well documented phenomenon of sarcopenic obesity (Lee et al., 2016b). The increase in adipose tissue is not a marker of sarcopenia, but rather a contributing factor in its onset, which is evident as muscle dysfunction and loss at the terminal stages of the mice lifespan. It is worth noting that weights of SOL are more conserved than EDL in elderly mice. This is evidence of SOL being more resistant of the effects of ageing then EDL, a phenomenon that has been observed before in other mammalian models (Demontis et al., 2013).

3.2.2 Effect of age on SNAT2 and LAT2 transporter protein expression.

Muscle mass is maintained by protein synthesis which in turn requires amino acid transport into muscle cells by amino acid transporters. An age dependent reduction in the expression or function of amino acid transporters such as SNAT2 and LAT2 could lead to a decline in muscle mass. The next experiment therefore analysed the expression of SNAT2 and LAT2 in mice in different age groups. Tissues were extracted and lysed using NP40 buffer and probed by western blot. The figures 3.2A and 3.2B show representative western blots while bar graphs show average expression in three mice calculated from densitometric analysis of blots. The results in figure 3.2 show, that when young mice were compared to elderly mice there was a decrease in the expression SNAT2 (Figure 3.2A) and LAT2 (Figure 3.2B) in both fibre types and in each case the decrease in SNAT2 (~31%) was slightly greater than that of LAT2 (~25%). In contrast the mature mice showed an increase in SNAT2 and LAT2 expression when compared to young or elderly mice.

This increase between young and mature mice may be due to mice of 100 days of age having not yet attained full maturity. As they undergo puberty and experience high levels of testosterone (and by proxy dihydrotestosterone) they will rapidly gain muscle mass, especially fast twitch muscle with increased physical activity. The 100 day old mice, having only reached their peak testosterone production, have not had the same length of time to produce the same quantity of amino acid transporters compared to the mature groups, which have been exposed to higher levels of anabolic stimulus for longer. Therefore, to rule out this anomaly we decided to compare the 300 day old mature mice to the 700+ day elderly mice for the rest of the experiments (Banerjee et al., 2014).

Figure 3.2A Effect of ageing on SNAT2 expression. Fast twitch extensor digitorum longus (EDL) and slow twitch soleus (SOL) muscles were isolated from young mice at ~100 days old, mature mice ~300 days old and elderly mice at over 700 days old. The figure shows a representative western blot while the bar graphs shows average expression calculated from densitometric analysis of blots from separate mice with SNAT2 expression normalised for actin used as a loading control. EDL are represented by white bars and SOL muscle by black bars. * and unmarked groups are statistically indifferent to each other($p>0.05$). Difference between mature EDL (#) to young, and elderly EDL (unmarked) is statistically significant ($p<0.05$) Elderly SOL (+) is significantly smaller to young or mature SOL (*)($p<0.05$). 2-way ANOVA used, n=4.

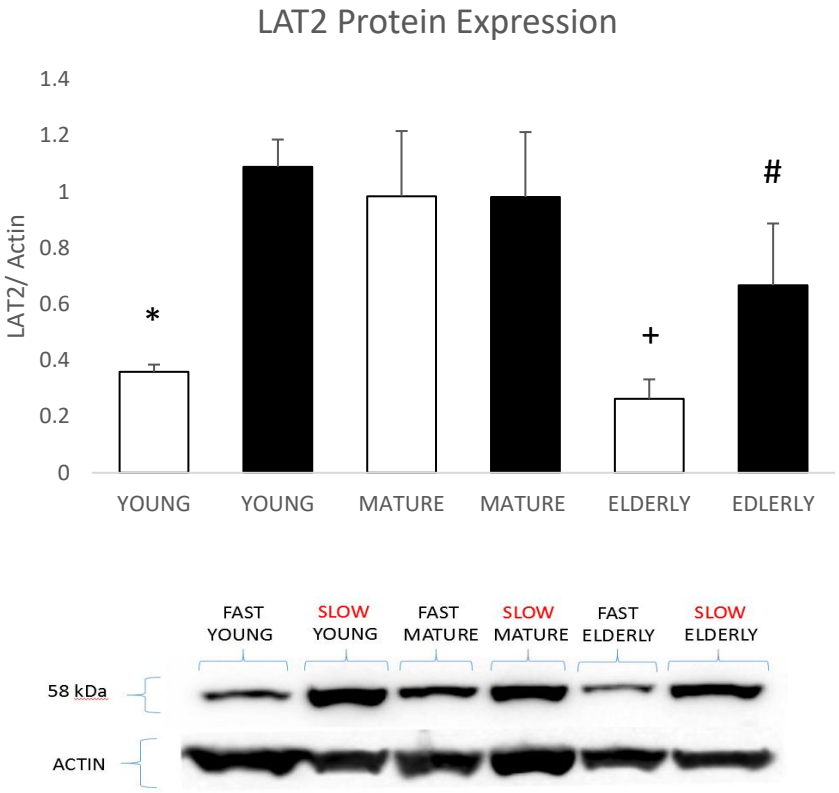

Figure 3.2B Effect of ageing on LAT2 expression. Fast twitch extensor digitorum longus (EDL) and slow twitch soleus (SOL) muscles were isolated from young mice at ~100 days old, mature mice at ~300 days old and elderly mice at over 700 days old. The figure shows a representative western blot while the bar graphs shows average expression calculated from densitometric analysis of blots from separate mice with LAT2 expression normalised for actin used as a loading control. EDL are represented by white bars and SOL muscle by black bars. All unmarked groups are statistically indifferent to each other($p>0.05$). Difference between mature EDL (unmarked) to elderly EDL (+) is statistically significant ($p<0.05$) Elderly SOL (#) is also significantly smaller to both young or mature SOL (unmarked)($p<0.05$). 2-Way ANOVA used with n=4.

3.2.3 Effect of ageing on amino acid transport into muscle

A marked reduction was evident in SNAT2 and LAT2 protein levels when skeletal muscle from mature mice was compared to that of elderly mice as shown in section 3.2. The next step was to determine whether this reduction in expression would translate to reduced amino acid transport into the muscle. In the next experiment the uptake of amino acids into the muscle tissue was assessed by incubating muscle fibres with C_{14} conjugated MeAIB. MeAIB is an N-methylated amino acid analogue that is transported exclusively through the SNAT family of amino acid transporters, in particular SNAT2 (Zhang and Grewer, 2007). Importantly, MeAIB is not a substrate for LAT2 (Yao et al., 2000). Therefore, measuring C_{14}MeAIB uptake into muscle can be used to accurately quantify changes in transport through SNAT2.

Transport through LAT2 was assessed using C_{14}-Isoleucine, a branched chain amino acid conjugated to the C_{14} radioisotope. Isoleucine is one of the preferred substrates for LAT2, (Lingrel and Kuntzweiler, 1994) and importantly, unlike leucine it does not stimulate protein synthesis (Anthony et al., 2000). Fast and slow-twitch muscle fibre bundles were incubated in Ringer's solution (See Buffers 2.1.1) containing C_{14}MeAIB or C_{14}Isoleucine for 1hr, the fibre bundles were washed in PBS and snap frozen in liquid nitrogen, pulverised and lysed with NP40 buffer. The mixture was centrifuged and the supernatant was collected for scintillation counting to assess amino acid transport as described in methods.

Figure 3.3A shows uptake of MeAIB into muscle fibres over one hour as a measure of transport through SNAT2 and shows that SNAT2 transport was significantly reduced in elderly (>700 day) muscle compared to mature (300 days). For fast twitch EDL muscle and slow twitch SOL muscle SNAT2 transport fell by nearly half in the elderly cohorts. The SOL group showed higher transport in both the mature and elderly animals, compared to the respective EDL groups. When the extent of loss from mature to elderly groups were compared statistically there was no significant difference between muscle types, but a trend toward higher remaining function in SOL was observed ($p=0.119$).

Similarly Figure 3.3B shows total transport of C_{14}Isoleucine into the cell. We see the same pattern as before. SOL groups show approximately a third higher uptake than EDL in both age groups. There is a significant ($p<0.05$) decrease in both EDL and SOL with ageing as seen before in C_{14}MeAIB uptake.

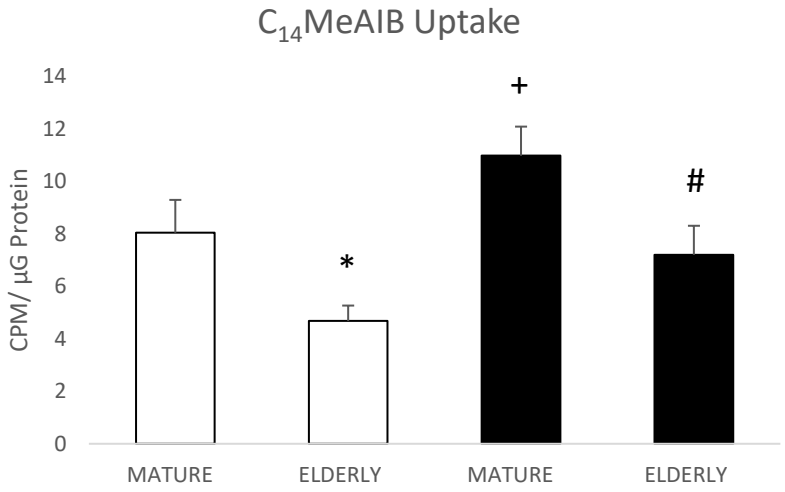

Figure 3.3A Effect of ageing on SNAT2-mediated amino acid transport in muscle fibres. Fast and slow-twitch muscle fibre bundles of ~300 day old (mature) and 700+day old (elderly) CD-1 mice were incubated Ringer's solution containing C_{14}MeAIB for 1hr, the fibre bundles were washed in PBS and snap frozen in liquid nitrogen, pulverised and lysed with NP40 buffer and scintillation counting used to quantify. The white bars represent fast twitch EDL fibres and the black bars represent slow twitch SOL. All groups were statistically different from each other ($p<0.05$). Mature EDL (unmarked) showed a significant difference to elderly EDL (*). Likewise, the elderly SOL (#) showed a significant decline in transport to mature SOL (+) 2-way ANOVA used, n=3.

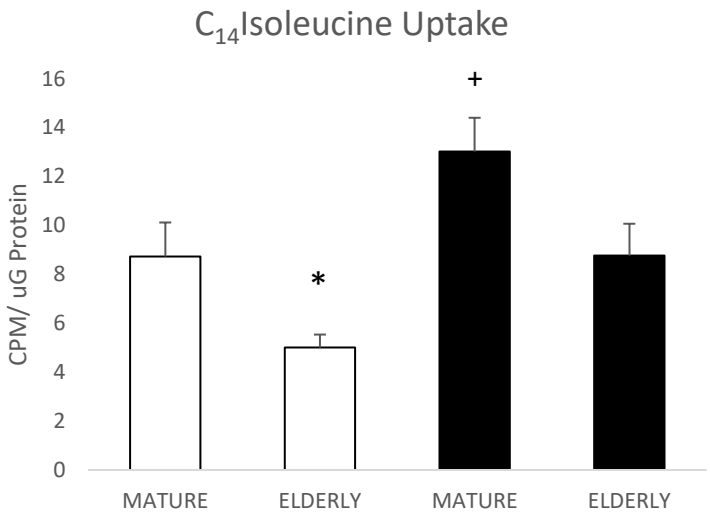

Figure 3.3B Effect of ageing on amino acid LAT2-mediated transport in muscle fibres. Fast and slow-twitch muscle fibre bundles of ~300 day old (mature) and 700+day old (elderly) CD-1 mice were incubated Ringer's solution containing C_{14}Isoleucine for 1hr, the fibre bundles were washed in PBS and snap frozen in liquid nitrogen, pulverised and lysed with NP40 buffer and scintillation counting used to quantify. The white bars represent fast twitch EDL fibres and the black bars represent slow twitch SOL. Unmarked groups (mature EDL and elderly SOL) were statistically indifferent ($p>0.05$). Elderly EDL (*) showed a significant reduction as compared to mature EDL (unmarked) ($p<0.05$). Likewise, the elderly SOL (unmarked) showed a significant decline in transport to mature SOL (+) 2-way ANOVA used, n=3.

3.2.4 The effect of ageing on incorporation of amino acids into protein.

The experiments above (3.2A-B and 3.3A-B) have shown that there was reduced expression of SNAT2 and LAT2 transporters in elderly muscle and this correlated with reduced transport of amino acids through these transporters into muscle fibres 'in vitro'. The next experiment determined if incorporation of amino acids into protein was also compromised with age. Fast and slow-twitch muscle fibre bundles were incubated Ringer's solution containing C_{14} Isoleucine for 1hr, the fibre bundles were washed in PBS and snap frozen in liquid nitrogen, pulverised and lysed with NP40 buffer as before. An additional step was incorporated, the mixture was centrifuged and the supernatant was mixed with ice-cold TCA and acetone to precipitate protein. Precipitates dissolved in KOH were analysed by for incorporation of amino acids by scintillation counting.

The results in figure 3.4 show ageing led to a decrease in protein synthesis in both muscle fibre types when >700 day elderly mice were compared to mature 300 day old mice. The graph also shows that in each case protein synthesis was significantly higher in the slow-twitch than in the corresponding fast-twitch fibres. The loss of amino acid incorporation was greater in the fast-twitch elderly fibres which showed a reduction of 47.33% (±4.92%) compared to mature muscle. The slow muscle fibres on the other hand, showed a reduction of only 30.95% (±5.36%) in protein synthesis compared to mature controls. These results further reinforced the notion that fast twitch muscle is affected to a greater extent than slow twitch muscle during ageing. Slow twitch muscle appears more resistant to ageing, by both retaining greater total muscle weight and retaining function of amino acid transporters. The same trend is shown in the ability of older muscle fibres to incorporate amino acids into protein as shown in fig 3.4.

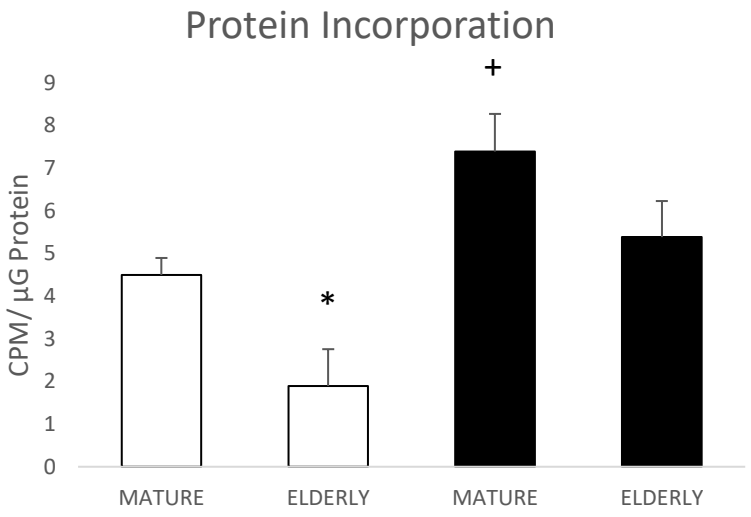

Figure 3.4 Effect of ageing on amino acid incorporation into muscle protein. Fast and slow-twitch muscle fibre bundles were incubated Ringer's solution containing C_{14}Isoleucine for 1hr, the fibre bundles were washed in PBS and snap frozen in liquid nitrogen, pulverised and lysed with NP40 buffer. The mixture was centrifuged and the supernatant was precipitated in TCA and dissolved in KOH. Scintillation counting was used to assess amino acid incorporation into protein. The white bars represent fast twitch EDL fibres and the black bars represent slow twitch soleus. Mature mice were ~300 days old and elderly mice were over 700 days old. Elderly EDL (*) showed a significant reduction to mature EDL (unmarked) ($p<0.05$). Likewise, elderly SOL (unmarked) showed a significant reduction from mature SOL (+)($p<0.05$). 2-way ANOVA used, n=4.

3.2.5 Effect of ageing on SNAT2 and LAT2 mRNA expression

To determine the mechanism underlying this age-dependent decline in SNAT2 protein expression, the effects of age on SNAT2 and LAT2 expression at the mRNA level was investigated. Real Time PCR was performed at 35 cycles for both transporters, using S29 as the house keeper gene. ΔΔCT values are presented as relative mRNA expression to more easily compare proportional levels of expression.

There was a significant ($p<0.05$) decline in SNAT2 mRNA expression with ageing as seen in Fig 3.5B. This reduction in mRNA expression likely contributes to the decline in protein seen with ageing in SNAT2 seen in 3.2A. Fast twitch EDL fibres show that 58.40±3.77% of mRNA expression remains in elderly muscle, while for slow twitch SOL this value is 52.94±2.11%.

As the results displayed in figure 3.5A shows, age had no statistically significant effect on LAT2 mRNA expression. However, there was a trend noticed toward a reduction with ageing which did not reach significance level ($p=0.127$). Fast twitch elderly muscle shows 76.42±4.36% expression, while slow twitch elderly muscle retains 83.59±3.18% expression.

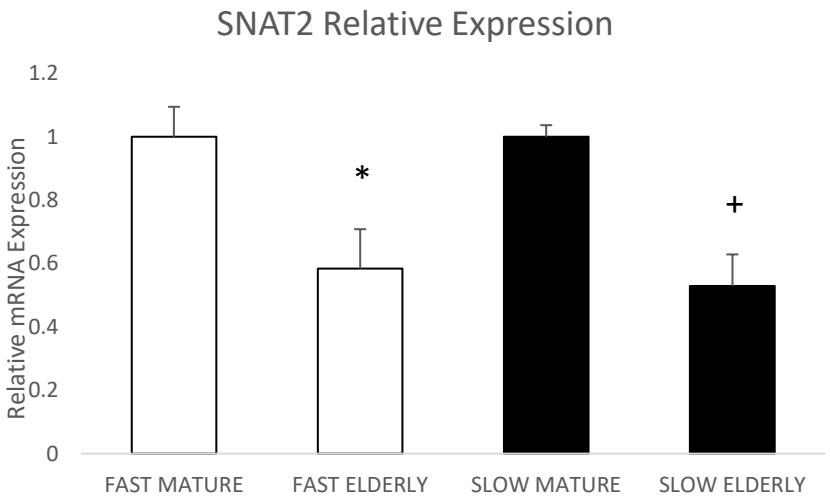

Figure 3.5A. Effect of ageing on SNAT2 mRNA expression. Total RNA was extracted from fast-twitch and slow-twitch muscle fibre bundles using TRIzol® reagent. 1µg of RNA was reverse transcribed and expression of SNAT2 determined after 35 cycles of amplification at 55°C. The white bars represent fast twitch EDL fibres and the black bars represent slow twitch soleus. Mature mice were ~300 days old and elderly mice were over 700 days old. EDL elderly group (*) showed a statistically significant reduction from EDL of mature group (unmarked)($p<0.05$). Likewise SOL elderly (+) mice showed a significant reduction ($p<0.05$) from SOL mature cohort (unmarked). 2-way ANOVA used, n=4.

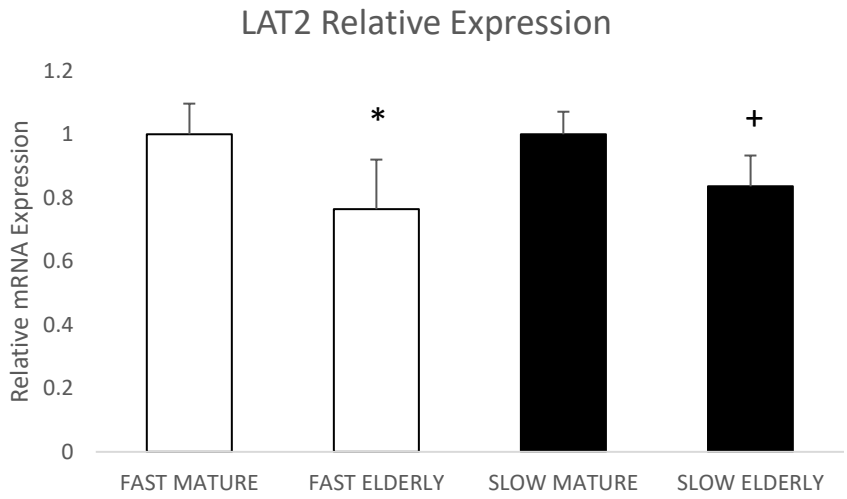

Figure 3.5B. Effect of ageing on LAT2 mRNA expression. Total RNA was extracted from fast-twitch and slow-twitch muscle fibre bundles using TRIzol® reagent. 1µg of RNA was reverse transcribed and expression of SNAT2 determined after 35 cycles of amplification at 55°C. The white bars represent fast twitch EDL fibres and the black bars represent slow twitch soleus. Mature mice were ~300 days old and elderly mice were over 700 days old. EDL elderly group (*) did not show a statistically significant reduction from EDL of mature group (unmarked)(p=0.119). Likewise SOL elderly (+) failed to show a statistically significant reduction (p=0.087) from SOL mature cohort (unmarked). A trend toward reduction was observed in both groups however. 2-way ANOVA used, n=4.

3.3 Discussion

In this chapter, we have shown that ageing has significant and quantifiably detrimental effects on mice skeletal muscle. We have shown that in the aged group, SNAT2 and LAT2 protein levels diminish which can be partly attributed to reductions in mRNA expression shown in Figures 3.5A-B. There was a trend towards reduction of mRNA levels in both SNAT2 and LAT2 with ageing, however only SNAT2 are found to be statistically significant. Note that this corresponds to the reductions in AA transporter protein expression seen in 3.2A and 3.2B.

These results are mirrored by the uptake studies showing a similar degree of reduction in AA transport, suggesting that the phenomenon involved is the reduction in the quantity of functional SNAT2 and LAT2 transporters rather than altered efficacy of transporter activity. It has been shown that the Km of SNAT2 does not change in response to hormonal stimulation, amino acid deprivation, or ageing (Franchi-Gazzola et al., 2006, Kashiwagi et al., 2009).

We have also established that these changes seem to be more profound in the fast twitch fibres then the slow twitch fibres as evidence from the uptake data in fig 3.3A-B and protein incorporation (fig3.4). The predominantly slow twitch fibres of the slow twitch soleus appear to be more resistant to the effects of ageing. This finding is in line with human data showing a trend toward a greater proportion of fibres exhibiting a slow twitch phenotype in elderly patients as compared to young. Elderly patients are found to be expressing myosin heavy chain type I (MHC-I is characteristic of slow twitch fibre) to a much greater extent than young subjects as well as showing evidence of old fibres switching from fast to slow twitch (Andersen, 2003). It is because of this rapid and profound switching that it may be possible to use fibre typing markers to aid the diagnosis of sarcopenia. The slow MLC2 isoform for instance, has been proposed as a possible biomarker indicative of sarcopenia onset (Gannon et al., 2009).

The sharp decline in SNAT2 or LAT2 levels during ageing could also serve as a diagnostic marker, due to the direct link of these AA transporters with muscle protein synthesis and function.

We have identified that SNAT2 and LAT2 are in fact greatly reduced in ageing at a protein level. This is likely manifested as a decrease in functional transporters available for utilisation of AA transport into elderly muscle cells.

It is still unclear why this age-related decline occurs. In the case of SNAT2, we have found a significant decrease in the mRNA of the transporter in elderly mice. This can at least partially explain the reduction in total protein expression of transporter levels seen in the elderly cells. However, in the case of LAT2 there was no statistically significant reduction at the mRNA level with age, although there was a clear trend observed toward reduction in both fibre types. Like in many biological processes, it is likely that the cause behind impaired function of these transporters is multifactorial.

These findings help elucidate an underlying mechanism of sarcopenic muscle dysfunction. As patients lose fast twitch fibres with age, they lack the power to initiate coordinated movements leading to increased risk of falls and greater disability, a hallmark of sarcopenia. To date there is little known about the role of SNAT2 and LAT2 in ageing, but based on the findings herein, it is likely that these amino acid transporters play a significant role.

There is more work needed to find the underlying causes of these changes in AA transport and to assess whether reversing these processes is a viable possibility. We theorise that the determining factor for AA transporter recruitment is a baseline anabolic signal mediated by DHT, the active metabolite of testosterone, that causes the movement of SNAT2 and LAT2 from an intercellular pool and determines the availability of said transporters on the plasma membrane. This theory will be tested in chapter 4.

Limitations of this chapter include the small sizes of animal cohorts, which were due to the high costs of aged animals. The studies were performed only on female CD-1 mice, and only in 1hr durations, with detection only possible at the end of experiments instead of throughout. Mice diet was kept consistent, but mice were not starved prior to sacrifice and dissection.

Table 8.3 Summary of Chapter 3

Baseline Ageing	MATURE FAST	MATURE SLOW	ELDERLY FAST	ELDERLY SLOW
SNAT2 Protein	●●	●●●●	●	●●●
LAT2 Protein	●●●●	●●●●	●	●●
SNAT2 mRNA	●●	●●●●	●	●●
LAT2 mRNA	●●●	●●	●●●	●●
C_{14}MeAIB Transport	●●●	●●●●	●	●●
C_{14}Isoleucine Transport	●●	●●●	●	●●
Protein Synthesis	●●	●●●	●	●●

Table 3.3 Summary of results derived from experiments on effects of ageing alone. Note that these differences are approximations for comparative purposes. We see a significant decline in all parameters tested aside from LAT2 mRNA expression, difference in which did not reach statistical significance.

Chapter 4: Effects of DHT on muscle ageing

4.1 Aim

4.2 Results

4.2.1 Effects of DHT on expression of SNAT2 and LAT2 in aged muscle.

4.2.2 Effects of DHT on transport of amino acids by SNAT2 and LAT2 in aged muscle.

4.2.3 Effects of DHT on incorporation of amino acids into protein in aged muscle.

4.2.4 Effects of chloroquine on DHT-induced increases in amino acid transport by aged muscle.

4.2.5 Effects of low temperature on DHT-induced increases in amino acid transport by aged muscle.

4.2.6 Effect of ageing and DHT on cellular location of SNAT2 in muscle fibres.

4.2.7 Effect of DHT on amino acid transport in C2C12 myoblasts and myotubes.

4.2.7 Effects of DHT and chloroquine on cellular location of SNAT2 in muscle fibres.

4.3 Discussion

4.1 Aim

To determine effect of acute DHT treatment on mature and elderly mice skeletal muscle. To assess whether age related dysfunction in AA transport and protein synthesis can be reversed with DHT treatment.

4.2 Results

4.2.1 Effects of DHT on expression of SNAT2 and LAT2 in aged muscle.

The ability of DHT to affect the expression and/or function of SNAT2 and LAT2 was tested by incubating muscle fibres with DHT for one hour. This time course was chosen to rule out classical genomic effects. Physiological concentrations of DHT were used at equivalent of 600pg/nL (normal biological range of 240-650 pg/nL) (Weng et al., 2010). Expression of SNAT2 and LAT2 protein were assessed by immune blotting of fibres isolated from ~100 day old mice representing young mice, ~300 day old representing fully mature mice, and elderly mice over 700 days old.

The results in chapter 3 (figures 3.2A-B) showed that expression of SNAT2 and LAT2 was reduced in muscle fibres isolated from elderly mice compared to young and mature mice. Figures 4.1A and 4.1B show that this decline in amino acid transporters was reversed when same age mouse fibres were incubated in DHT for one hour. The representative western blots show that muscle fibres of elderly mice treated with DHT express statistically equal levels ($p<0.05$) of SNAT2 protein compared to DHT treated mature mice. This is true in both the SOL and EDL muscles.

In the study of LAT2 protein expression (fig 4.1B) the data shows the average of three western blots normalised to the actin loading control. Levels of LAT2 in EDL fibres are no different in DHT treated elderly muscle than in DHT treated mature muscle. The ability of DHT to rescue LAT2 expression in elderly slow twitch SOL was less pronounced, evidenced by the LAT2 elderly SOL showing lower expression than the mature group ($p<0.05$). This data potentially shows preliminary evidence of the EDL exhibiting a greater response to the DHT treatment than SOL.

As before the young ~100 day old mice are not discussed here due to the high variability of results. Interestingly the fast twitch EDL in young mice is not receptive to DHT treatment, showing expression of both SNAT2 and LAT2 below that of the other ae groups ($p<0.05$). However, the slow twitch SOL of young mice is responsive to DHT treatment, showing the same levels as the other age groups in LAT2 expression.

Further study is needed to elucidate the link in early development and AA transporter expression.

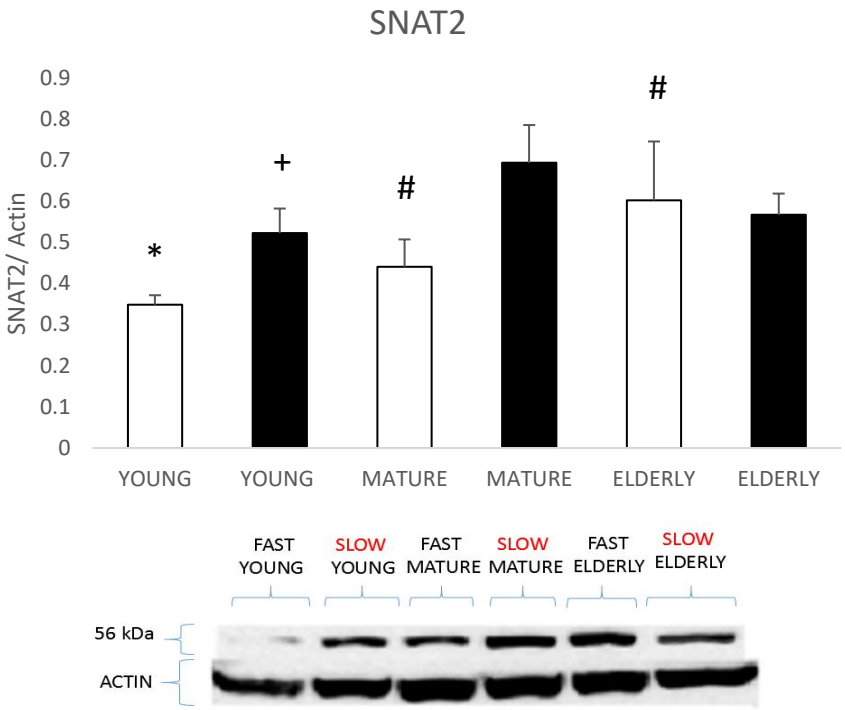

Figure 4.1A Effect of DHT in SNAT2 protein expression in muscle fibres 'in vitro'. Fast twitch extensor digitorum longus (EDL) and slow twitch soleus (SOL) muscles were isolated from: young mice (~100 day old), mature mice (~300 days old) and elderly mice (over 700 days old). Muscles were incubated in Ringers solution with or without DHT for one hour at 37^0C. Fibres were extracted using NP40 buffer and expression of SNAT2 analysed by western blotting. The figure shows a representative western blot while the bar graphs shows average expression calculated from densitometric analysis of blots from three mice with SNAT2 expression normalised for actin used as a loading control actin. EDL is represented by white bars, while SOL is represented by black bars. In fast twitch EDL, the mature (#) and elderly (#) groups were statistically indifferent ($p>0.05$), while the young EDL (*) showed lower expression ($p<0.05$). In the slow twitch SOL, mature (unmarked) and elderly (unmarked) groups were similar ($p=0.069$), while young (+) was lower to mature ($p<0.05$). Two-way ANOVA used, n=3.

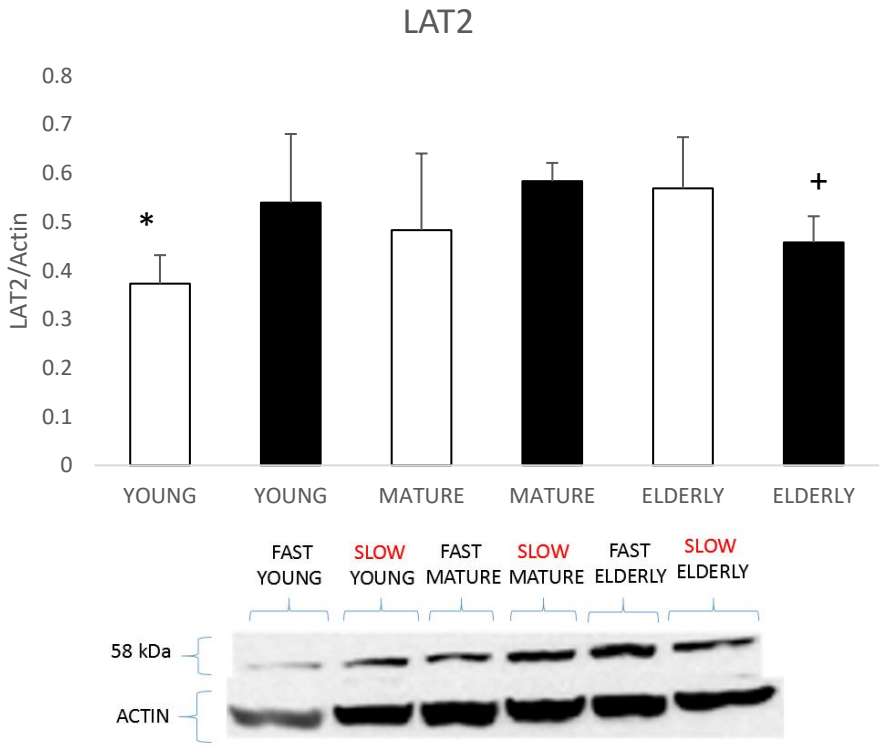

Figure 4.1B Effect of DHT in LAT2 protein expression in muscle fibres 'in vitro'.
Fast twitch extensor digitorum longus (EDL) and slow twitch soleus (SOL) muscles were isolated from: young mice (~100 day old), mature mice (~300 days old) and elderly mice (over 700 days old). Muscles were incubated in Ringers solution with or without DHT for one hour at 37^0C. Fibres were extracted using NP40 buffer and expression of LAT2 analysed by western blotting. The figure shows a representative western blot while the bar graphs shows average expression calculated from densitometric analysis of blots from three mice with LAT2 expression normalised for actin used as a loading control actin. EDL is represented by white bars, while SOL is represented by black bars. In fast twitch EDL group, mature (unmarked) and elderly (unmarked groups were statistically the same ($p>0.05$), whilst the young (*) group showed significantly lower expression ($p<0.05$). In the slow SOL group, the young (unmarked) and mature (unmarked) showed no difference ($p>0.05$), whilst the elderly SOL (+) showed statistically lower LAT2 expression with DHT treatment ($p<0.05$) Two-way ANOVA used, n=3.

4.2.2 Effects of DHT on transport of amino acids by SNAT2 and LAT2 in aged muscle.

The next experiments studied the effect of DHT on uptake of C_{14} conjugated MeAIB and Isoleucine to assess if DHT treatment increased transport through SNAT2 and LAT2 transporters. Figure 4.2A shows uptake of C_{14} conjugated MeAIB as an assay for SNAT2 activity and compares fibres from mature mice (~300 day old) with fibres from elderly mice (over 700 days old). Young mice (~100day old) were not studied from this point forward. In line with the increased levels of SNAT2 protein detected by western blot of elderly fibres incubated with DHT (figure 4.1A), there was evidence for increase in uptake of MeAIB in response to DHT in the elderly cohorts. There was also a trend for increased uptake in mature fibres, but this change was not significant ($p>0.05$).

DHT treatment increased uptake of MeAIB in the elderly mice, and this was most obvious for fast twitch EDL fibres. The DHT treatment rescued the elderly EDL fibres to a level that showed no statistical difference from that of mature treated EDL fibres ($p>0.05$). The percentage increase in transport presented in figure 4.2A shows a 46% increase for elderly EDL fibres with DHT, and only 10% for mature fibres. Slow muscle fibres showed less marked responses to DHT, increasing 21% in elderly and 8% in mature mice (Fig 4.2B).

The experiment was repeated using C_{14}Isoleucine to measure LAT2 transport in figure 4.2C. As before, DHT increased uptake of the radioisotope, and this was most profound in the elderly EDL. As with MeAIB uptake, the fast EDL of the elderly group showed no difference to the fast EDL of mature controls ($p>0.05$). This again suggested that the age-related reduction in LAT2 transport was reversed with DHT treatment. The % increase in transport from data in fig 4.2C shows a 72% increase for elderly EDL fibres with treatment, and only 9% for mature fibres. Slow muscle fibres (fig 4.2D) showed less marked responses to DHT of 17% in elderly and 0.2% in mature.

As before, these experiments offer strong evidence that the response to DHT is far greater in the elderly muscle than mature. Also, fast EDL is more responsive to treatment than SOL, shown by the percentage increase figures from the data.

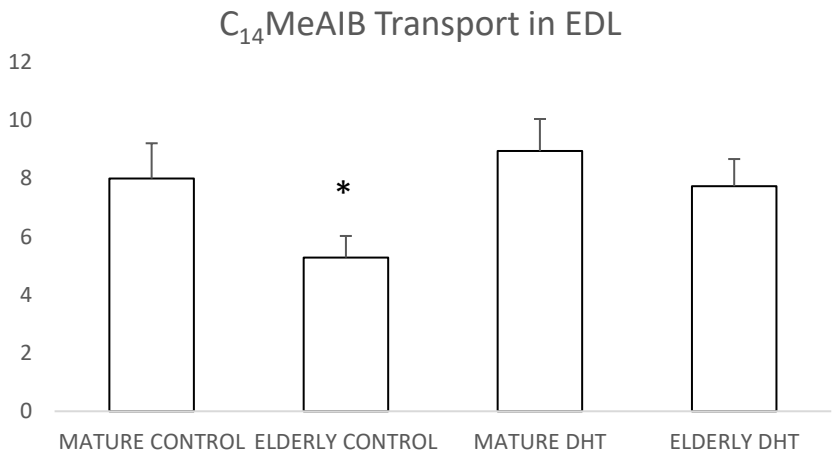

Figure 4.2A. Effect of DHT on C_{14}MeAIB transport in EDL muscle fibres 'in vitro'. Fast twitch muscle fibre bundles were incubated Ringer's solution containing DHT and C_{14} MeAIB for 1hr, the fibre bundles were washed in PBS and snap frozen in liquid nitrogen, pulverised and lysed with NP40 buffer. The mixture was centrifuged and the supernatant was collected for scintillation counting to assess amino acid transport. Mature mice were ~300 days old and elderly mice were over 700 days old. Only statistical difference was found in elderly controls (*) which were significantly reduced ($p<0.05$) compared to mature control, mature DHT and elderly DHT (all unmarked). 1-way ANOVA used, n=4.

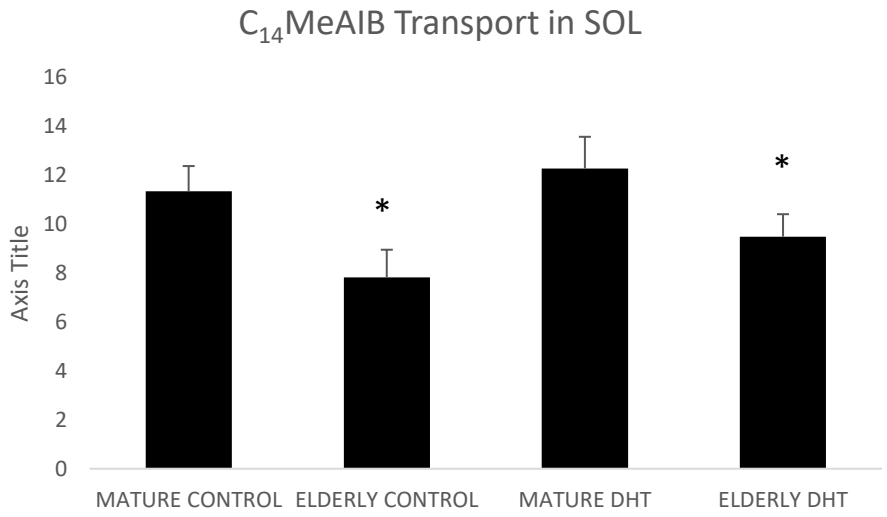

Figure 4.2B. Effect of DHT on C_{14}MeAIB transport in SOL muscle fibres 'in vitro'. Slow twitch muscle fibre bundles were incubated Ringer's solution containing DHT and C_{14} MeAIB for 1hr, the fibre bundles were washed in PBS and snap frozen in liquid nitrogen, pulverised and lysed with NP40 buffer. The mixture was centrifuged and the supernatant was collected for scintillation counting to assess amino acid transport. Mature mice were ~300 days old and elderly mice were over 700 days old. Although there was a trend seen toward increase in both groups, DHT treatment did not result in statistically significant increases ($p<0.05$) in either mature or elderly SOL. 1-way ANOVA used, n=4.

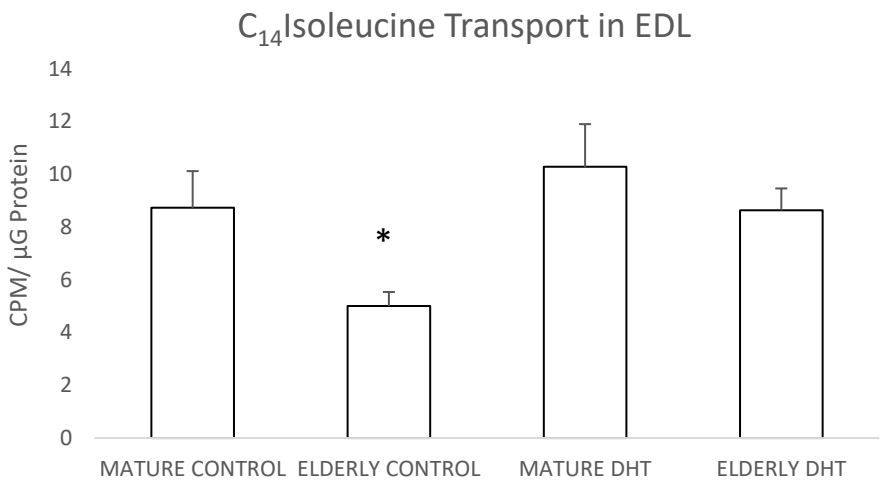

Figure 4.2A. Effect of DHT on C_{14}Isoleucine transport in EDL muscle fibres 'in vitro'. Fast twitch muscle fibre bundles were incubated Ringer's solution containing DHT and C_{14} MeAIB for 1hr, the fibre bundles were washed in PBS and snap frozen in liquid nitrogen, pulverised and lysed with NP40 buffer. The mixture was centrifuged and the supernatant was collected for scintillation counting to assess amino acid transport. Mature mice were ~300 days old and elderly mice were over 700 days old. Only statistical difference was found in elderly controls (*) which were significantly reduced ($p<0.05$) compared to mature control, mature DHT and elderly DHT (all unmarked). 1-way ANOVA used, n=4.

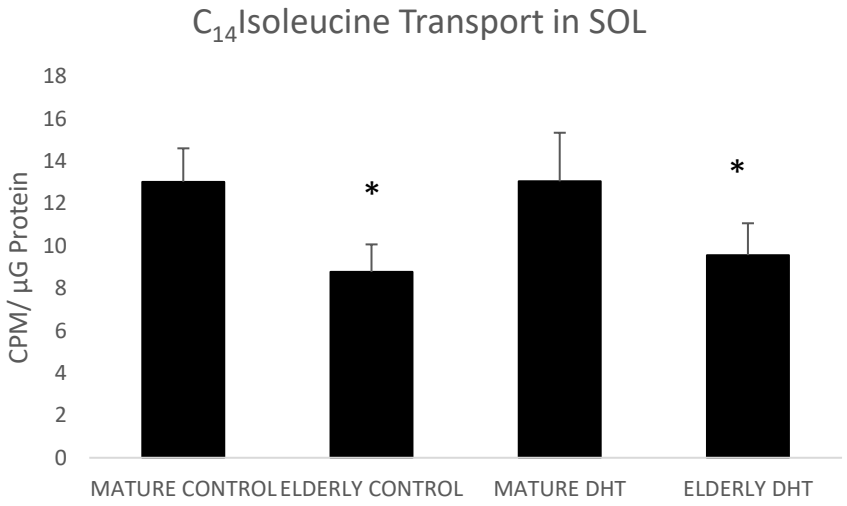

Figure 4.2B. Effect of DHT on C_{14}Isoleucine transport in SOL muscle fibres 'in vitro'. Slow twitch muscle fibre bundles were incubated Ringer's solution containing DHT and C_{14} MeAIB for 1hr, the fibre bundles were washed in PBS and snap frozen in liquid nitrogen, pulverised and lysed with NP40 buffer. The mixture was centrifuged and the supernatant was collected for scintillation counting to assess amino acid transport. Mature mice were ~300 days old and elderly mice were over 700 days old. There was a trend seen toward increase in elderly group (*), but DHT treatment did not result in statistically significant increases ($p<0.05$) in either the mature or elderly SOL. 1-way ANOVA used, n=4.

4.2.3 Effects of DHT on incorporation of amino acids into protein in aged muscle.

The work in chapter 3 showed that incorporation of amino acids into protein was reduced in muscle fibres from elderly mice compared to those of mature aged mice (figure 3.4). The possibility that the increased activity of SNAT2 and LAT2 might increase amino acid incorporation into muscle protein was tested by analysing incorporation of radioactive isoleucine into TCA-insoluble material. Figure 4.3A shows that DHT increased incorporation of radioactive isoleucine into protein, and that DHT restored levels of incorporation in elderly EDL muscles to levels seen in mature muscle fibres.

The percentage increase in incorporation seen in the fast twitch EDL (fig 4.3A) fibres showed an impressive 72% increase in the elderly cohort, compared to only 17% increase for the control mature fibres. The percentage increase resulting from DHT treatment was significantly greater for elderly fibres compared to mature muscle fibres, as seen with in AA transport in figures 4.2A-D. Slow muscle fibres (fig 4.3B) showed a less marked responses to DHT at increases of 15% in the elderly SOL cohort and only 0.1% in the mature SOL. This data correlates with the previous experiments measuring C_{14}MeAIB and C_{14}Isoleucine transport. This data offers evidence that DHT treatment can rescue the age-related deficits in both AA transport and subsequent protein synthesis, at least in the fast twitch EDL fibres.

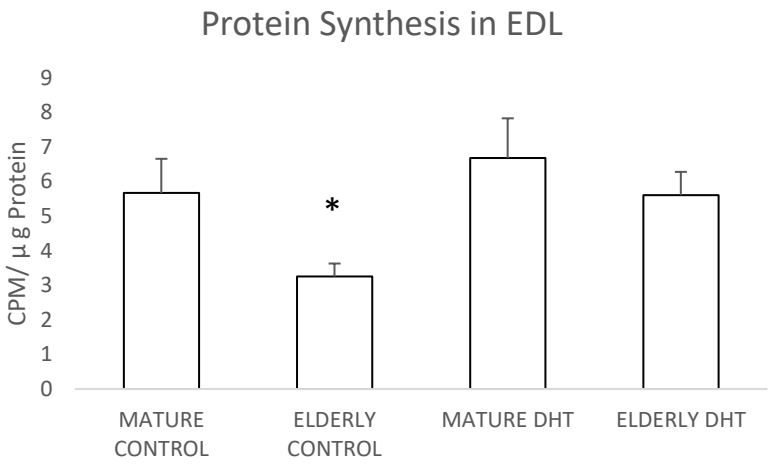

Figure 4.3A. Effect of DHT on incorporation of isoleucine into protein in fast and slow by muscle fibres 'in vitro'. Fast twitch muscle fibre bundles were incubated in Ringer's solution containing DHT and C_{14}Isoleucine for 1hr, the fibre bundles were washed in PBS and snap frozen in liquid nitrogen, pulverised and lysed with NP40 buffer. The mixture was centrifuged and the supernatant was precipitated with TCA for scintillation counting to assess amino acid incorporation into protein. Mature mice were ~300 days old and elderly mice were over 700 days old. Only statistical difference was found in elderly controls (*) which were significantly reduced ($p<0.05$) compared to mature control, mature DHT and elderly DHT (all unmarked). 1-way ANOVA used, n=4.

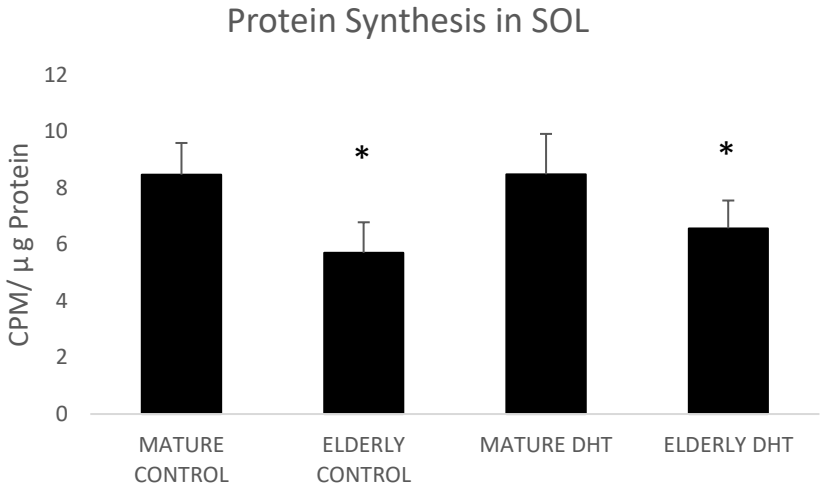

Figure 4.3B. Comparison of effect of DHT on incorporation of isoleucine into protein in fast and slow by muscle fibres 'in vitro'. Slow twitch muscle fibre bundles were incubated in Ringer's solution containing DHT and C_{14}Isoleucine for 1hr, the fibre bundles were washed in PBS and snap frozen in liquid nitrogen, pulverised and lysed with NP40 buffer. The mixture was centrifuged and the supernatant was precipitated with TCA for scintillation counting to assess amino acid incorporation into protein. Mature mice were ~300 days old and elderly mice were over 700 days old. There was a trend seen toward increase in elderly group (*), but DHT treatment did not result in statistically significant increases ($p<0.05$) in either the mature or elderly SOL. 1-way ANOVA used, n=4.

4.2.4 Effects of chloroquine on DHT-induced increases in amino acid transport by aged muscle.

Taken together the results show that incubation of elderly fibres 'in vitro' with DHT is in some way able to increase levels of transporters extracted through our lysis method (Figures 4.1A-B) as well as increase activity of SNAT2 and LAT2 transporters and protein synthesis. This increase in activity brings the elderly EDL muscles to the same levels as mature muscle (Fig 4.2B, 4.2D, 4.3B). One possible explanation for these results is that DHT is able to change the cellular distribution of amino acid transporters so that they are more susceptible to extraction with mild detergent and have better access to extracellular amino acids. One mechanism could involve movement of intracellular pool of transporters to the plasma membrane with consequent increased sensitivity to extraction by NP40.

To test this hypothesis, experiments were repeated in the presence of chloroquine, a known blocker of vesicular recruitment (Chapman and Munro, 1994, Kashiwagi et al., 2009). The effects of chloroquine on SNAT2 activity assessed using C_{14}MeAIB are shown in figures 4.4A-B. In these experiments the concentration of DHT was doubled over physiological levels to 4nM. A higher concentration of DHT was chosen because all animals used are at an age of ~300 days, which we have shown do not elicit a statistical upregulation at physiological doses of DHT.

Chloroquine alone did not affect baseline amino acid transport. As shown before, DHT increased uptake of C_{14}MeAIB ($p<0.05$), and this increase was reversed by chloroquine in both fast and slow twitch muscle fibres. Chloroquine treated tissues showed no difference to baseline controls, suggesting that the accumulation of transporters as well as recycling back into storage compartments were blunted.

Figure 4.4C-D show the same experiment for the uptake of C_{14}Isoleucine to assess LAT2 activity. DHT increased the uptake of C_{14}Isoleucine as expected and this was blocked by chloroquine in both fast and slow twitch muscle fibres. As before, chloroquine abolished the DHT effect completely and chloroquine treatment alone was equal to the uptake seen with controls ($p>0.05$). A combination of CQ and DHT still blunted the DHT effect and was equal to baseline untreated control ($p>0.05$).

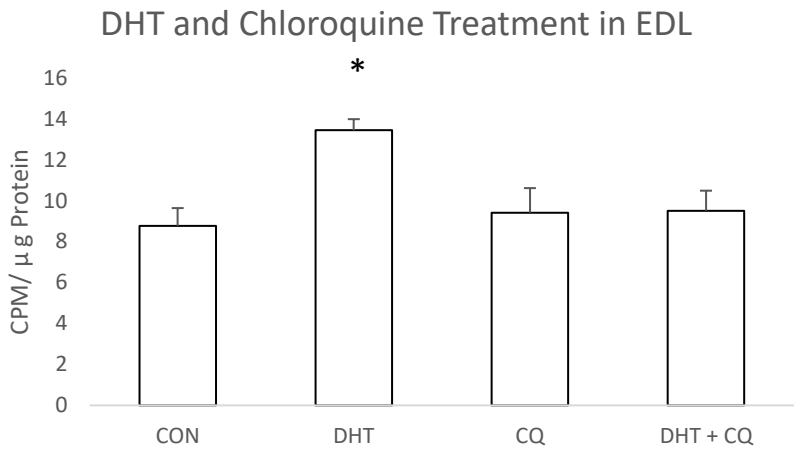

Figure 4.4A Effect of chloroquine on DHT induced elevation of C_{14}MeAIB transport by EDL muscle fibres 'in vitro'. Fast twitch EDL muscle fibre bundles were incubated Ringer's solution containing C_{14}MeAIB for 1hr, in the presence or absence of chloroquine (CQ) and DHT as indicated. The fibre bundles were washed in PBS and snap frozen in liquid nitrogen, pulverised and lysed with NP40 buffer. The mixture was centrifuged and the supernatant was collected for scintillation counting to assess amino acid transport. Mature mice were used at ~300 days old. Only DHT cohort (*) was found statistically different ($p<0.05$) to control, CQ, and DHT+CQ (unmarked). 1-way ANOVA used, n=3.

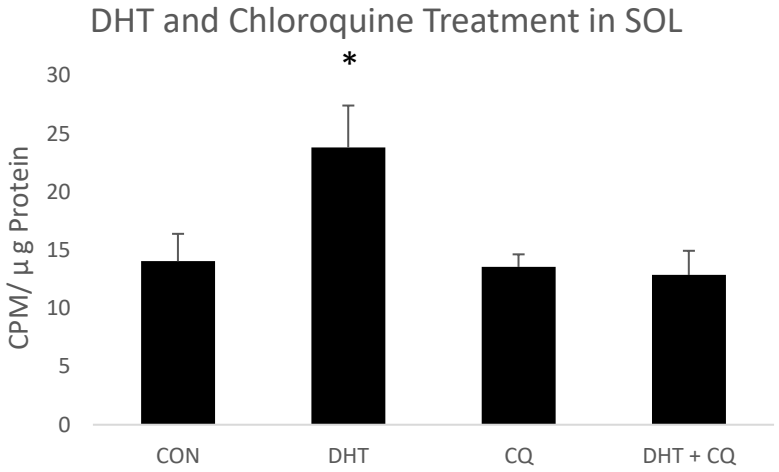

Figure 4.4B Effect of chloroquine on DHT induced elevation of C_{14}MeAIB transport by SOL muscle fibres 'in vitro'. Slow twitch SOL muscle fibre bundles were incubated Ringer's solution containing C_{14}MeAIB for 1hr, in the presence or absence of chloroquine (CQ) and DHT as indicated. The fibre bundles were washed in PBS and snap frozen in liquid nitrogen, pulverised and lysed with NP40 buffer. The mixture was centrifuged and the supernatant was collected for scintillation counting to assess amino acid transport. Mature mice were used at ~300 days old. As before, only DHT cohort (*) was found statistically different ($p<0.05$) to control, CQ, and DHT+CQ (unmarked). 1-way ANOVA used, n=3.

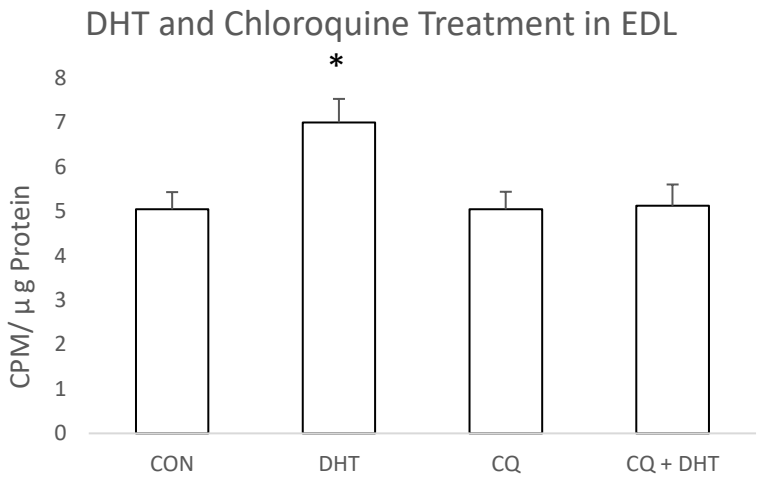

igure 4.4A Effect of chloroquine on DHT induced elevation of C_{14}Isoleucine transport by EDL muscle fibres 'in vitro'. Fast twitch EDL muscle fibre bundles were incubated Ringer's solution containing C_{14}Isoleucine for 1hr, in the presence or absence of chloroquine (CQ) and DHT as indicated. The fibre bundles were washed in PBS and snap frozen in liquid nitrogen, pulverised and lysed with NP40 buffer. The mixture was centrifuged and the supernatant was collected for scintillation counting to assess amino acid transport. Mature mice were used at ~300 days old. Only DHT cohort (*) was found statistically different ($p<0.05$) to control, CQ, and DHT+CQ (unmarked). 1-way ANOVA used, n=3.

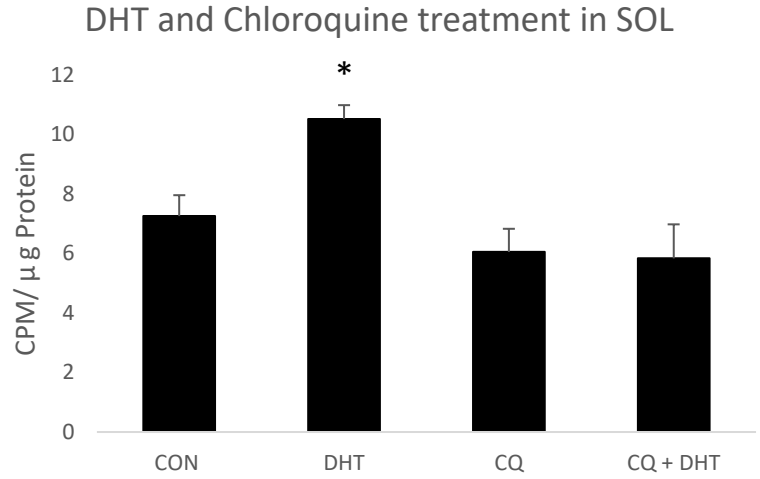

Figure 4.4B Effect of chloroquine on DHT induced elevation of C_{14}Isoleucine transport by SOL muscle fibres 'in vitro'. Slow twitch SOL muscle fibre bundles were incubated Ringer's solution containing C_{14}Isoleucine for 1hr, in the presence or absence of chloroquine (CQ) and DHT as indicated. The fibre bundles were washed in PBS and snap frozen in liquid nitrogen, pulverised and lysed with NP40 buffer. The mixture was centrifuged and the supernatant was collected for scintillation counting to assess amino acid transport. Mature mice were used at ~300. DHT cohort (*) was found statistically different ($p<0.05$) to control, CQ, and DHT+CQ (unmarked). 1-way ANOVA used, n=3.

4.2.5 Effects of low temperature on DHT-induced increases in amino acid transport by aged muscle.

The transport of intracellular receptors can be blocked by lowered temperature. It has been previously shown that temperatures of 4°C block membrane transport and pathways such as endocytosis are halted completely at this temperature(Wilson and King, 1986) The effects of incubation at 4°C on increased SNAT2 and LAT2 activity induced by DHT was compared to control conditions of 22°C. This was run over the course of 2hr instead of the usual 1hr. The ice-cold experiment would determine what portion of the increase in amino acid transport could be attributed to only SNAT2 and LAT2 transport as opposed to diffusion or any other unforeseen transport mechanism. Thus, this was done as an additional control to determine if the amino acid uptake observed was real.

Figure 4.5 shows again that DHT increased uptake of MeAIB at 22°C in both fast and slow twitch muscle and that uptake of MeIAB was greatly reduced at 4°C. In fact radioactive signals were barely above baseline when the experiment was carried out at 4°C. The bulk of amino acid transport seen in the assay could therefore be attributed mainly to active transport through SNAT2 and Lat2 rather than adsorption of radioactive amino acids to the tissue or any other form of transport into the tissue.

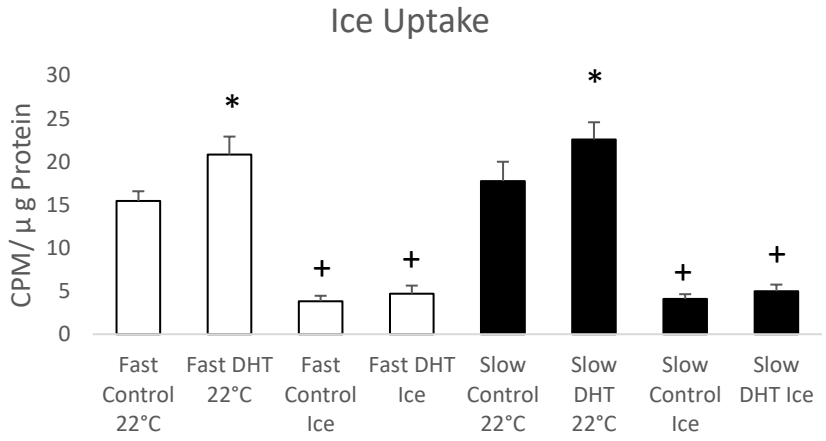

Figure 4.5 Effect of low temperature on isoleucine transport by muscle fibres 'in vitro'. Fast and slow-twitch muscle fibre bundles were incubated Ringer's solution containing C_{14}Isoleucine for 2hr, and incubated with DHT, either at room temperature (22^0C) or 4^0C as indicated. The fibre bundles were washed in PBS and snap frozen in liquid nitrogen, pulverised and lysed with NP40 buffer. The mixture was centrifuged and the supernatant was collected for scintillation counting to assess amino acid transport. The white bars represent fast twitch EDL fibres and the black bars represent slow twitch soleus. 2-Way ANOVA used, n=3.

4.2.6 Effect of DHT on cellular location of SNAT2 in muscle fibres

Elderly and mature tibialis anterior fibre bundles were incubated in Ringer's solution in the absence and presence of 2nM DHT as indicted. The fibre bundles were snap frozen, sectioned and adsorbed onto slides for use in immunofluorescence microscopy. Figures 4.6B-C show mixed muscle (TA) from mature (~300 day old) mice. Figures 4.6D-E show mixed muscle from elderly (700 day old) mice. Regions of interest are shown at higher magnification.

Quantification of the data using pixel densitometry is show in figure 4.6A. Image J was used to quantify the signal at the plasma membrane and the data analysed. The densitometry confirms both the SNAT2 protein expression and C_{14}MeAIB uptake data. Elderly TA fibres treated with DHT are statistically the same as mature control, suggesting reversal of SNAT2 dysfunction with DHT in the aged muscle.

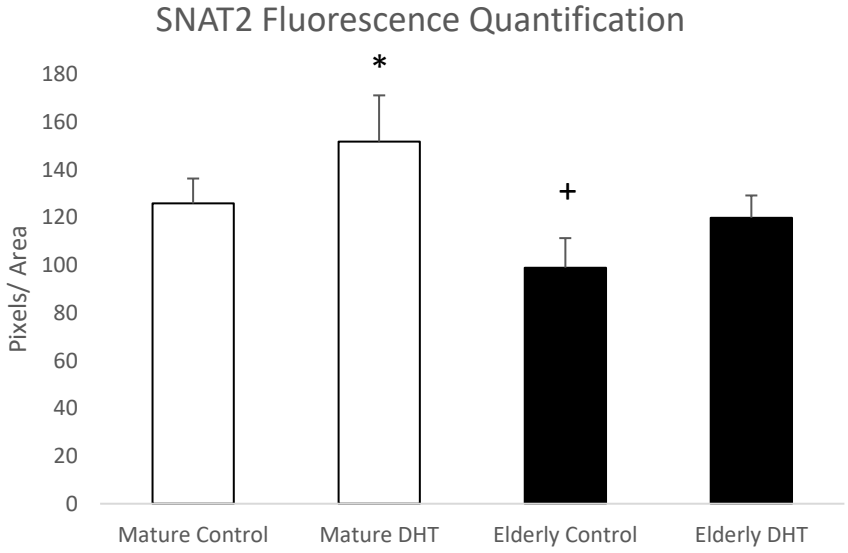

Figure 4.6A Effect of DHT on cellular location of SNAT2 in muscle fibres 'in vitro' densitometry quantification. Tibialis anterior muscle fibre bundles from 3 different mice were incubated for an hour in Ringer's solution in the absence (Control) or presence of DHT. The fibre bundles were snap frozen, sectioned and adsorbed onto slides for immunofluorescence microscopy. The images were then quantified for magnitude of signal at the plasma membranes using ImageJ. Although a trend toward increase is seen, statistically there is no change in the mature groups response to DHT treatment (*) ($p>0.05$). Elderly DHT (unmarked) shows a significant increase ($p<0.05$) with DHT treatment from untreated elderly (+). Elderly DHT (unmarked) shows no difference to mature control group (unmarked) ($p=0.137$). 1-way ANOVA used, n=3.

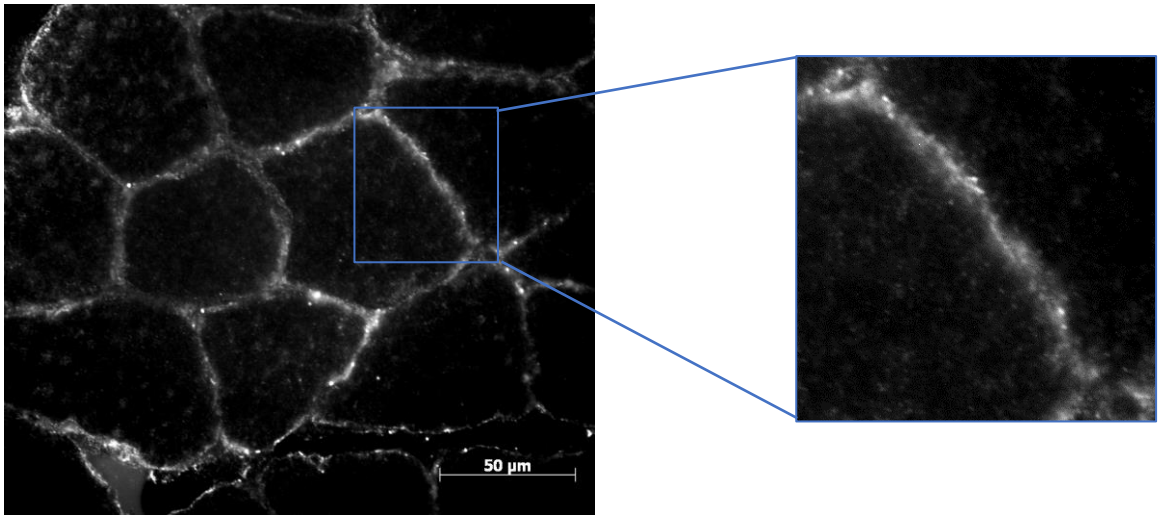

Figure 4.6B Effect of DHT on cellular location of SNAT2 in mature muscle fibres 'in vitro'. Tibialis anterior muscle fibre bundles from mature (300 day old) mice were incubated for an hour in Ringer's solution in the absence of DHT. The fibre bundles were snap frozen, sectioned and adsorbed onto slides for immunofluorescence microscopy. Representative image.

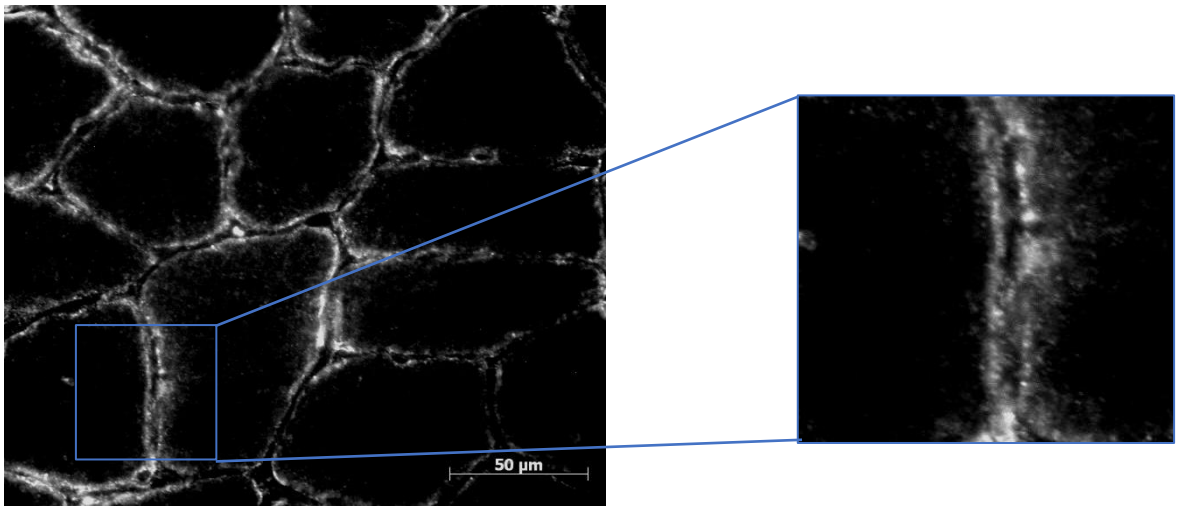

Figure 4.6C Effect of DHT on cellular location of SNAT2 in mature muscle fibres incubated with DHT 'in vitro'. Tibialis anterior muscle fibre bundles from mature (300 day old) mice were incubated for an hour in Ringer's solution in the presence of 4nM DHT. The fibre bundles were snap frozen, sectioned and adsorbed onto slides for immunofluorescence microscopy. Representative image.

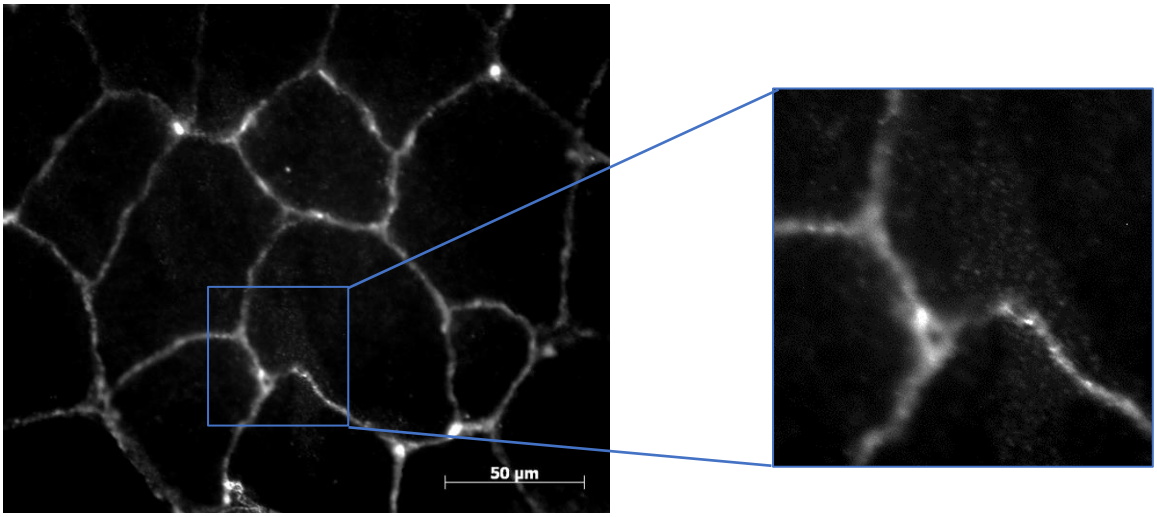

Figure 4.6D Effect of DHT on cellular location of SNAT2 in elderly skeletal muscle fibres 'in vitro'. Tibialis anterior muscle fibre bundles from elderly (+700 day old) mice were incubated for an hour in Ringer's solution in the absence of DHT. The fibre bundles were snap frozen, sectioned and adsorbed onto slides for immunofluorescence microscopy. Representative image.

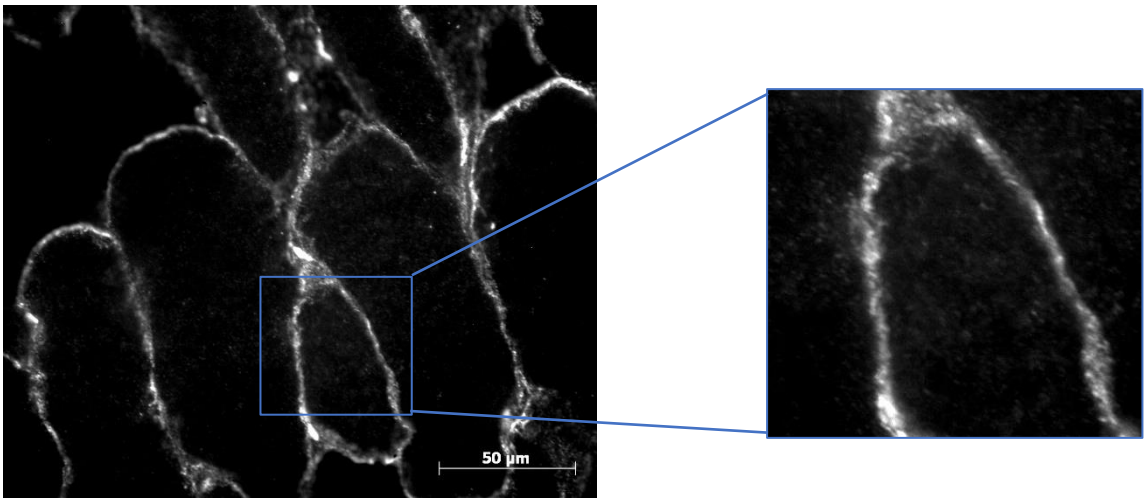

Figure 4.6E Effect of DHT on cellular location of SNAT2 in elderly skeletal muscle fibres incubated with DHT 'in vitro'. Tibialis anterior muscle fibre bundles from elderly (+700 day old) mice were incubated for an hour in Ringer's solution in the presence of 4nM DHT. The fibre bundles were snap frozen, sectioned and adsorbed onto slides for immunofluorescence microscopy. Representative image.

4.2.7 Analysis of effects of DHT on C2C12 myoblasts and myotubes.

The experiments to this point have analysed muscle fibres. However, a typical muscle fibre is not homozygous in cell type throughout and the tissue lysates used in previous experiments consist of a mixture of both satellite progenitor cells, collagen, smooth muscle, plasma cells as well as fully formed muscle fibres. The aim of the next experiments was to see if the data observed in tissue could be replicated in the C2C12 skeletal myoblast cell line. If successful, the cell line could be used for cell biology experiments based on exogenous gene expression and gene silencing to probe mechanisms further.

C2C12 cells are similar in structure and function to commited skeletal myoblasts.These cells arise from the activation of satellite cells, which lie underneath the basal lamina of skeletal muscle and are triggered during injury (Le Grand and Rudnicki, 2007). As discussed before, these are critical for the regeneration and repair of skeletal muscle. The myoblast strain used here will serve to simulate the response of myoblasts alone to treatment with DHT. Myoblasts incubated in MEM with 2% horse serum differentiate into myotubes. This is because of the different proportion of growth factors present in horse serum compared to normal growth media and the sudden reduction in the concentration of growth factors initiates the differentiation into myotubes (Lawson and Purslow, 2000). Myotubes behave very much like mature myofibers, reacting to electrical stimuli with contraction although not as sustained and rapidly fatiguing. They serve as a model for the effects of DHT on skeletal muscle cells alone. Chloroquine has been extensively shown to inhibit vesicular trafficking (Puertollano and Alonso, 1999, Kashiwagi et al., 2009). CQ was used in the following experiments to test whether DHT was working through vesicle recruitment to increase SNAT2 and LAT2 transport. Flutamide (FLU) is a potent selective, competitive silent antagonist of the androgen receptor (Sarrabay et al., 2015). It was used to ascertain whether the DHT response is mediated through an AR element or through some other non-genomic receptor. Figures 4.7A-B show the effects of DHT, FLU, CQ, CQ + DHT and FLU + DHT on uptake of C_{14}MeAIB (fig 4.7A) and C_{14}Isoleucine (fig 4.7B). The same interventions are tested in myotubes shown in figures 4.7C-D on the uptake of C_{14}MeAIB (fig 4.7C) and C_{14}Isoleucine (fig 4.7D).

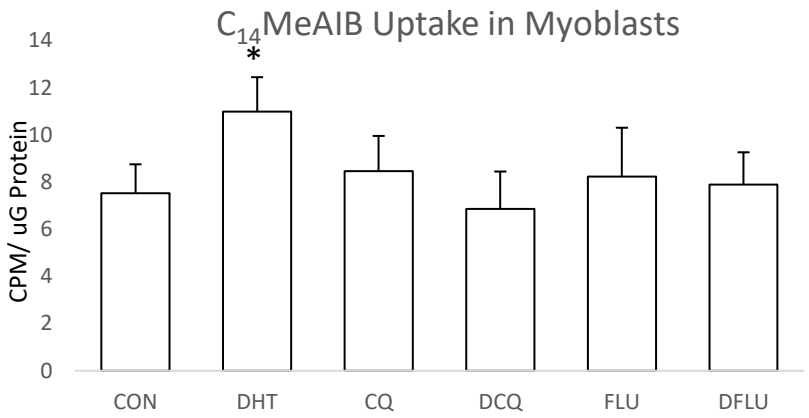

Figure 4.7A Effect of DHT, Flutamide and Chloroquine on C_{14}MeAIB Uptake in myoblasts. Myoblasts were incubated in full media with C_{14}MeAIB over one hour with 1 hr prior pre-incubation of antagonists (CQ and FLU) without radioisotope. Incubation and experiment ran at 37°C. Cell wells washed in PBS and snap frozen in liquid nitrogen, pulverised and lysed with NP40 buffer. The mixture was centrifuged and the supernatant was collected for scintillation counting to assess amino acid transport. Only group showing significant difference ($p<0.05$) from control is DHT treatment alone(*). Chloroquine treatment group (CQ) shows no difference to DHT + Chloroquine (DCQ). Flutamide (FLU) also abolishes the DHT mediated increase in transport, showing no difference to control (CON) or DHT + flutamide (DFLU)(unmarked). 1-way ANOVA used, n=3.

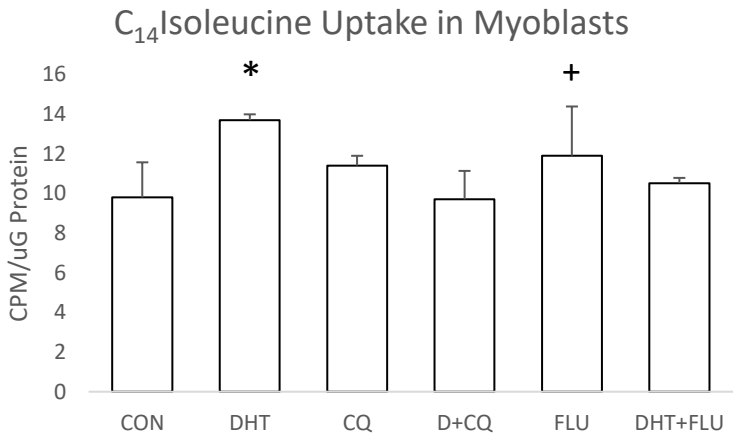

Figure 4.7B Effect of DHT, Flutamide and Chloroquine on C_{14}Isoleucine Uptake in myoblasts. Myoblasts were incubated in full media with C_{14} Isoleucine over one hour with 1 hr prior pre-incubation of antagonists (CQ and FLU) without radioisotope. Incubation and experiment ran at 37°C. Cell wells washed in PBS and snap frozen in liquid nitrogen, pulverised and lysed with NP40 buffer. The mixture was centrifuged and the supernatant was collected for scintillation counting to assess amino acid transport. DHT treatment alone(*) showed significance ($p<0.05$) to all other groups (unmarked) except Flutamide (FLU, +)($p>0.05$). Chloroquine treatment group (CQ) shows no difference to DHT + Chloroquine (DCQ)($p>0.05$). Flutamide (FLU, +) shows no difference to any groups ($p>0.05$). 1-way ANOVA used, n=3.

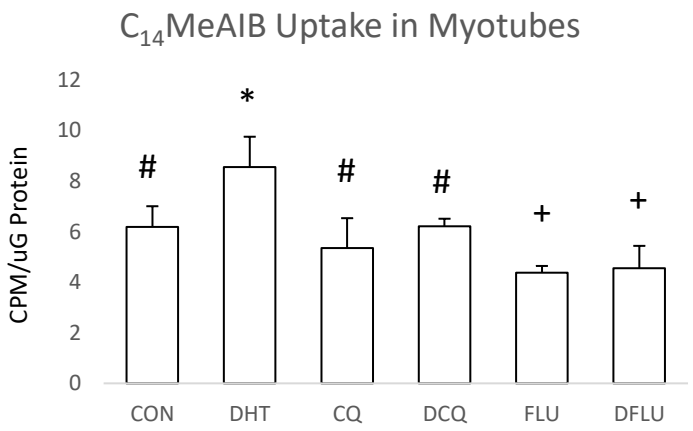

Figure 4.7C Effect of DHT, Flutamide and Chloroquine on C_{14}MeAIB Uptake in myoblasts. Myoblasts were incubated in full media with C_{14}MeAIB over one hour with 1 hr prior pre-incubation of antagonists (CQ and FLU) without radioisotope. Incubation and experiment ran at 37°C. Cell wells washed in PBS and snap frozen in liquid nitrogen, pulverised and lysed with NP40 buffer. The mixture was centrifuged and the supernatant was collected for scintillation counting to assess amino acid transport. DHT treatment alone (*) was significantly higher then all other groups(# and + $p<0.05$) . Chloroquine treatment group (CQ,#) shows no difference to DHT + Chloroquine (DCQ,#) nor control (#)($p>0.05$). Flutamide (FLU +) also abolishes the DHT mediated increase in transport, showing reduction from # and * groups ($p<0.05$) but no difference to DHT+FLU (DFLU +)($p>0.05$). 1-way ANOVA used, n=3.

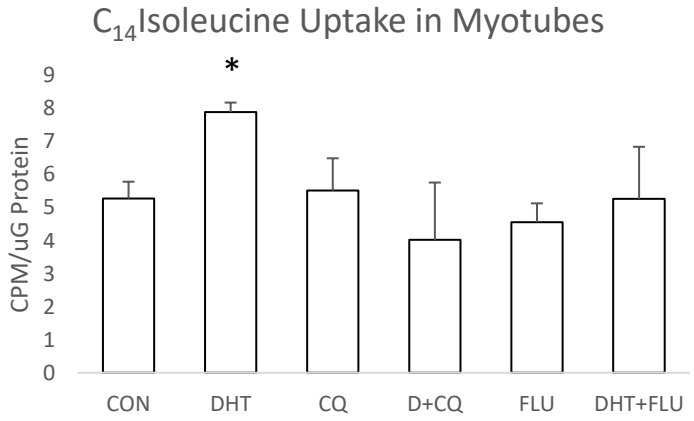

Figure 4.7D Effect of DHT, Flutamide and Chloroquine on C_{14}Isoleucine Uptake in myotubes. Myotubes were incubated in full media with C_{14} Isoleucine over one hour with 1 hr prior pre-incubation of antagonists (CQ and FLU) without radioisotope. Incubation and experiment ran at 37°C. Cell wells washed in PBS and snap frozen in liquid nitrogen, pulverised and lysed with NP40 buffer. The mixture was centrifuged and the supernatant was collected for scintillation counting to assess amino acid transport. DHT treatment alone(*) showed significance ($p<0.05$) to all other groups (unmarked). Chloroquine treatment group (CQ unmarked) shows no difference to DHT + Chloroquine (DCQ unmarked) nor control (CON unmarked) ($p>0.05$). Flutamide (FLU, unmarked) shows no difference to control (CON unmarked) ($p>0.05$). 1-way ANOVA used, n=3.

4.2.8 Fluorescence imaging of SNAT2 and LAT2 localisation with DHT and Chlorquine treatment

To assess the impact of CQ on SNAT2 localisation, TA muscle sections from mature mice were stained for SNAT2. Densitometry was used to compare the effects of no treatment to 4nM DHT, chloroquine and 4nM DHT + chloroquine. The densitometry quantification of the imaging results in figure 4.2A confirm the previous AA uptake and western blotting data. This serves as further evidence that DHT likely increases the quantity of functional SNAT2 transporters on the plasma membrane of skeletal muscle. Chloroquine inhibits vesicle trafficking and recruitment by increasing vesicular pH and directly abolishes the DHT effect (Puertollano and Alonso, 1999, Kashiwagi et al., 2009). This effect can be seen by the absence of increased total plasma membrane signal of SNAT2 as compared to controls in 4.8B.

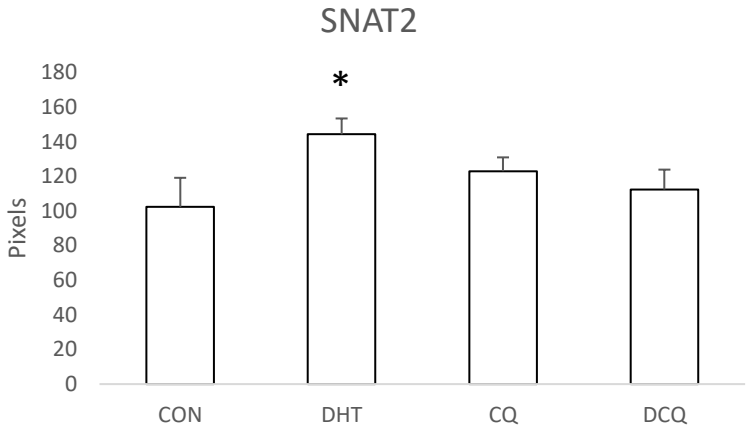

4.8A Effect of DHT and CQ on cellular location of SNAT2 in muscle fibres 'in vitro' densitometry quantification Tibialis anterior muscle fibre bundles from 3 separate mature (300 day old) mice were incubated for an hour in Ringer's solution in the presence of 4nM (supraphysiological) DHT or 40µM chloroquine. The fibre bundles were snap frozen, sectioned and adsorbed onto slides for immunofluorescence microscopy. DHT (*) group showed significantly higher plasma membrane fluorescence than all other groups (unmaked)($p<0.05$). CQ treatment reduced signal to control levels ($p>0.05$). 1-way ANOVA used, n=3.

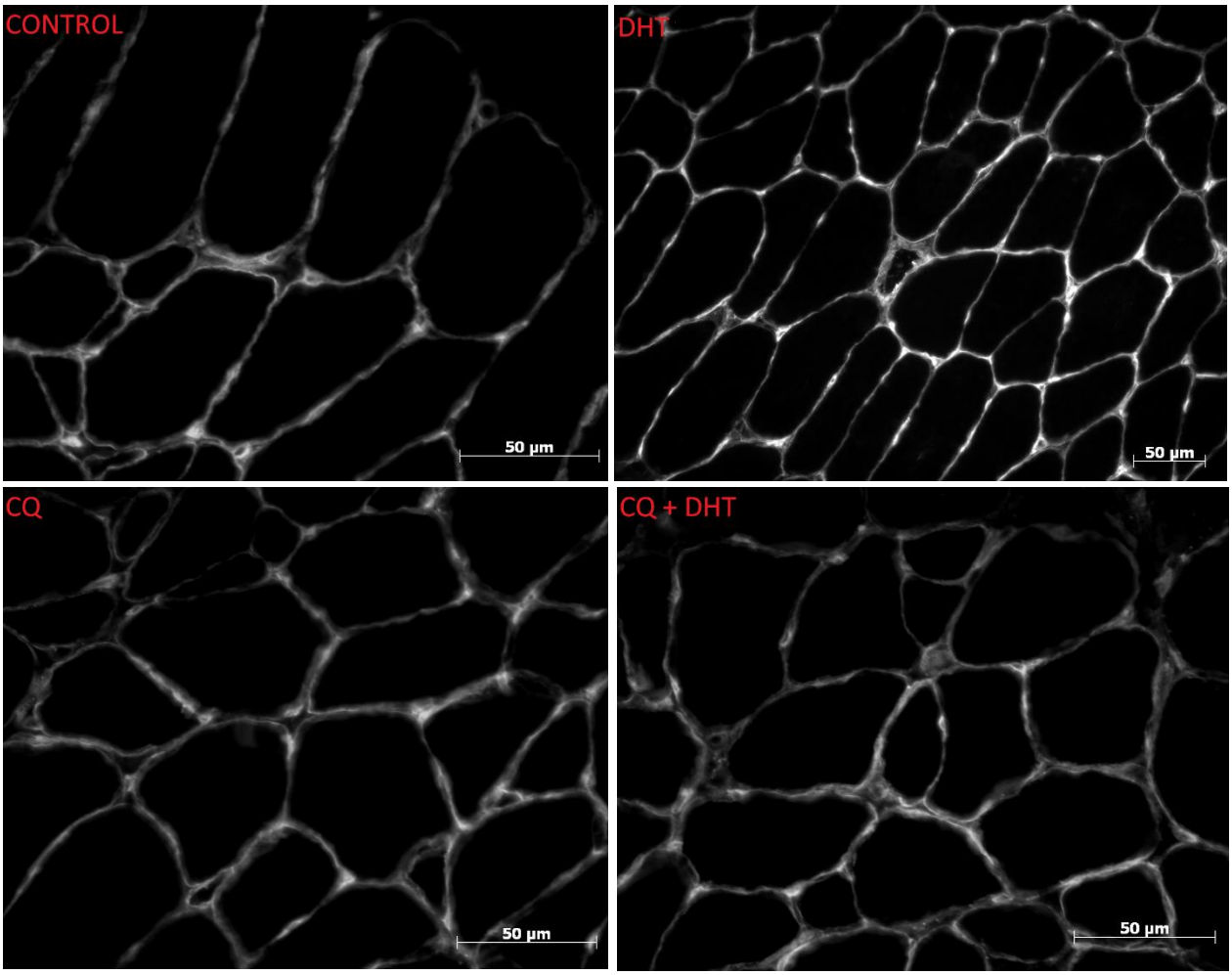

Figure 4.8B Fluorescence imaging of SNAT2 localisation in response to DHT and Chlorquine treatment Tibialis anterior muscle fibre bundles from mature (300 day old) mice were incubated for an hour in Ringer's solution in the presence of 4nM (supraphysiological) DHT, 40µM chloroquine. The fibre bundles were snap frozen, sectioned and adsorbed onto slides for immunofluorescence microscopy. Representative image.

4.3 Discussion

4.3.1 SNAT2 and LAT2 Protein Expression

To determine the mechanism underlying the effects of DHT-treatment on amino acid transport in elderly mice, western blotting was used to investigate the expression of SNAT2 and LAT2 protein in fast-twitch and slow-twitch muscles isolated from young, middle aged and elderly mice. As the results displayed in Figures 4.1A and 4.1B show, DHT treatment reversed the age-dependent decline in SNAT2 and LAT2 protein expression that was evident in our previous studies of the ageing effect on SNAT2 and LAT2 protein expression (Fig. 3.2A and 3.2B). With DHT treatment of 1 hr, we saw the protein expression of SNAT2 and LAT2 in elderly fast twitch muscle return to a level which was not different from that of the mature mice ($p<0.05$). Fast twitch fibres were rescued completely in this regard. While there was a trend toward the reversal of age related decline in SNAT2 and LAT2 in slow SOL, the difference was not statistically significant. This data suggests that an acute 1hr treatment with DHT has recovered functional SNAT2 and LAT2 levels in elderly fast muscle to that equal to much younger animals. While slow SOL also benefits from DHT treatment as we can see from the positive trends, the effect is not profound enough to reach statistical significance. It should however be noted that the slow SOL is more resistant to age related decline in the first place and experiences a lesser magnitude of dysfunction in ageing.

In experiments of protein expression, young animals of around 100 days were tested as well as mature and elderly but ignored after the amino acid transporter protein expression studies. This is because the expression of both SNAT2 and LAT2 was found to be significantly reduced in comparison to their mature counterparts and inconsistent. Amino acid uptake was also shown to be impaired when compared to the mature (around 300 day old) counterparts. It was concluded that these mice were too young to use for the study of SNAT2 and LAT2 function. This is of course the opposite to what was initially expected. It is intuitive to think that the expression of these transporters would be at their highest during the developmental stages of an animal's life, as this has been shown to be the time of the highest rate of growth. This is

attributed to greater nitrogen retention and increased protein synthesis rates (Davis et al., 1989, Davis and Fiorotto, 2009). However, our findings contradict this dogma.

There are several plausible reasons for this result. It is known that testosterone concentrations in serum peak at around 15 weeks in mice, then decline in senescent animals (Banerjee et al., 2014). Banerjee et al. also shows that the expression of the transporter GLUT3 declines as mice get closer to the 100-day mark, then increases into maturity. It is possible a similar phenomenon is at work in SNAT2 and LAT2 expression. This could be due to these mice simply not having had sufficient time to produce large stores of the transporters in the intracellular pools when compared to fully mature mice. Thus, the limiting factor is likely to be the reserve pools of transporters available. It is also possible that there is a reduced response to the stimulation from anabolic steroids in immature mice stemming from a reduction in AR expression. In fact, it has been found that amino acids such as leucine and higher levels of insulin may act as the dominant anabolic triggers in very young animals rather than anabolic hormones (Suryawan and Davis, 2011). Whatever the underlying reason, more research needs to be completed to elucidate the role of SNAT2 and LAT2 in early development.

4.3.2 AA uptake in tissue

The results of the amino acid uptake studies mirror the increase in SNAT2 and LAT2 expression. In elderly mice, DHT treatment on fast twitch skeletal tissue results in a significant increase ($p<0.05$) from untreated tissue. This is true in the uptake of both C_{14}MeAIB and C_{14}Isoleucine as seen in figures 4.2A-B and 4.2C-D. There is a trend towards greater uptake in both mature and elderly slow twitch muscle, but it does not show statistical significance ($p>0.05$). This data suggests that DHT rescues the age-related decline in SNAT2 and LAT2 in fast twitch fibres.

The increases in AA uptake correlates with the increases seen in the SNAT2 and LAT2 protein expression data. The increase in both C_{14}MeAIB and C_{14}Isoleucine may be directly attributed to an increased amount of SNAT2 and LAT2 present at the plasma membrane. Mature mice did not see any significant benefit from 2nm physiological DHT treatment. This is likely because of the higher levels of testosterone and by proxy DHT in the mature cohort mice compared to the elderly (Banerjee et al., 2014).

The attenuated response seen in slow twitch muscle to DHT compared to the fast twitch remains to be fully elucidated. It is possible that the decreased response to anabolic stimuli in slow fibers is due to a reduction in AR expression, which has been documented in slow fibres (Hulmi et al., 2008). This finding also implies that the non-genomic DHT effect might be AR mediated.

The experiments using chloroquine were run using mature tissue to understand the physiological effect of these drugs in isolation. No elderly group was used. Tissues were pre-treated with chloroquine for 1hr prior to start of experiments to ensure vesicle alkylation (Ramm et al., 1994). DHT treatment was initiated at start of experiments for 1hr as before. Supra-physiological level of DHT was used (4nm) equal to roughly double that of physiological to assess the ability of CQ to blunt the DHT effect.

As before, a significant ($p<0.05$) effect with DHT was noted. This effect was completely abolished in both chloroquine and chloroquine + DHT groups. This suggests that chloroquine is acting to prevent the recruitment of SNAT2 and LAT2 from storage vesicles. This effect of chloroquine has been observed in system A transporters (Hyde et al., 2002, Kashiwagi et al., 2009) as well as in GLUT4 trafficking as well (Romanek et al., 1993). This is due to the accumulation of chloroquine inside the storage vesicles and protonation, which results in a net alkylation of the entire vesicle (Chapman and Munro, 1994).

Table 4.1. Summary of DHT effects on Skeletal Tissue

DHT Treatment	MATURE FAST	MATURE SLOW	ELDERLY FAST	ELDERLY SLOW
SNAT2 Protein	●●●	●●●●	●●	●●●
LAT2 Protein	●●●●	●●●●	●●●●	●●●
C_{14}MeAIB Transport	●●●	●●●●	●●●	●●
C_{14}Isoleucine Transport	●●	●●●	●●	●●
Protein Synthesis	●●	●●●	●●	●●

4.3.3 Fluorescence Imaging of SNAT2 localisation with ageing and DHT treatment

The fluorescence imaging yielded results confirming the western blot and amino acid uptake data. There was a statistically higher membrane localised signal found in the DHT treated groups, as compared to their age equivalent controls. The magnitude of increase was also roughly consistent with what was found in the previous protein expression and amino acid uptake experiments. Clusters of fluorescence were observed either at the plasma membrane or surrounding the nuclei. This is consistent localisation studies involving GLUT4, which have shown that there is very little movement of actual vesicles in cytoplasm of cells but rather large accumulation around nuclei, and smaller storage sites along the plasma membrane (Lauritzen et al., 2008). Intentional disruption of the trans-Golgi network has had no effect on uptake of amino acids, lending more credibility to the theory that in fact the second storage pool of amino acid transporters responsible for acute recruitment lies in close proximity to the plasma membrane (Hundal et al., 1994).

4.3.4 AA uptake in C2C12 myoblasts and myotubes

In preliminary experiments, we found varying expression levels of androgen receptor in myoblasts and myotubes, being significantly greater in myoblasts. In fact, myoblast

cells have been found to be the prime expressors of androgen receptors out of all cell types (Sinha-Hikim et al., 2004). In order to account for this potential confounding factor, uptake in both myoblasts and myotubes was measured independently.

Myoblasts and myotube C2C12 cell lines were used for these experiments. Both our cell types have shown a significant increase ($p<0.05$) in the uptake of both C_{14}MeAIB and C_{14}Isoleucine in response to DHT (Fig 4.7A-B and 4.7C-D). Both of the antagonists were used to pretreat the tissues 1hr prior to commencement of experiments. This was a step that was not followed by Hamdi et al. in their tissue experiments, which showed an impartial abolishment of DHT effects with flutamide. It was essential to achieve complete blockade of the androgen receptor with flutamide and inhibition of vesicular recruitment and turnover with chloroquine.

As before, C_{14}MeAIB quantified SNAT2 transport, while C_{14}Isoleucine quantified LAT2 transport. Myoblast C_{14}MeAIB uptake with 4nM DHT showed an increase of 45.91% + 6.82% and increase of 39.8% $\pm$ 4.02% with C_{14}Isoleucine uptake. These results were mirrored in myotubes, with and 38.12% 5.177 increase in C_{14}MeAIB uptake and 49.67% $\pm$ 3.32% increase in C_{14}Isoleucine.

In all groups this DHT mediated increase in transport was abolished completely with chloroquine treatment. Chloroquine groups showed no statistical difference to controls. Combined DHT and chloroquine treatment group fared the same, an abolishment of the DHT was seen with not significant variance from controls. This supports the theory that DHT works to recruit SNAT2 and LAT2 from an internal vesicular pool. Once the movement of these stored transporters to the plasma membrane is inhibited by chloroquine, the acute effect of DHT treatment is completely abolished. This also shows that the recruitment of transporters is a rapid non-genomic process, being able to occur in under an hour. This is consistent with the rapid recruitment of the well-studied GLUT4 transporter (Becker et al., 2001). The equivalence in transport between control groups and chloroquine treated are consistent with the evidence that chloroquine disrupts all vesicular trafficking, both the recruitment of SNAT2 and its turnover (Michihara et al., 2005).

A similar blunting effect was seen in the flutamide treated groups. Flutamide is a selective competitive antagonist of the androgen receptor, which binds strongly to the receptor resulting in an inactive conformation that is unable to propagate a signalling cascade (Suh et al., 2015). Flutamide treatment completely abolished the DHT mediated increase in amino acid uptake in both the myoblasts and myotubes. Treatment with a combination of flutamide and DHT resulted in the same effect, the uptake was blunted back to baseline uptake not significantly different to controls ($p>0.05$). This was an interesting finding, as it suggests the action of DHT is likely mediated by an AR element.

Previous data by Hamdi et al. has proposed that this mechanism is also mediated by the EGF receptor (Hamdi and Mutungi, 2010). However more recent evidence points to DHT working downstream of the EGFR. DHT is shown to greatly potentiate MAPK signalling, but only in the presence of baseline EGF binding (Lee et al., 2014). It is also possible that DHT is working as a co-activator of the EGFR, through an androgen receptor element. More work is required to elucidate the exact mechanism of the acute action of DHT.

4.3.5 Fluorescence imaging of SNAT2 localisation with DHT and Chloroquine treatment

Our imaging results confirm the AA uptake and Western blotting data. DHT increases the quantity of functional SNAT2 transporters on the plasma membrane of skeletal muscle. We suggest that this fast (1hr) recruitment of functional transporters is obtained from plasma membrane proximal storage vesicles. Chloroquine inhibits vesicle trafficking and recruitment by increasing vesicular pH (Kashiwagi et al., 2009). This effect can be seen by the absence of increased total plasma membrane signal of SNAT2 as compared to controls.

Interestingly, the chloroquine groups seem to show more pinpoint signals close to the membranes. This suggests that translocation of transporters into the plasma membrane proximal storage vesicles is still occurring, even in the presence of chloroquine. If this is accurate, it means that DHT is not only initiating the recruitment of transporters in plasma membrane localised vesicles but also the movement of any

transporters located in the Golgi into these vesicles. We do not see this effect in non CQ treatment groups, which gives more support to this theory.

During the course of this chapter some limitations arose. Due to difficulty with fluorescence imaging of LAT2, only SNAT2 fluorescence data was obtained. This might have been a result of the relatively early availability of LAT2 antibodies and poor binding for use in the technique. Further work is necessary to assess LAT2 localisation in myoblast cells as a result of DHT and CQ treatment.

Due to the scarcity of mice, the TA was chosen for use in sectioning and immunofluorescence. This made it impossible to assess fibre type differences between groups. See summary of limitations in section 6.7 for overview of all limitations.

Chapter 5

5.1 Aim

5.2 Results

5.2.1 SNAT2 encoding plasmid transfection in C2C12 myoblasts

5.2.2 Effects of DHT on SNAT2 transport in transfected and control C2C12 myoblasts

5.2.3 Effects of starvation on SNAT2 transport in transfected and control C2C12 myoblasts

5.2.4 Effects of SNAT2 blockade on LAT2 transport in C2C12 myoblasts

5.2.5 Effects of SNAT2 blockade with MeAIB on C_{14}Isolecuine transport in C2C12 myoblasts

5.2.6 Effects of Wartmannin, SP600125, and DHT on starvation induced increase in LAT2 transport in C2C12 myoblasts

5.3 Discussion

5.3.1 SNAT2 Expression Vector

5.3.2 Effect of SNAT2 blocking on LAT2

5.3.3 Investigation of starvation induced LAT2 upregulation with JNK and wortmannin

5.3.4 Limitations

5.1 Aim

In this chapter, the focus lies on investigating the relationship between SNAT2 and LAT2. The aim is to gain more insight into the trafficking involved in the recruitment of these amino acid transporters. Specifically, the hypothesis that SNAT2 is a limiting factor determining LAT2 function. The focus is shifted to the study of modulating SNAT2 function rather than LAT2, because SNAT2 is a likely determining driver of LAT2 transport.

5.2 Results

5.2.1 SNAT2 encoding plasmid Transfection in C2C12 myoblasts

C2C12 myoblasts were transfected with an expression vector coding for the SNAT2 sequence. Cells were tested for SNAT2-GFRP using immunofluorescent imaging, determined by a strong luminescent signal in transfected cells. A positive fluorescent signal can be seen in figures 5.1C and 5.1D. Restrictive digest was also performed on expression vector and ran using agarose gel electrophoresis, which obtained a fragment of expected 1001 base pairs.

C_{14}MeAIB uptake experiments were run in order to test whether transfection would resort in greater SNAT2 mediated transport. A trend was found toward increase in C_{14}MeAIB uptake with SNAT2 plasmid transfection as seen in figure 5.1E. This suggests that artificially creating a greater quantity of SNAT2 may have led to higher translocation to the membrane and thus more functional SNAT2. However, the difference between groups was not statistically significant. It is very likely that as with GLUT4, the recruitment of SNAT2 to the plasma membrane is limited at the uptake and release of transporter into and out of storage vesicles, which are the only route directly to the plasma membrane (Leto and Saltiel, 2012).

As seen before in our imaging our transfection was successful. However, our transfection success rate was around 20% of total cells based on cell counts of fluorescent images (based on cell counts). This means that our uptake experiments using cell lysates were effectively an average of transfected and untransfected cells. While there was a trend seen towards higher uptake in the transfected group, the difference was not significant ($p=0.1653$). This shows that there likely only a small increase of functional SNAT2 at the plasma membrane as a result of the transfection at baseline conditions.

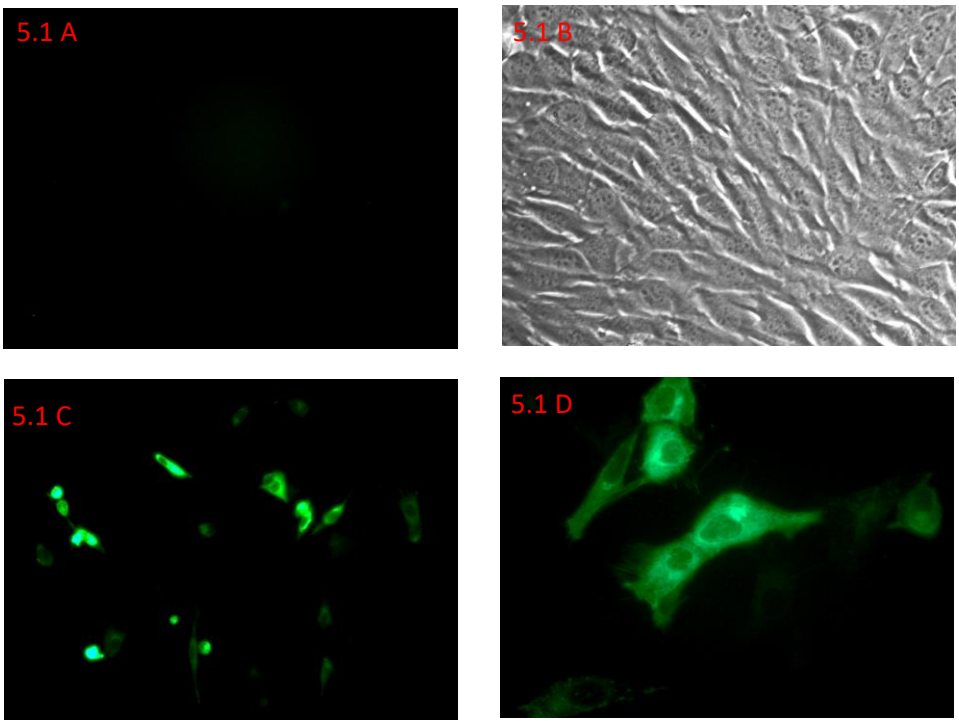

Figures 5.1A-D Fluoresence imaging of transfected and control untransfected C2C12 myoblasts 5.1A- Control image at 509nm of untransfected C2C12 myoblasts. 5.1B- Corresponding brightfield image of 5.1A showing the same area. 5.1C-Representative image of C2C12 cells with SNAT2 plasmid in lipofectamine at 10x magnification at 509nm. 5.1C Representative image of C2C12 cells transfected with SNAT2 plasmid in lipofectamine at 40x magnification at 509nm.

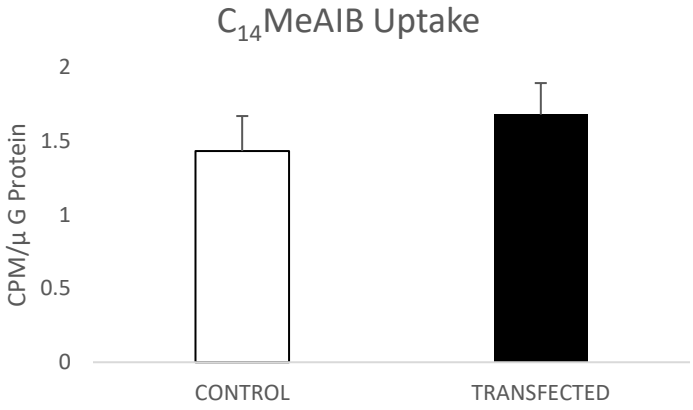

Graph 5.1E C_{14}MeAIB Uptake in transfected and control untransfected C2C12 myoblasts Bar graph of C_{14}MeAIB uptake in control C2C12 cells and those transfected with SNAT2 expression vector. Increase is noted in cells transfected with SNAT2 plasmid, however this is not significant (p=0.1653). 1-way ANOVA used, n=3.

5.2.2 Effects of DHT on SNAT2 transport in transfected and control C2C12 myoblasts

The next step in testing the transfection of C2C1 myoblasts with the SNAT2 vector was to assess the functional uptake of C_{14}MeAIB through SNAT2 when treated with 4nm DHT. If the hypothesis of the SNAT2 plasmid increasing an intracellular pool of functional SNAT2 was correct then acute treatment should potentially recruit these to the plasma membrane leading to increased transport.

The results in figure 5.2A validates this assumption and shows that with DHT stimulation the uptake of C_{14}MeAIB was significantly increased ($p<0.05$) in the transfected cells compared to untransfected cells treated with the same concentration of DHT. This finding suggests that the transfection has increased the quantity of SNAT2 available for recruitment, leading to a higher level of functional SNAT2 at the plasma membrane. This process, as before is facilitated by DHT treatment.

Figure 5.2B shows that the magnitude of increase in the transfected cells was over 60% that of untransfected cells treated with same concentrations of DHT. Cells were cultured in full media as normal, and DHT was added at start of experimental run, which was run at 37°C in full media for 1hr.

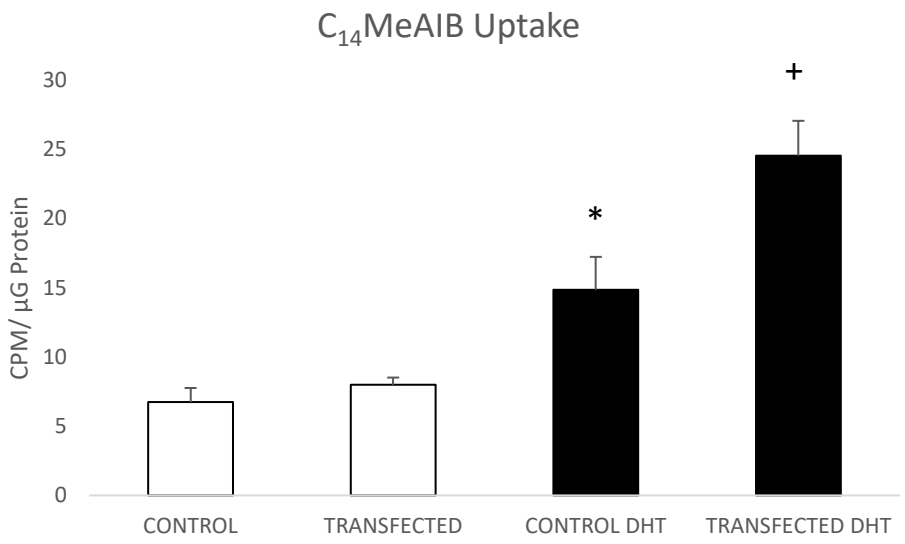

Figure 5.2A Effect of DHT on C_{14}MeAIB in transfected and untransfected C2C12 myoblasts Bar graph showing effect of DHT treatment on transfected C_2C_{12} cells, cultured in full media at 37°C, treated with 4nM DHT for 1hr in full media. White bars represent no DHT, black bars are DHT treated. Control and transfected do not show significant difference ($p>0.05$). DHT treated control (*) shows greater uptake to both control and transfected (unmarked)($p<0.05$). DHT treated transfected (+). Transfected treated with DHT (+) show higher uptake than all other groups ($p<0.05$). 1-way ANOVA used, n=3.

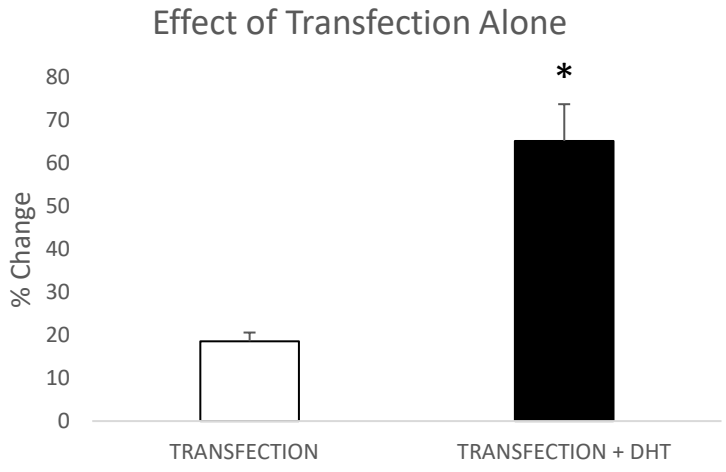

Figure 5.2B Extent of change with transfection alone compared to transfection and DHT C2C12 myoblasts cultured in full media at 37°C, treated with 4nM DHT for 1hr. Bar graph showing percentage change in C_{14}MeAIB uptake represents effect of transfection in control (white) group and DHT treated (black) group. Baseline used are untransfected and untransfected DHT treated respectively. The magnitude of change is significantly greater ($p<0.05$) in transfected + DHT than in transfected alone. 1-way ANOVA used, n=3.

5.2.3 Effects of starvation on SNAT2 transport in transfected and control C2C12 myoblasts

Experiments were repeated to assess the effects of starvation on SNAT2 recruitment. Starvation is a known up regulator of SNAT2 and works through a distinct pathway from DHT (Kashiwagi et al., 2009). Therefore, starvation treatment serves to show whether the overexpressed SNAT2 was fully functional and responsive to physiological triggers other than direct hormone stimulation.

Figure 5.3A shows that starvation did increase the uptake of C_{14}MeAIB in transfected C2C12 myoblasts when compared to untransfected cells ($p<0.05$). Figure 5.3B shows the magnitude of change. Cells were starved for 3hrs in HBSS prior to start of experiment, which was then incubated at 37°C in HBSS for 1hr.

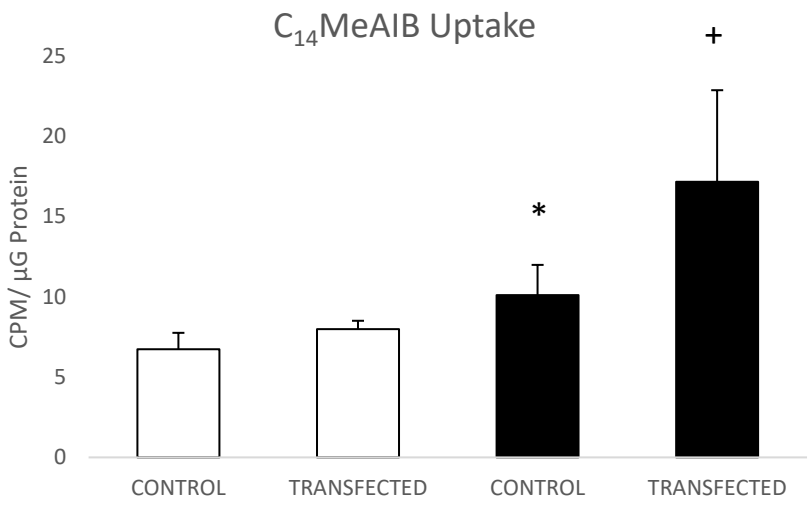

Figure 5.3A Effect of starvation on C_{14}MeAIB in transfected and untransfected C2C12 myoblasts Bar graph showing effect of starvation on transfected C_2C_{12} cells, cultured in full media at 37°C, pre-starved for 3hr in HBSS and incubated for 1hr in HBSS. As before, control and transfected do not show significant difference (unmarked) ($p>0.05$). Starved control (*) is different from all other groups ($p<0.05$). Transfected starved (+) is statistically higher than all groups ($p<0.05$). 1-way ANOVA used, n=3.

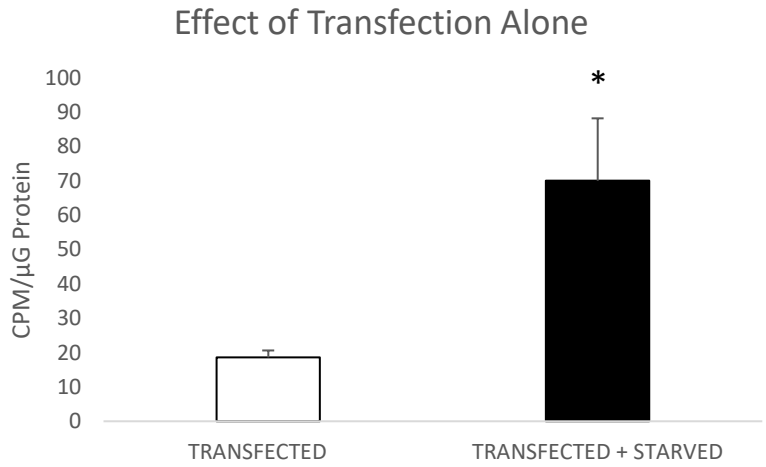

Figure 5.3B Extent of change with starvation alone compared to transfection and starvation C2C12 myoblasts cultured in full media at 37°C prestarved for 3hr in HBSS, then incubated for 1hr in HBSS. Bar graph showing percentage change of C_{14}MeAIB uptake. White bar represents effect of transfaction alone, whilst black bar represents the effect of transfection between starved cells. Baseline are untransfected and untransfected starvation groups respectively. The magnitude of change is significantly greater ($p<0.05$) in transfected starvation (+) then in transfection alone (unmarked). 1-way ANOVA used, n=3.

5.2.4 Effects of SNAT2 plasmid transfection on C_{14}Isoleucine transport in C2C12 myoblasts

As stated before, an assumption was made that SNAT2 activity is directly correlated to LAT2 transport. Therefore, effect of artificially upregulating SNAT2 transporter protein in C2C12 myoblasts on LAT2 transport was assessed by measuring C_{14}Isoleucine transport in transfected C2C12 myoblasts. As figure 5.2A has shown a significant increase in C_{14}MeAIB transport with DHT treatment, this experiment was performed to determine if an abundance of intracellular SNAT2 would likewise increase LAT2 transport. As figure 5.4 shows, there is no statistically significant difference between the DHT response in untransfected cells when compared to those transfected with the SNAT2 plasmid. There is however a trend toward increased transport.

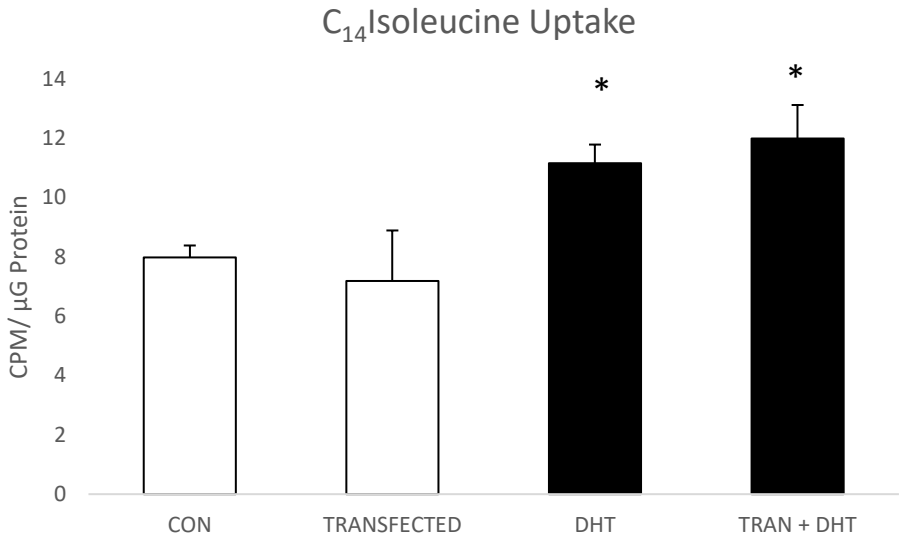

Figure 5.4 Effect of SNAT2 plasmid transfection on C2C12 myoblasts treated with DHT. Bar graph showing C2C12 myoblast uptake of C_{14}Isoleucine. Cells were transfected with plasmid coding for SNAT2. Myoblasts were cultured in full media at 37°C, and treated with 4nM DHT for 1hr in full media for experimental runs. Control untransfected showed no difference to transfected (unmarked white) ($p>0.05$). DHT treated controls (DHT *) showed no difference to transfected DHT (TRAN + DHT *) ($p>0.05$). Both DHT treated showed significantly higher uptake than non DHT groups ($p<0.05$). 1-way ANOVA used, n=3.

5.2.5 Effects of SNAT2 blockade with MeAIB on C_{14}Isolecuine transport in C2C12 myoblasts

The above experiments suggested that artificially increasing SNAT2 protein content in C2C12 myoblasts did not lead to increases in LAT2 transport, even in the presence of DHT. The next step was to test whether the blocking of SNAT2 would in turn have a negative impact on LAT2 function. This was achieved by preincubating C2C12 myoblasts in varying concentrations of MeAIB (non-radioactive). At high concentrations MeAIB blocks the SNAT2 transporter, a phenomenon known as trans inhibition (Kashiwagi et al., 2009).

Figure 5.5A shows two concentrations of MeAIB used, 3.3mM and 5.0mM and the effect of this block on C_{14}Isoleucine uptake in C2C12 cells in full media. All blocking groups were significantly lower than control ($p<0.05$) 3.3mM MeAIB resulted in 52.83% (±5.22%) reduction in blocking from control group, while maximal block was achieved with 5.0mM MeAIB at a reduction of 77.03% (±2.51%). MeAIB used at 5mM provided maximal reduction in LAT2 transport. In this instance MeAIB serves to block entry of small amino acids necessary to drive LAT2 (Hatanaka et al., 2001).

Figure 5.5B illustrates the blunting of the magnitude of the starvation response in LAT2 transport, a very large increase is noted in starved cells compared to unnstarved controls. Interestingly, MeAIB still acts to blunt this large increase by approximately half. Because the cells are in AA free media (HBSS) this effect cannot be attributed to prevention of AA uptake.

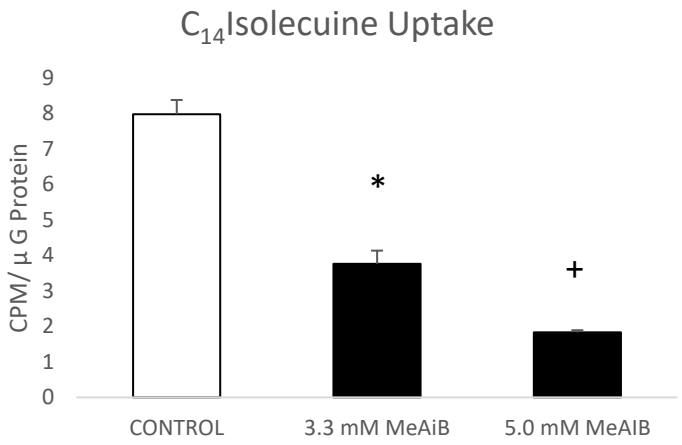

Figure 5.5A Effects of blocking concentrations of MeAIB on C_{14}Isolecuine transport in C2C12 myoblasts in full media Bar graph showing effect of high concentration MeAIB on C_2C_{12} cells, cultured in full media at 37°C. Cells were pre-treated with various concentrations of MeAIB for 1hr in full media, experiment was performed over the course of 1hr in full media in the presence of corresponding concentrations of MeAIB. Both 3.3nM and 5.0nM MeAIB were statistically lower (* and +, $p<0.05$) than control (unmarked). 1-way ANOVA used, n=3.

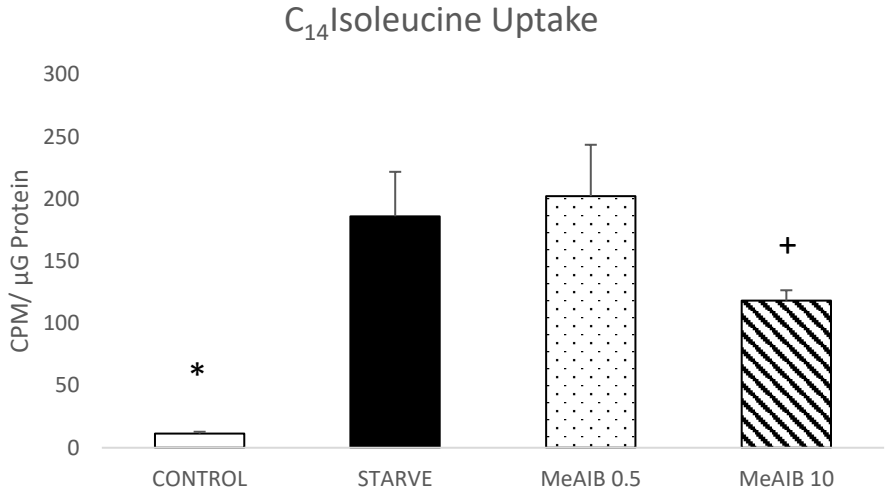

Figure 5.5B Effects of blocking and normal concentrations of MeAIB on C_{14}Isolecuine transport in C2C12 myoblasts under starvation Bar graph showing effect of blocking and non-blocking concentrations of MeAIB on C_2C_{12} cells, cultured in full media at 37°C. Cells were pre starved for 3hrs in HBSS, pre-treated with various concentrations of MeAIB for 1hr in HBSS. Experiment was performed over the course of 1hr in HBSS in the presence of corresponding concentrations of MeAIB. Starvation control (black, unmarked) showed no difference to 0.5nM MeAIB (dotted, unmarked). Control unstarved cells (white, *) showed significantly lower uptake to all groups ($p<0.05$). Maximal blocking concentration of 10µM MeAIB (dashed, +) blunted the starvation effect (seen in starved and 0.5nM MeAIB) significantly ($p<0.05$). 2-way ANOVA used, n=3.

5.2.6 Effects of Wartmannin, SP600125, and DHT on starvation induced increase in LAT2 transport in C2C12 Myoblasts

When comparing the starvation induced increase in transport between SNAT2 and LAT2, it was noted that LAT2 transport increased to a greater extent than SNAT2 transport. As seen in figure 5.6A, there is a much greater effect seen in LAT2 transport then SNAT2 transport. ($p<0.05$) This quantified as a percentage from baseline (non-starved cohorts) equates to 1534.09% increase in LAT2 transport VS a 49.96% increase for SNAT2 transport. LAT2 transport is 30.62 times greater than SNAT2 transport under starvation conditions.

Because these experiments were run in HBSS after 3hr of starvation, the question of where LAT2 is obtaining small amino acids to drive the exchange for C_{14}Isoleucine arises. A hypothesis that SNAT2 and LAT2 act as transceptors and signal through the JNK pathway to initiate proteolysis in response to starvation was proposed.

To test our hypothesis of SNAT2 signalling through the JNK pathway, we used the anthrapyrazolone selective JNK inhibitor SP600125 (Sigma Aldrich, UK). In these experiments, cells were pre-starved for three hours in HBSS before the commencement of uptake experiments as before. SP600125 was used at a concentration of 10nM which has maximal effect without significantly effecting any other physiological processes (Kashiwagi et al., 2009).

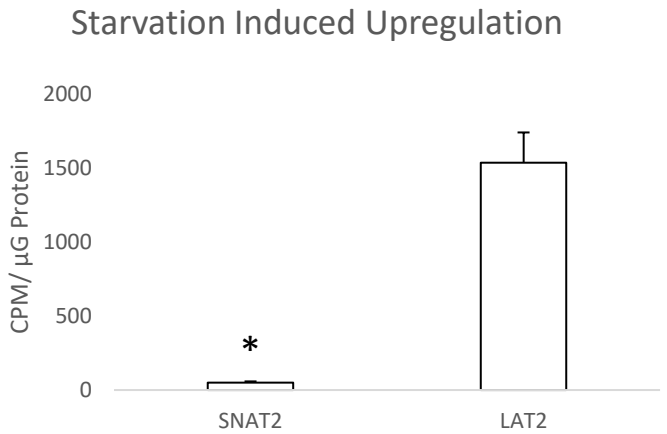

Figure 5.6A Comparison of starvation induced upregulation of C_{14}MeAIB and C_{14}Isoleucine in C2C12 myoblasts Bar graph showing effect of starvation on transfected C_2C_{12} cells, cultured in full media at 37°C, pre-starved for 3hr in HBSS and ran for 1hr in HBSS. SNAT2 signifies C_{14}MeAIB and LAT2 signifies C_{14}Isoleucine. There is a significant difference ($p<0.05$) between the two groups, n=3.

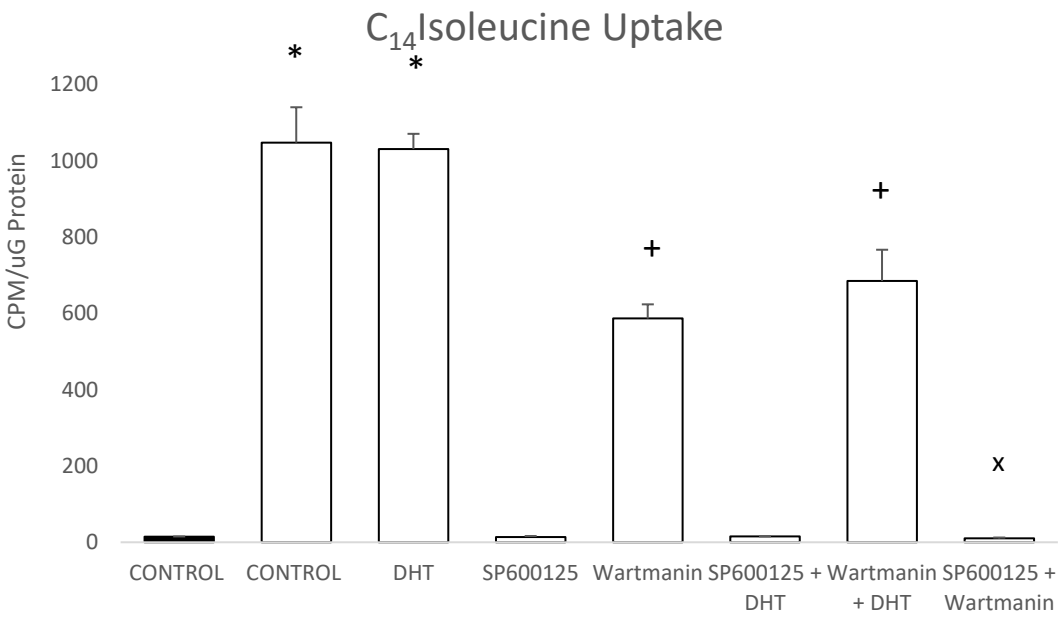

Figure 5.6B Effects of Wartmannin and SP600125 on starvation induced increase in LAT2 transport. C2C12 myoblasts were cultured in full media at 37°C, pre starved for 3hr in HBSS alone and then incubated for 1hr in HBSS with or without drug treatments as indicated. Black bars represent control fed full media and white bars starvation in HBSS. Fig 26B is the same data isolated to show differences. DHT (*) shows no increase in comparison to control starved ($p<0.05$). Wartmannin shows 44.02% ±3.89% reduction compared to starvation control ($p<0.05$). Wartmanin (+) shows no difference to DHT+Warmanin (+)($p>0.05$). 2-way ANOVA used, n=3.

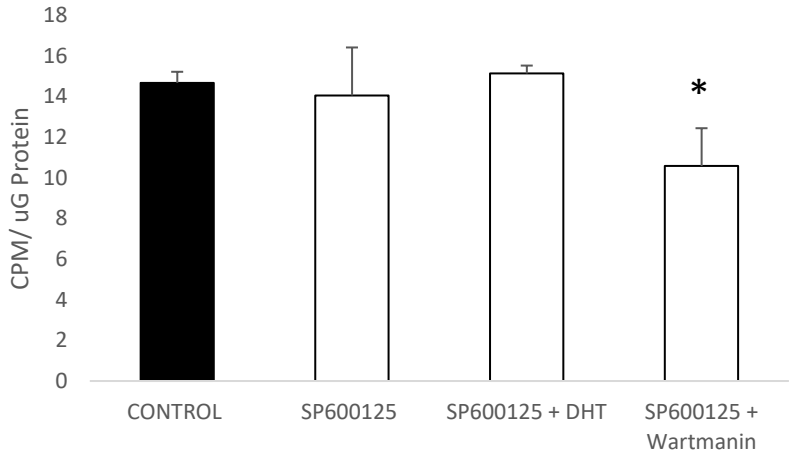

Figure 5.6C Effects of Wartmannin and SP600125 on starvation induced increase in LAT2 transport. Data from Figure 5.6B, 4 groups isolated to show differences more clearly. SP6000125 blunts the starvation induced upregulation completely, showing no difference to control ($p>0.05$). SP600125+DHT shows no difference to either control nor SP600125 alone ($p>0.05$). SP600125+Wartmanin suggest additive effect, showing reduced uptake to all groups tested ($p<0.05$) 2-way ANOVA used, n=3**.**

5.3 Discussion

5.3.1 SNAT2 Expression Vector

We developed a SNAT2 expression vector with the aims of artificially upregulating SNAT2 in C2C12 myoblasts. This made it possible to assess whether LAT2 transport was directly limited by the small amino acid gradient produced by SNAT2. It also tested the possibility of SNAT2 upregulation as a means of increasing LAT2 transport, leading to increased net protein synthesis. Studies with GLUT4 have shown that upregulating expression of the transporter do not lead to proportionally higher levels of active GLUT4 on the plasma membrane, because the amount of transporter available for recruitment in vesicular compartments is tightly controlled (Brozinick et al., 1997). The aim of these experiments was to determine if this was also the case with SNAT2.

The transfection of the plasmid was successful as evidenced by figures 5.1A-D. The results in figure 5.1E however shows no significant increase in C_{14}MeAIB with transfection. This suggests that transfection alone likely does not translate to a significant upregulation of functional SNAT2 transporter on the plasma membrane. This is consistent with findings from studies on GLUT4, which show that extra cytoplasmic transporter levels do not correlate proportionally with increased concentrations of the transporter on the plasma membrane (Leto and Saltiel, 2012).

However, as shown in our figures 5.2B and 5.3B the magnitude of response to both DHT and amino acid starvation is significantly higher in the transfected cells. This suggests that there is an increased capacity for SNAT2 recruitment, potentially stemming from increased packaging and availability of SNAT2 inside terminal storage vesicles proximal to the plasma membrane.

As evidenced by the data in figure 5.4 there is no change on LAT2 transport in response to SNAT2 overexpression using an SNAT2 plasmid transfection in C2C12 cells. This holds true in both control C2C12 myoblasts as well as DHT treated groups. This was not surprising, as the increased expression of SNAT2 in transfected cells did not increase C_{14}MeAIB transport. This provides more evidence that there was little increase in functional SNAT2 protein at the plasma membrane resulting from transfection alone.

This has also shown that total protein SNAT2 overexpression alone using a SNAT2 plasmid in C2C12 myoblasts is likely not a feasible method for the direct upregulation of LAT2 activity.

However, using DHT to upregulate LAT2 in transfected cells also did not lead to higher uptake of Isoleucine (fig 5.4). This suggests that increasing the small amino acid gradient over baseline does not lead to increased LAT2 activity. It is likely that small amino acid availability is not a rate limiting factor in LAT2 function and that increasing the substrate concentration is not a feasible way to induce LAT2 activity.

5.3.2 Effect of SNAT2 blocking on LAT2

When SNAT2 transport is significantly impaired, LAT2 activity suffers. This is evidenced by our blocking experiments using blocking concentrations of MeAIB as seen in figure 5.5. When SNAT2 was completely blocked, the small neutral amino acid gradient was impaired, reducing LAT2 transport. It has been shown that blocking cells for prolonged periods of 5 days with saturable concentration of MeAIB results in significant depletion of branched chain amino acids such as leucine (Pinilla et al., 2011). However the connection to LAT2 has not been previously made in these findings.

It is likely that under SNAT2 impairment LAT2 is unable to function at its normal capacity, due to the unavailability of small neutral amino acid substrates necessary for its normal function as an AA exchanger. It should be noted that even at full block of SNAT2, LAT2 still retained roughly 23% of activity as seen in figure 5.5. This may be due simply to incomplete depletion of small amino acids in the cell. This is further supported by the abundance of amino acids inside the skeletal muscle cell. Our chosen pre-blockade of 3 hours with MeAIB results in about 20% residual small neutral amino acid concentration without activating autophagy (Evans et al., 2008). Even without an external source of new small neutral amino acids, the cell is in a constant state of protein turnover, producing potential substrates for LAT2 (Bevington et al., 2002).

We can conclude from our findings that SNAT2 is likely the main regulator of the small neutral amino acid gradient necessary for LAT2 function in conditions of nutrient scarcity, SNAT2 transport accounting for the great majority of the latter's substrates.

This has possible implications for further research. LAT2 provides much of the necessary protein building blocks for fast dividing cancer cells, and its downregulation has shown to halt the pervasiveness of these cells (Janpipatkul et al., 2014). Instead of targeting LAT2 directly, it may be possible to partially blunt its function with the use of a compound that is relatively benign like MeAIB. This could be a feasible targeted therapy, as fast dividing cells rely on higher LAT2 function and have higher substrate requirements (Barollo et al., 2016).

5.3.3 Starvation induced LAT2 upregulation and effects of JNK inhibition and wortmannin

As noted in the previous section, saturable concentrations of MeAIB (>5nM) blunt the starvation induced LAT2 upregulation. This effect can be explained by a possible transceptor function of SNAT2. It has been shown that SNAT2 blockade using a saturable concentration of MeAIB results in decrease in the starvation induced upregulation of SNAT2 (Gazzola et al., 2001, Ling et al., 2001, Lopez-Fontanals et al., 2003). It has also been proven that amino acid deprivation causes an activation of the JNK pathway, leading to both an increased transcription of amino acid transporters and proteolysis (Kashiwagi et al., 2009, Zhou et al., 2015a). Because of these findings, the role of JNK was studied further.

Interestingly, starvation did not produce as a profound effect on SNAT2 function compared to LAT2. LAT2 uptake was 30.62 times greater under starvation conditions then SNAT2. This suggests that SNAT2 is not as sensitive to the JNK pathway, which has been found to be instrumental in starvation induced SNAT upregulation. (Kashiwagi et al., 2009) It is however possible that SNAT2 simply does not respond quickly enough through this pathway, requiring more time than our experimental runs allowed to achieve full transporter regulation.

MeAIB itself does not inhibit the phosphorylation of JNK at concentration tested up to 10mM (Hyde et al., 2007). However as Bracy et al. have shown, the use of MeAIB at saturable concentrations effectively locks the MeAIB substrate in an inward facing direction SNAT2, resulting in the phenomenon of trans-inhibition (Bracy et al., 1986). This likely produces an unstable confirmation of SNAT2 associated with no JNK

phosphorylation (Nardi et al., 2015). This is opposed to SNAT2 in purely starved conditions which takes a stable outward facing form that is able to activate the JNK pathway likely leading to increases in both its own recruitment from vesicular pools and increased transcription (Hyde et al., 2007). In other words, if there is amino acid flux through the transporter no starvation induced cascade effects are propagated by SNAT2. When amino acid availability dwindles and no amino acids are moving through the SNAT2 domain, the stable form of the transporter is preferred, which leads to JNK phosphorylation and initiation of autophagy most likely by dissociating bcl-2 from Beclin1 leading to the formation of Beclin1/PI3K complexes (Zhou et al., 2015a). Figure 5.3.3 illustrates this process in more detail. In this way it is possible that SNAT2 acts to regulate its own activity with changing nutrient availability controls the small neutral amino acid gradient inside the cell.

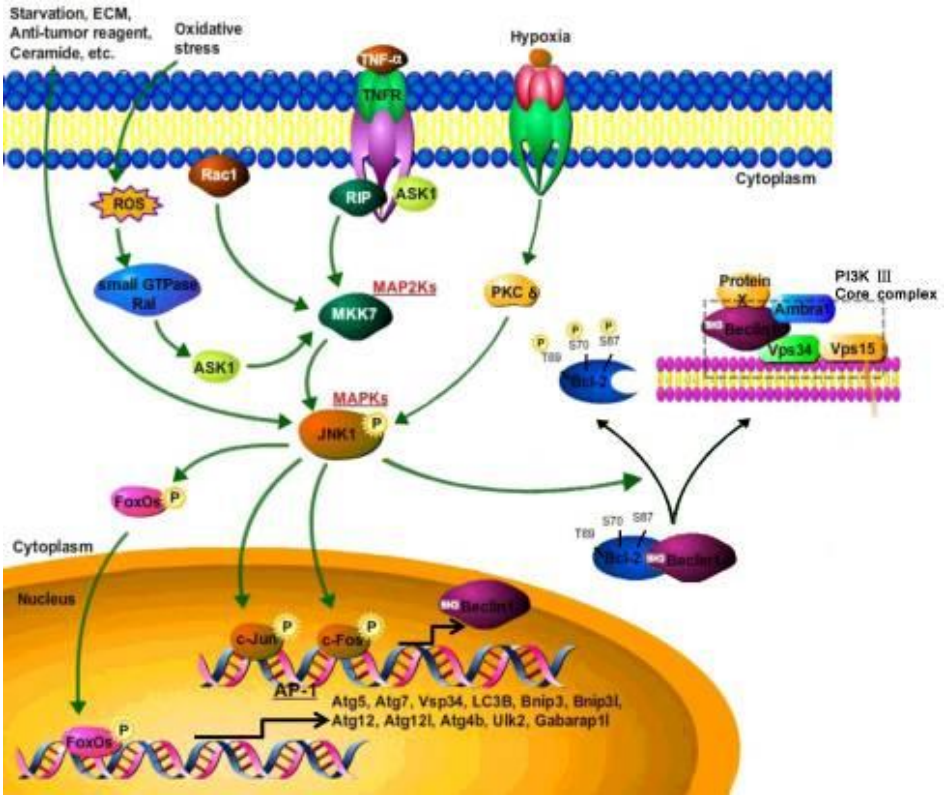

5.3.3 Illustration of JNK signalling in autophagy Starvation induced JNK signalling works through numerous different mechanisms, of which the fast non genomic involves formation of Beclin1/PI3K complexes. Illustration used from: (Zhou et al., 2015a).

It is plausible that starvation induced increase in AA transport are mediated primarily through JNK. In Figure 5.6B we see that under normal starvation conditions, transport of C_{14}Isoleucine through LAT2 is significantly increased when compared to control fed conditions. The magnitude of this effect is so great that It was not possible to show these two data points on the same linear graph, having to isolate the lower reading groups on figure 5.6C. However, when the cells were treated with SP600125, there was no observable increase in uptake when compared to fed controls. In other words, the starvation effect was completely abolished back to baseline.
On the other hand Wortmannin, a non-reversible PI3K inhibitor produced only a 44.02% (±3.89%) reduction in the observed starvation effect. This was noted using a relatively high concentration of wortmannin at 200nM (IC50= 1nM) (Akinleye et al., 2013) It has been shown that wortmannin at these concentrations does not interfere with JNK phosphorylation. This suggests that JNK mediated signalling is not acting solely through PI3K but potentially via another undefined mechanism, possibly downstream from PI3K (Xing et al., 2008).

Another notable finding arising from the previous set of experiments was that the DHT effect is absent in starvation conditions. This is clearly illustrated in figure 5.6B and contrasts with experiments ran in full media, which show a significant increase in transport with DHT treatment. This data provides additional evidence for the hypothesis stating that DHT is working through an EGFR mediated mechanism (Hamdi and Mutungi, 2010). In the absence of EGF signal in our HBSS starvation media, it is likely that DHT is not sufficient to elicit the EGFR mediated response and induce SNAT2 recruitment.

5.3.4 Limitations

During this chapter certain limitations arose. Due to the limited availability of the radioactive tracers C_{14}MeAIB and C_{14}Isoleucine, only a limited variety of antagonists were used. More work is also needed to assess the use of EGF agonists in starvation conditions to provide further evidence to the non-genomic acute pathway of AA transporter recruitment. See limitations section 2.14 for all experimental limitations.

Chapter 6: Conclusion

6.1 Effects of Ageing on Mice Skeletal Muscle

6.2 Effects of DHT treatment on ageing

6.3 Study of SNAT2 and LAT2 recruitment

6.4 SNAT2 plasmid transfection

6.5 SNAT2 and LAT2 transceptor function

6.6 Significant findings

6.7 Further Work

6.1 Effects of ageing on mice skeletal muscle

During these experiments, we have uncovered several potentially novel findings. The preliminary work in Chapter 3 has set out the groundwork for elucidating some of the mechanisms at play in age related muscle dysfunction. Our data suggests that there is a marked decline in mice skeletal muscle size and function with ageing. In the studies of the effects of ageing on skeletal muscle a significant decrease in most measured parameters have been shown: total muscle weight (fig 3.1A), muscle to total weight ratio (Fig 3.1B), SNAT2/LAT2 protein expression (figs 3.2A-B), AA transport levels (figs 3.3A-C), protein synthesis (figs 3.4A-B), and SNAT2 mRNA levels (figs 3.5A-B) in our elderly cohorts compared to mature mice.

As expected, we found a significant decrease in total muscle weight in mice which only occurs in the elderly group, and not in young or mature (Fig 3.1A). Young and mature mice showed statistically similar muscle weights. Age related muscle dysfunction manifests as skeletal muscle atrophy and reduced mass, explaining the findings in our elderly cohort.

The observed reduction in muscle mass to total body weight ratio (Fig 3.1B) was also predicted as this is a product of adipose tissue accumulation and hallmark of sarcopenic obesity. The ratio of muscle mass in comparison to total body weight is reduced in a linear fashion, with a steady decline shown between age groups. This suggests the accumulation of adipose tissue is a part of normal ageing in these animals, possibly partially attributed to the levels of anabolic hormones which also decline in a gradual fashion throughout life (Chen et al., 2015a). Levels of anabolic steroids are unlikely to be the sole reason behind this, as the difference in testosterone levels between the young and mature animals is negligible compared to the difference between mature and elderly cohorts. This suggests that another factor is at play, whether that be metabolic changes or perhaps a result of reduced physical activity of the mice with ageing.

As fat tissue is abundant in aromatase, an increasing amount of testosterone is converted to oestrogen with greater obesity (Chan et al., 2014). The increase in adipose cell size seen in obese human patient drives a metabolic cycle that results in decreases in testosterone levels (Bekaert et al., 2015). It is possible that fat tissue

accumulation therefore is a self-perpetuating cycle in the mice cohorts, that occur throughout the lifespan only reaching a measurable detrimental effect on muscle function once an animal has reached a critical elderly age. It should be noted that only three age points were used in our experiments however, which limits extrapolation of these effects on the broader course of the mice lifespan (see experimental limitations 2.14).

It has been shown in Chapter 3 that age related muscle dysfunction affects some muscle types more than others. It is generally believed that ageing affects mainly type 2 fibres while sparing type 1 fibres in humans (Lexell et al., 1988, Balagopal et al., 2001). This effect has been seen repeatedly in our experiments. The fast twitch fibres showed a greater reduction in both SNAT2 and LAT2 protein levels, AA transport and protein synthesis with ageing compared to their slow twitch counterparts. In other words, slow twitch muscle was more resistant to detrimental age induced changes.

The mechanism underlying this observation remains unknown. It has been shown that fast twitch EDL mice skeletal muscle undergo much greater denervation compared to slow twitch SOL (Chai et al., 2011). The fibre transition observed by Chai et al. involved a trend toward the phenotype majority in a given muscle, in other words in slow SOL there was a fast to slow fibre type transition observed, while in fast muscle there was a slow to fast transition (Gannon et al., 2009). Considering that the fast twitch fibres are more prone to a loss in enervation and subsequent atrophy, it makes sense that our fast fibres show a greater overall decline in function when compared to slow muscle.

It has been shown in chapter 3 (Figures 3.4A and 4.3A) that the rate of protein synthesis, regardless of age group, is consistently higher in slow-twitch predominant muscle as opposed to corresponding fast-twitch muscle. This finding is supported by techniques measuring in vivo muscle protein synthesis (Chen et al., 2015a). It has been shown that exercise upregulates the expression of AR density in both skeletal muscle fibre types, in this way modulating the local anabolic response to the same circulating testosterone levels and resulting in increased hypertrophy of the muscle (Aizawa et al., 2011, Horii et al., 2016). It is plausible that in mice, the slow twitch SOL undergoes more frequent use, which leads to increased androgen receptor expression and thus

higher response to DHT. It should also be noted that he results from Chapter 3 show that the drop in amino acid transport associated with ageing is relatively proportional to the decrease in protein synthesis, suggesting a deficiency in the synthesis of amino acids into proteins in aged muscle is unlikely.

Protein synthesis declines with age in both fibre types. However, we have shown that the magnitude of decrease is lower in slow twitch fibres, which appear to be more resistant to ageing (3.4A-B). Although a number of studies have reported a loss in mixed muscle and myofibrillar proteins with age (Welle et al., 1993, Rooyackers et al., 1996, Balagopal et al., 1997), these particular studies were performed on muscle biopsies derived from humans. As most muscles in the body consist of a mixture fast-twitch and slow-twitch fibres, from these studies it is difficult to assess exactly which of these fibres are affected most by ageing.

We can relate these findings to development of sarcopenic muscle dysfunction. The loss of fast twitch muscle has been shown in sarcopenia with the use of other analytical techniques (Deschenes et al., 2013). Consistent with our work, ageing has also been shown be Deschenes et al. to decrease the fractional synthetic rates of type 2a and 2x myosin heavy chains in human muscle biopsies. Together, these findings suggest that sarcopenia may arise from the sum of an age-dependent fibre type shift and overall decline in muscle protein synthesis.

As shown before in this thesis, the reduction in protein synthesis is coupled with a decline in both SNAT2 and LAT2 protein (Figs 3.4A-B). The effect on amino acid transporter protein levels directly mirrors the effects of overall transport in muscle fibre types. Like the decrease in protein synthesis with age, the decline in SNAT2 expression was greater in the fast-twitch fibres than in the slow-twitch ones.

When looking at SNAT2 expression on the mRNA level, a significant reduction has been found with ageing (3.5A-B). It would seem logical that this would translate to a lower response to DHT, however this was not seen. SNAT2 levels rise roughly proportionally to LAT2 levels with DHT treatment. This is likely because DHT, especially at physiological levels, does not initiate total recruitment of all available SNAT2 from internal storage pools. In other words, total SNAT2 reserve in the cell is higher than

can be additionally recruited with DHT treatment. It can be speculated that the decrease in protein synthesis and SNAT2 expression with age are linked and that they may be directly responsible for the development of sarcopenia.

On the other hand, while it has been shown that the levels of LAT2 protein decline with age (3.5C-D), this reduction is seen independent of mRNA levels, which remain stable through the lifespan of the mice. Again, this does not seem to effect LAT2 recruitment in response to DHT in elderly cohorts. We can speculate that as with SNAT2, physiological levels of DHT do not induce the total recruitment of LAT2 from intracellular pools. In fact, as seen in the pronounced response of LAT2 to starvation in mature mice, (Fig 5.3) there is a significant reserve of LAT2 in the cell.

Table 6.1: Summary of Effects of Ageing on Mice Skeletal Muscle

Baseline Ageing	**MATURE FAST**	**MATURE SLOW**	**ELDERLY FAST**	**ELDERLY SLOW**
SNAT2 Protein	●●	●●●●	●	●●●
LAT2 Protein	●●●●	●●●●	●	●●
SNAT2 mRNA	●●	●●●●	●	●●
LAT2 mRNA	●●●	●●	●●●	●●
C_{14}MeAIB Transport	●●●	●●●●	●	●●
C_{14}Isoleucine Transport	●●	●●●	●	●●
Protein Synthesis	●●	●●●	●	●●

6.2 Effects of DHT treatment on ageing

Total and free plasma testosterone reduces gradually with ageing in human subjects, leading to almost 50% of men defined as hypogonadal at the age of 80 (Stanworth and Jones, 2008). Ageing has the opposite effect on the plasma concentration of steroid hormone binding globulin which increase with age (Vermeulen et al., 1971). This severely curtails the levels of free testosterone in plasma and hence its bioavailability. Moreover, the decrease in plasma testosterone concentrations parallels the decline in skeletal muscle mass and function with age suggesting again that the reduced bioavailability of DHT may be one of the causes of sarcopenia.

Our findings also show that treating small muscle fibre bundles, isolated from the elderly mice, with physiological concentrations of DHT rescues the age-dependent decline in amino acid transport in both muscle fibre types. However, the effects of DHT treatment, like those of age related decline on protein synthesis, were greater in the fast-twitch than in the slow-twitch fibres (Figs 4.3A-B). DHT treatment was also accompanied by an increase in the expression of SNAT2 and LAT2 expression in both fibre types (Figs 4.1A-B).

Although the exact non- genomic mechanism involved was not investigated fully at present, we suggest that it involves the recruitment of SNAT2 from an intracellular compartment. The expression of SNAT2 is regulated by many factors including pH, amino acid deprivation growth factors and hormones (Hyde et al., 2002). These factors have been shown to rapidly increase the function and expression of SNAT2, on the scale of minutes rather than hours (Hundal et al. 1994), providing further evidence for the storage compartment theory. It is also thought that these effects act independently from changes in transcription and translation rates, as these require a longer timescale then our 1hr experiments (Oliver et al., 2013).

Table 6.2: Summary of the Effects of DHT treatment on Elderly Mice Skeletal Muscle.

DHT Treatment	MATURE FAST	MATURE SLOW	ELDERLY FAST	ELDERLY SLOW
SNAT2 Protein	●●●	●●●●	●●	●●●
LAT2 Protein	●●●●	●●●●	●●●●	●●●
C_{14}MeAIB Transport	●●●	●●●●	●●●	●●
C_{14}Isoleucine Transport	●●	●●●	●●	●●
Protein Synthesis	●●	●●●	●●	●●

6.3 Study of SNAT2 and LAT2 recruitment

The experimental data suggests that the stimulation of the recruitment of SNAT2 from an intracellular compartment by DHT is similar in manner to the effects of insulin on GLUT4 activation (Hyde et al., 2002). There are many parallels which can be drawn from the study of GLUT4 function. Because GLUT4 mechanisms are so extensively studied (Huang and Czech, 2007), study of this transporter system gives us a broader perspective as to which avenues to test to assess likely mechanisms involved. This, coupled with limited research in other system A transporters showing storage vesicle pool localisation and recruitment in response to insulin (Hyde et al., 2002) led to the initial hypothesis of SNAT2 and LAT2 recruitment from vesicle model.

To test the theory of SNAT2 being held and utilised inside intracellular vesicles, chloroquine was used to inhibit vesicle movement to the cell membrane (figures 4.4A and 4.4B). The protein uptake studies were done as noted before using untreated mouse skeletal muscle tissue, myoblasts and myotubes. Groups were split into control, DHT treated, and Chloroquine and DHT plus chloroquine treated. Chloroquine completely blunted the DHT induced SNAT2 and LAT2 increase in AA transport (Figures 4.4A and 4.4B). These results were confirmed in the Immunohistochemical image studies, (Figure 4.8B) showing increases in signal in DHT treated groups, and no difference to controls in chloroquine and DHT + chloroquine groups.

The work on SNAT2 and LAT2 transporters in starvation conditions resulted in several interesting findings. We saw that with complete blockage of SNAT2 by MeAIB saturation in normal media conditions, LAT2 activity would drop to around 20% of normal transport. This is most likely due to the gradient of small neutral amino acids being disrupted by impaired transport of any usable substrate for LAT2. This suggests that LAT2 is dependent on SNAT2 to function at full capacity.

It also shows that targeting SNAT2 by blocking can artificially reduce LAT2 transport without initiating proteolysis and an autophagic response. This is an important finding, because LAT2 is a potential therapeutic target that is over expressed in numerous cancer cells (Fuchs and Bode, 2005, Nawashiro et al., 2006, Sakata et al., 2009). It also shows that SNAT2 is likely the predominant supplier of small neutral amino acids inside the mouse skeletal muscle cell.

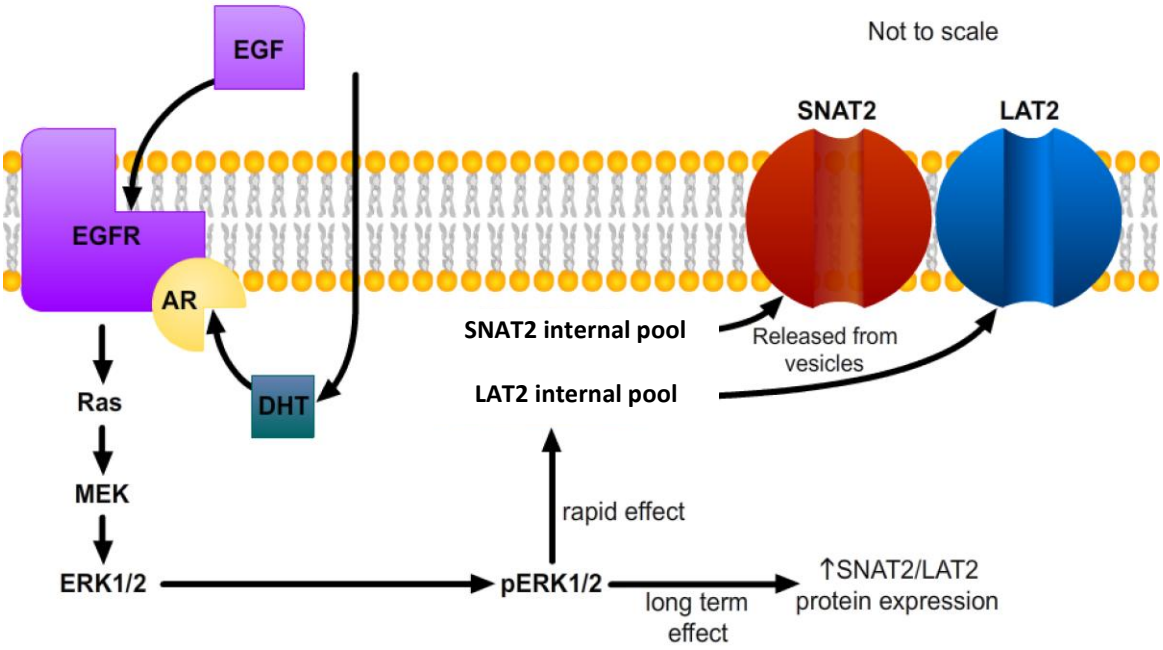

Figure 6.4 Proposed mechanism of SNAT2 and LAT2 recruitment form intracellular vesicle pools in response to DHT. EGF in needed for the acute non-genomic DHT response, as evidenced by its lack of efficacy under starvation conditions. EGFR signals through RAF/MEK/ERK1/2 causing ERK phosphorylation. pERK1/2 causes recruitment from vesicular pools as well as long term increase in transcription. Image produced with Adobe Flash.

6.4 SNAT2 plasmid transfection

The upregulation of SNAT2 by means of plasmid transfection has also yielded interesting results. The studies in Chapter 5 have shown that with upregulation of SNAT2, no further transport over baseline was seen with LAT2 (figure 5.1E). Therefore, LAT2 function at baseline SNAT2 transport level is likely not limited by small neutral AA availability as there is likely more than sufficient reserve created by SNAT2 under control conditions. Increasing this cytoplasmic small neutral amino acid reserve by artificially increasing SNAT2 levels does not increase transport through LAT2 even with the use of DHT (figure 5.4). DHT treatment in transfected cells does elicit a heightened response through SNAT2 (Fig 5.2A) showing that the increase in reserve SNAT2 from transfection is being recruited to a greater extent. Starvation also induces an increased response in C_{14}MeAIB transport (Fig5.3A).

The work shows further evidence for an interaction between the EGFR and androgen receptor in skeletal muscle. This phenomenon has been shown to be true in prostate cells (Bonaccorsi et al., 2004). It has been shown that EGF in combination with DHT elicit a greater anabolic response than DHT alone (Mukherjee and Mayer, 2008). There is evidence that EGFR signalling is greatly potentiated by DHT, suggesting that DHT acts as a coactivator of EGFR (Bonaccorsi et al., 2004, Lee et al., 2016a). However, a baseline EGF level is necessary for this pathway to function and to maintain healthy muscle function. These findings explain why under starvation conditions in HBSS (devoid of EGF) DHT treatment even at a high level of 4nM does not elicit any additional response over untreated cells (figure 5.6B).

6.5 SNAT2 and LAT2 transceptor function

There have been many recent advancements in the field of transceptor research in the recent years. This has been especially plentiful in the study of yeast cells, where numerous transcectors have been identified (Conrad et al., 2014). These transporters have been shown to be integral in cell signalling, namely in the mTOR pathway (Van Zeebroeck et al., 2014).

Recently, an uncharactarised transported related to SNAT2 and member of the SLC38 solute carrier family, SLC38A9 was the centre of research. An 11-pass transmembrane protein, SLC38A9 has been found to be involved in mTOR signalling through the Rag-Ragulator complex in response to varying nutrient levels (Jung et al., 2015, Rebsamen and Superti-Furga, 2016). These findings provide support for the crucial role of these related transporters in regulating homeostasis.

The studies with JNK inhibitor SP600125 have yielding promising results. As graphs 5.6B and 5.6C show, JNK inhibition completely abolishes the starvation induced proteolytic mechanism that greatly upregulates LAT2 function. It is possible that this is because SNAT2 is locked into a non-signalling conformation (signified as SNAT2^), this LAT2 induction is significantly attenuated. It is plausible that both SNAT2 and LAT2 signal through JNK, which induces proteolysis inside the cell providing substrate for LAT2 (and to a much lesser degree SNAT2). The current research implicates the JNK pathway in SNAT2 signalling in response to starvation (Kashiwagi et al., 2009), however there is little research in elucidating LAT2 signalling at present.

In the blocking experiments using saturable concentrations of MeAIB in full media (Fig 5.5A), LAT2 transport was blocked approximately 80%. However, when this same experiment was used after starvation (Fig 5.5B) the result of MeAIB blocking was only an approximate 50% reduction in the starvation induced increase in C_{14}Isoleucine. This provides evidence that under normal conditions (full media) reducing SNAT2 transport reduces LAT2 transport, whilst under starvation both SNAT2 and LAT2 are likely both inducing a proteolytic response through JNK signalling. This is why SNAT2 block only elicits a 50% reduction in starved conditions. Fig 6.5 Illustrates a normal starvation response, compared to MeAIB block in Fig 6.6.

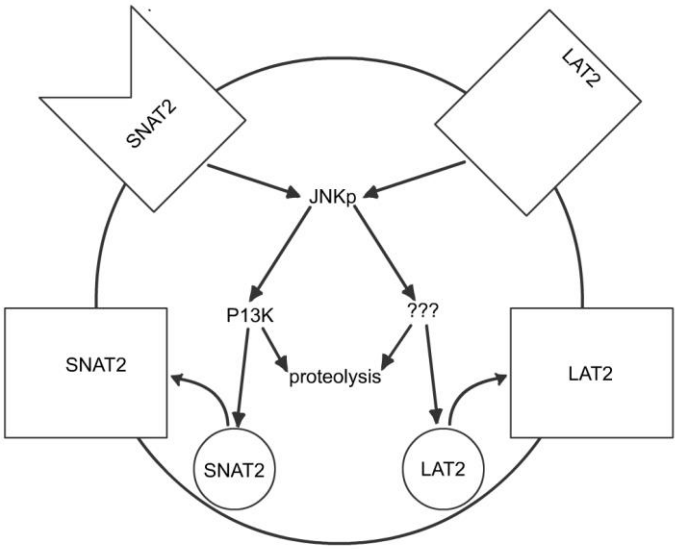

Figure 6.5 SNAT2 and LAT2 response in starved conditions. Proposed mechanism for response of SNAT2 and LAT2 to starvation. Both trigger a JNK mediated response which initiates proteolysis resulting in intracellular AA increase and self-upregulation of both transporters. Image created using Adobe Illustrator.

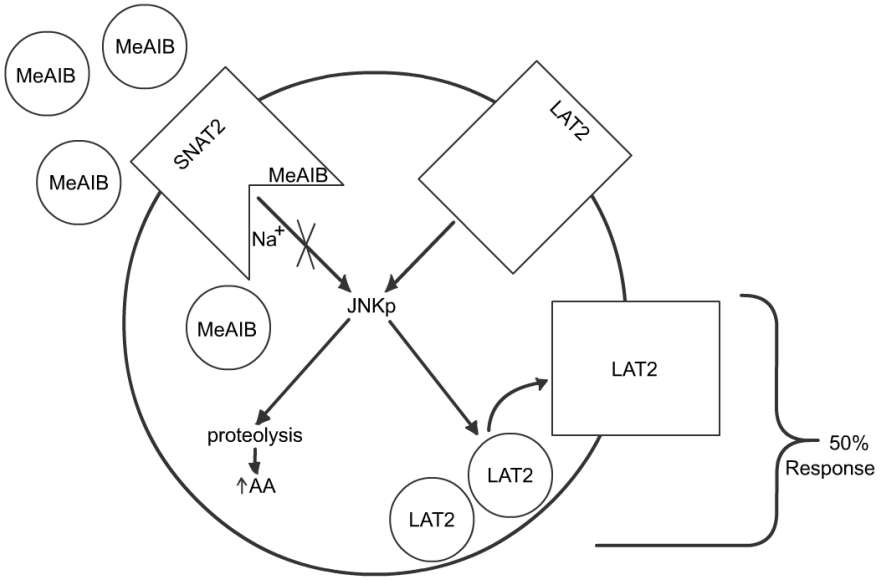

Figure 6.6 MeAIB saturable block of SNAT2 in starvation conditions. Only a partial reduction in starvation induced upregulation is possible due to the remaining LAT2 transceptor signalling, initiating AA release and its own upregulation. Image created with Adobe Illustrator.

A novel nomenclature is proposed of identifying SNAT2 and LAT2 transporter confirmations in order to differentiate signalling from non-signalling conformations of the protein. SNAT2^{V} denotes an outward facing protein conformation that is ready to accept substrate, while SNAT2^ donates an inward locked conformation that is associated with AA saturation and does not initiate JNK signalling. There is evidence of this conformational change in the clear discrimination of SNAT2 between extracellular and intracellular AA concentrations (Hundal and Taylor, 2009).

Once the substrates leave SNAT2 and enter the cytoplasm, the conformation is returned to SNAT^{V} state. When using MeAIB in saturable conditions, there is a sufficient quantity of MeAIB inside the cell to prevent the MeAIB substrate from entering the cell, it being kinetically more stable at the transporter site (Nardi et al., 2015).

It is proposed here that the stable SNAT^{V} conformation is associated in JNK transmission and initiation of proteolysis. Under normal starvation conditions, the SNAT2 transport is found predominantly in this state due to lack of substrate needed for conformational shift. Under MeAIB saturation, the transporter finds itself locked into the unstable SNAT^{V} conformation, which cannot initiate JNK transmission and downstream proteolysis. In this way MeAIB saturation blunts the amino acid deprivation response.

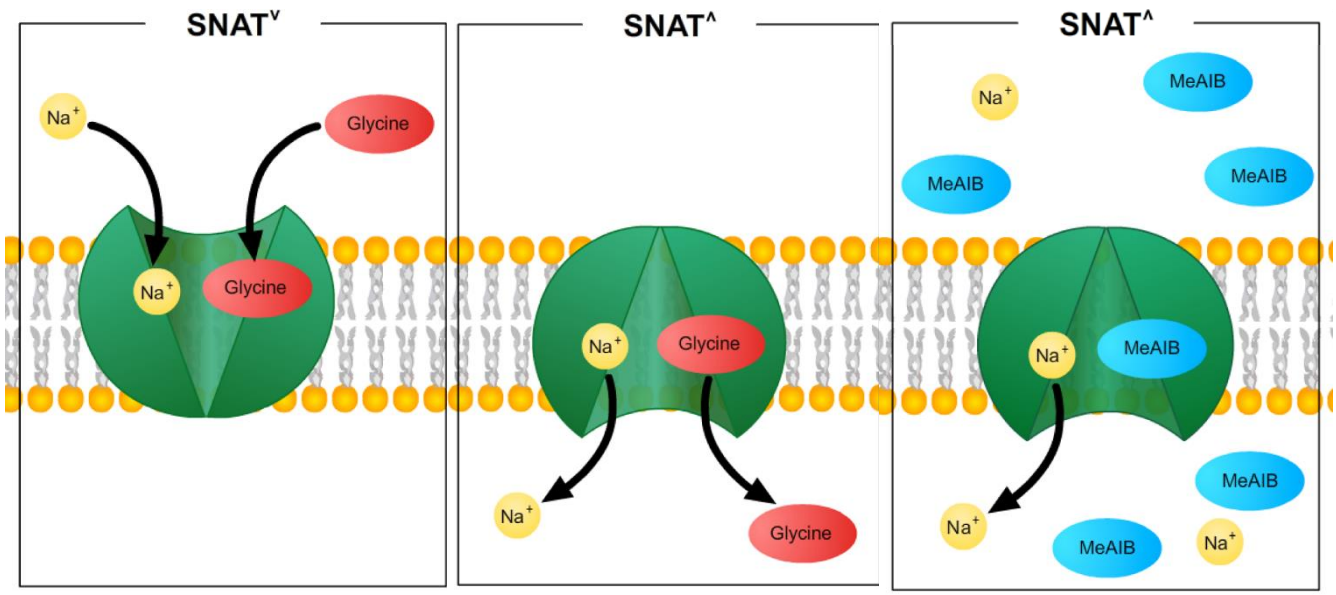

Figure 6.7 SNAT2 transceptor function Proposed two configuration states of SNAT2. SNAT^{V} protein configuration accepts one sodium ion and one small amino acid. The gradient of sodium pushes the sodium molecule further into the complex, causing a conformational change to SNAT$^{\wedge}$. SNAT^{V} is the predominant "stable" conformation under starvation conditions and potentially facilitates JNK signalling. A saturation of MeAIB results in a more preferable SNAT$^{\wedge}$ conformation due to the reduced dissociation of MeAIB from the active site, resulting in no JNK signalling.

6.6 Significant findings

1. Elderly CD-1 mice exhibit a marked reduction in EDL and soleus muscle weight compared to young and mature mice. They also show a linear increase in total body weight to EDL and SOL weight ratio.
2. SNAT2 and LAT2 protein levels are markedly reduced in elderly CD-1 mice as compared to mature mice.
3. Transport of C_{14}MeAIB, C_{14}Isoleucine, and protein incorporation is reduced in elderly CD-1 mice compared to mature mice. The extent of reduction is greater in fast twitch EDL than in slow twitch soleus. Slow twitch muscles are more resistant to age related amino acid transport dysfunction.
4. mRNA expression of SNAT2 is reduced in elderly CD-1 mice compared to controls but LAT2 mRNA levels remains statistically the same with age.
5. DHT treatment increases C_{14}MeAIB and C_{14}Isoleucine transport into cells. It also increases SNAT2 and LAT2 protein level.
6. Both Chloroquine and Flutamide treatment completely blunt the DHT effect. This suggests that SNAT2/LAT2 are recruited from an intracellular pool and that an AR element is required for DHT signalling.
7. Under starvation conditions, LAT2 exhibits a much greater increase in transport than SNAT2.
8. SNAT2 saturable block with MeAIB results in 77% reduction of baseline transport in LAT2. This suggests baseline SNAT2 transport is chiefly necessary to supply small amino acid gradient to drive LAT2.
9. SNAT2 upregulation using expression vector has no effect on LAT2 function. This shows that increasing the SNAT2 reserve pool does not proportionally increase LAT2 transport and is likely not a limiting step.
10. SNAT2^, SNAT2^{v}, LAT2^, and LAT2^{v} nomenclature proposed to identify stable signalling conformations of these transporters, and unstable extracellular binding conformations.
11. Data suggests that it is possible that SNAT2 and LAT2 signal through JNK to initiate proteolysis which mainly drives LAT2 transport under starvation conditions.

6.7 Further Work

As in all fields of science, with answers often come more questions. There are many exciting developments under way in the field of muscle ageing. The best way forward is to study individual pathways in further detail to understand the role anabolics such as DHT play in concert with other biological processes on the broader scope of organism ageing.

With further studies, it would be possible to better understand the mechanism DHT is using to activate the movement of vesicles containing SNAT2 and LAT2 to the cellular membrane. Live cell imaging can be used to study the internal localisation of SNAT2 and LAT2 in response to stimuli. During the course of this work, LAT2 was found to be very difficult to image successfully (see experimental limitations 2.14). Therefore, better antibodies and imaging techniques are needed to quantify LAT2 localisation accurately.

The transceptor action of SNAT2 and LAT2 need to be further elucidated. Specifically, to understand by what means SNAT2 is initiating proteolysis. This could be done using more specific inhibitors of different steps of the JNK and PI3K cascade. It is also likely that LAT2 serves a similar transceptor function. Molecular modelling of this receptor has identified possible interaction domains between PKA and PKB (Pochini et al., 2014). These potential binding sites need further research, and the means in which LAT2 is capable of signalling needs to be elucidated.

Inhibition of specific pathways in JNK/ PI3K pathway would enable us to elucidate the phosphorylation cascades at work. As stated before, it is suggested that DHT is signalling through the EGFR and MAPK/ERK pathway to initiate recruitment of amino acid transporters. The exact nature of DHT binding to initiate this pathway is still not known. Molecular modelling of the EGF receptor complete with identification of an androgen responsive element or evidence of direct AR interaction would prove the theory that DHT is acting as a coactivator of the EGFR. Specifically, we require more evidence that DHT is working as a co activator of EGFR receptor, which in conjunction with a baseline signal leads to increased phosphorylation in the ERK1/ERK2 cascade.

Although experiments using inhibitors are useful, molecular imaging would give a clearer and more definite picture of what is happening.

One recurrent problem in these studies was the poor binding of our LAT2 antibodies to the LAT2 transporter. This led to long incubation times due to very low initial signals. It is not surprising that more robust antibodies are not available, as LAT2 has only been identified relatively recently. Therefore, the creation of improved LAT2 antibodies would aid in the quantification of this important amino acid transporter. Better antibodies would allow for running live cell studies with adequate precision. Naturally as current antibodies are refined, better examples should be available.

These experiments have studied only the acute, non-genomic pathway of DHT induced AA transporter recruitment. Therefore, further work is necessary in running in vivo DHT treatment in mice. This would be a better assessment of the suitability of DHT as a long-term treatment of sarcopenic muscle dysfunction in elderly mice. The most efficient way of doing this would be using sub dermal injections of a DHT impregnated pellet (McCullough et al., 2012, Okabe et al., 2013). This would eliminate the need for frequent injections and limit the stress caused to the animals. By exposing the animals to DHT for long durations, we could assess the effects not only of recruitment, but also of mRNA expression, total reserve protein, and AR expression. This would also elucidate any negative feedback and sensitisation issues surrounding chronic DHT treatment. Rudimentary safety profile of such treatment could also be assessed.

In an in vivo model, it would also be possible to treat the animals using MeAIB in the aim to stop cell proliferation and prevent or reverse the growth of tumors. Very little research has been done in this regard. One group showing MeAIB inhibiting liver collagen formation after injury, showed that MeAIB halts the cell cycle by limiting nutrient availability (Freeman et al., 2004). The use of MeAIB did not show any overt toxicity in this study. Because LAT2 is increasingly found to be upregulated in tumours (Barollo et al., 2016), MeAIB could be used to artificially lower transport through LAT2 by reducing the amount of small neutral amino acids available for co transport of branched chain AAs. In this way MeAIB could be used to control both AA type levels in the cell, without initiating proteolysis as SNAT2 would possibly remain in the unstable

SNAT2^ confirmation, which is not conductive to pro proteolytic signalling. This could be of great therapeutic benefit in the treatment of malignancy and needs further study.

The breakdown or recycling of both SNAT2 and LAT2 also require further study. To do this, one would need to look at levels of post translational modifications such as ubiquitination on SNAT2 and LAT2. Recent studies have suggested that mTOR might have an action on ubiquitination of SNAT, which in turn reduces its recruitment (Chen et al., 2015b). It is necessary to assess the extent of the role these ubiquitination steps serve in overall transporter function.

There is also scope to study the effect of DHT on satellite cell number in greater detail. It has long been believed that satellite cell reserve decreases with age. It is known from animal and human studies, that satellite cell density is heavily dependent on the fibre type (Mackey et al., 2014). It is also excepted that ageing causes a transition from fast twitch fibres to a slow phenotype (Neunhauserer et al., 2011). The relationship between these two factors needs further clarification. It is possible that the fibre type transition is a compensatory response to loss in satellite cell reserve.

More work is required on assessing the extent of 5αReductase expression in different fibre types. Preliminary work shows that the cause of resistance to ageing we have seen in slow muscle fibres is likely related to increased expression of 5αReductase in this tissue. This means of course, that more testosterone is converted to DHT, exerting a greater anabolic response. However, from our experience the quantities of 5α-Reductase present are so small that a more sensitive quantification methods are needed in the study of skeletal muscle.

References

AIZAWA, K., IEMITSU, M., MAEDA, S., MESAKI, N., USHIDA, T. & AKIMOTO, T. 2011. Endurance exercise training enhances local sex steroidogenesis in skeletal muscle. *Med Sci Sports Exerc,* 43**,** 2072-80.

AKINLEYE, A., AVVARU, P., FURQAN, M., SONG, Y. & LIU, D. 2013. Phosphatidylinositol 3-kinase (PI3K) inhibitors as cancer therapeutics. *J Hematol Oncol,* 6**,** 88.

ALDINGER, K. A., SOKOLOFF, G., ROSENBERG, D. M., PALMER, A. A. & MILLEN, K. J. 2009. Genetic variation and population substructure in outbred CD-1 mice: implications for genome-wide association studies. *PLoS One,* 4**,** e4729.

ANDERSEN, J. L. 2003. Muscle fibre type adaptation in the elderly human muscle. *Scand J Med Sci Sports,* 13**,** 40-7.

ANTHONY, J. C., YOSHIZAWA, F., ANTHONY, T. G., VARY, T. C., JEFFERSON, L. S. & KIMBALL, S. R. 2000. Leucine stimulates translation initiation in skeletal muscle of postabsorptive rats via a rapamycin-sensitive pathway. *J Nutr,* 130**,** 2413-9.

AUDY, M. C., VACHER, P. & DULY, B. 1996. 17 beta-estradiol stimulates a rapid Ca2+ influx in LNCaP human prostate cancer cells. *Eur J Endocrinol,* 135**,** 367-73.

BAIRD, F. E., PINILLA-TENAS, J. J., OGILVIE, W. L., GANAPATHY, V., HUNDAL, H. S. & TAYLOR, P. M. 2006. Evidence for allosteric regulation of pH-sensitive System A (SNAT2) and System N (SNAT5) amino acid transporter activity involving a conserved histidine residue. *Biochem J,* 397**,** 369-75.

BALAGOPAL, P., ROOYACKERS, O. E., ADEY, D. B., ADES, P. A. & NAIR, K. S. 1997. Effects of aging on in vivo synthesis of skeletal muscle myosin heavy-chain and sarcoplasmic protein in humans. *Am J Physiol,* 273**,** E790-800.

BALAGOPAL, P., SCHIMKE, J. C., ADES, P., ADEY, D. & NAIR, K. S. 2001. Age effect on transcript levels and synthesis rate of muscle MHC and response to resistance exercise. *Am J Physiol Endocrinol Metab,* 280**,** E203-8.

BANERJEE, A., ANURADHA, MUKHERJEE, K. & KRISHNA, A. 2014. Testicular glucose and its transporter GLUT 8 as a marker of age-dependent variation and its role in steroidogenesis in mice. *J Exp Zool A Ecol Genet Physiol,* 321**,** 490-502.

BAROLLO, S., BERTAZZA, L., WATUTANTRIGE-FERNANDO, S., CENSI, S., CAVEDON, E., GALUPPINI, F., PENNELLI, G., FASSINA, A., CITTON, M., RUBIN, B., PEZZANI, R., BENNA, C., OPOCHER, G., IACOBONE, M. & MIAN, C. 2016. Overexpression of L-Type Amino Acid Transporter 1 (LAT1) and 2 (LAT2): Novel Markers of Neuroendocrine Tumors. *PLoS One,* 11**,** e0156044.

BASARIA, S. & DOBS, A. S. 2001. Hypogonadism and androgen replacement therapy in elderly men. *Am J Med,* 110**,** 563-72.

BECKER, C., SEVILLA, L., TOMA, S. E., PALACIN, M., ZORZANO, A. & FISCHER, Y. 2001. The Endosomal Compartment Is an Insulin-Sensitive Recruitment Site for GLUT4 and GLUT1 Glucose Transporters in Cardiac Myocytes. *Endocrinology,* 142**,** 5267-5276.

BEKAERT, M., VAN NIEUWENHOVE, Y., CALDERS, P., CUVELIER, C. A., BATENS, A. H., KAUFMAN, J. M., OUWENS, D. M. & RUIGE, J. B. 2015. Determinants of testosterone levels in human male obesity. *Endocrine,* 50**,** 202-11.

BENTEN, W. P., LIEBERHERR, M., SEKERIS, C. E. & WUNDERLICH, F. 1997. Testosterone induces Ca2+ influx via non-genomic surface receptors in activated T cells. *FEBS Lett,* 407**,** 211-4.

BENTEN, W. P., LIEBERHERR, M., STAMM, O., WREHLKE, C., GUO, Z. & WUNDERLICH, F. 1999. Testosterone signaling through internalizable surface receptors in androgen receptor-free macrophages. *Mol Biol Cell,* 10**,** 3113-23.

BERNET, J. D., DOLES, J. D., HALL, J. K., KELLY TANAKA, K., CARTER, T. A. & OLWIN, B. B. 2014. p38 MAPK signaling underlies a cell-autonomous loss of stem cell self-renewal in skeletal muscle of aged mice. *Nat Med,* 20**,** 265-71.

BEVINGTON, A., BROWN, J., BUTLER, H., GOVINDJI, S., K, M. K., SHERIDAN, K. & WALLS, J. 2002. Impaired system A amino acid transport mimics the catabolic effects of acid in L6 cells. *Eur J Clin Invest,* 32**,** 590-602.

BHASIN, S. & BUCKWALTER, J. G. 2001. Testosterone supplementation in older men: a rational idea whose time has not yet come. *J Androl,* 22**,** 718-31.

BHASIN, S., STORER, T. W., BERMAN, N., YARASHESKI, K. E., CLEVENGER, B., PHILLIPS, J., LEE, W. P., BUNNELL, T. J. & CASABURI, R. 1997. Testosterone replacement increases fat-free mass and muscle size in hypogonadal men. *J Clin Endocrinol Metab,* 82**,** 407-13.

BIRBRAIR, A. & DELBONO, O. 2015. Pericytes are Essential for Skeletal Muscle Formation. *Stem Cell Rev,* 11**,** 547-8.

BONACCORSI, L., CARLONI, V., MURATORI, M., FORMIGLI, L., ZECCHI, S., FORTI, G. & BALDI, E. 2004. EGF receptor (EGFR) signaling promoting invasion is disrupted in androgen-sensitive prostate cancer cells by an interaction between EGFR and androgen receptor (AR). *Int J Cancer,* 112**,** 78-86.

BONETTO, A., ANDERSSON, D. C. & WANING, D. L. 2015. Assessment of muscle mass and strength in mice. *Bonekey Rep,* 4**,** 732.

BOULPAEP, W. F. B. E. L. 2012. *Medical Physiology* Elsevier.

BRACY, D. S., HANDLOGTEN, M. E., BARBER, E. F., HAN, H. P. & KILBERG, M. S. 1986. Cis-inhibition, trans-inhibition, and repression of hepatic amino acid transport mediated by System A. Substrate specificity and other properties. *J Biol Chem,* 261**,** 1514-20.

BRADFORD, M. M. 1976. A rapid and sensitive method for the quantitation of microgram quantities of protein utilizing the principle of protein-dye binding. *Anal Biochem,* 72**,** 248-54.

BROOKS, N. E., SCHUENKE, M. D. & HIKIDA, R. S. 2009. No change in skeletal muscle satellite cells in young and aging rat soleus muscle. *J Physiol Sci,* 59**,** 465-71.

BROOKS, R. V. 1975. Androgens. *Clin Endocrinol Metab,* 4**,** 503-20.

BROWN, J. C., HARHAY, M. O. & HARHAY, M. N. 2016. Sarcopenia and mortality among a population-based sample of community-dwelling older adults. *J Cachexia Sarcopenia Muscle,* 7**,** 290-8.

BROZINICK, J. T., JR., MCCOID, S. C., REYNOLDS, T. H., WILSON, C. M., STEVENSON, R. W., CUSHMAN, S. W. & GIBBS, E. M. 1997. Regulation of cell surface GLUT4 in skeletal muscle of transgenic mice. *Biochem J,* 321 (Pt 1)**,** 75-81.

BRUCHOVSKY, N. & WILSON, J. D. 1968. The conversion of testosterone to 5-alpha-androstan-17-beta-ol-3-one by rat prostate in vivo and in vitro. *J Biol Chem,* 243**,** 2012-21.

CARCAILLON, L., BLANCO, C., ALONSO-BOUZON, C., ALFARO-ACHA, A., GARCIA-GARCIA, F. J. & RODRIGUEZ-MANAS, L. 2012. Sex differences in the association between serum levels of testosterone and frailty in an elderly population: the Toledo Study for Healthy Aging. *PLoS One,* 7**,** e32401.

CATO, A. C., SKROCH, P., WEINMANN, J., BUTKERAITIS, P. & PONTA, H. 1988. DNA sequences outside the receptor-binding sites differently modulate the responsiveness of the mouse mammary tumour virus promoter to various steroid hormones. *EMBO J,* 7**,** 1403-10.

CHAI, R. J., VUKOVIC, J., DUNLOP, S., GROUNDS, M. D. & SHAVLAKADZE, T. 2011. Striking denervation of neuromuscular junctions without lumbar motoneuron loss in geriatric mouse muscle. *PLoS One,* 6**,** e28090.

CHAN, J., SAUVE, B., TOKMAKEJIAN, S., KOREN, G. & VAN UUM, S. 2014. Measurement of cortisol and testosterone in hair of obese and non-obese human subjects. *Exp Clin Endocrinol Diabetes,* 122**,** 356-62.

CHAPMAN, R. E. & MUNRO, S. 1994. Retrieval of TGN proteins from the cell surface requires endosomal acidification. *EMBO J,* 13**,** 2305-12.
CHAUDHRY, F. A., SCHMITZ, D., REIMER, R. J., LARSSON, P., GRAY, A. T., NICOLL, R., KAVANAUGH, M. & EDWARDS, R. H. 2002. Glutamine uptake by neurons: interaction of protons with system a transporters. *J Neurosci,* 22**,** 62-72.
CHEN, C., WANG, J., CAI, R., YUAN, Y., GUO, Z., GREWER, C. & ZHANG, Z. 2016. Identification of a Disulfide Bridge in Sodium-Coupled Neutral Amino Acid Transporter 2(SNAT2) by Chemical Modification. *PLoS One,* 11**,** e0158319.
CHEN, H., JIN, S., GUO, J., KOMBAIRAJU, P., BISWAL, S. & ZIRKIN, B. R. 2015a. Knockout of the transcription factor Nrf2: Effects on testosterone production by aging mouse Leydig cells. *Mol Cell Endocrinol,* 409**,** 113-20.
CHEN, Y. & LIPPINCOTT-SCHWARTZ, J. 2013. Rab10 delivers GLUT4 storage vesicles to the plasma membrane. *Commun Integr Biol,* 6**,** e23779.
CHEN, Y. Y., ROSARIO, F. J., SHEHAB, M. A., POWELL, T. L., GUPTA, M. B. & JANSSON, T. 2015b. Increased ubiquitination and reduced plasma membrane trafficking of placental amino acid transporter SNAT-2 in human IUGR. *Clin Sci (Lond),* 129**,** 1131-41.
CHRISTENSEN, H. N., OXENDER, D. L., LIANG, M. & VATZ, K. A. 1965. The use of N-methylation to direct route of mediated transport of amino acids. *J Biol Chem,* 240**,** 3609-16.
COLMAN, R. J., MCKIERNAN, S. H., AIKEN, J. M. & WEINDRUCH, R. 2005. Muscle mass loss in Rhesus monkeys: age of onset. *Exp Gerontol,* 40**,** 573-81.
CONRAD, M., SCHOTHORST, J., KANKIPATI, H. N., VAN ZEEBROECK, G., RUBIO-TEXEIRA, M. & THEVELEIN, J. M. 2014. Nutrient sensing and signaling in the yeast Saccharomyces cerevisiae. *FEMS Microbiol Rev,* 38**,** 254-99.
CRUZ-JENTOFT, A. J., BAEYENS, J. P., BAUER, J. M., BOIRIE, Y., CEDERHOLM, T., LANDI, F., MARTIN, F. C., MICHEL, J. P., ROLLAND, Y., SCHNEIDER, S. M., TOPINKOVA, E., VANDEWOUDE, M., ZAMBONI, M. & EUROPEAN WORKING GROUP ON SARCOPENIA IN OLDER, P. 2010a. Sarcopenia: European consensus on definition and diagnosis: Report of the European Working Group on Sarcopenia in Older People. *Age Ageing,* 39**,** 412-23.
CRUZ-JENTOFT, A. J., LANDI, F., TOPINKOVA, E. & MICHEL, J. P. 2010b. Understanding sarcopenia as a geriatric syndrome. *Curr Opin Clin Nutr Metab Care,* 13**,** 1-7.
DAVIS, T. A. & FIOROTTO, M. L. 2009. Regulation of muscle growth in neonates. *Curr Opin Clin Nutr Metab Care,* 12**,** 78-85.
DAVIS, T. A., FIOROTTO, M. L., NGUYEN, H. V. & REEDS, P. J. 1989. Protein turnover in skeletal muscle of suckling rats. *Am J Physiol,* 257**,** R1141-6.
DEMONTIS, F., PICCIRILLO, R., GOLDBERG, A. L. & PERRIMON, N. 2013. Mechanisms of skeletal muscle aging: insights from Drosophila and mammalian models. *Dis Model Mech,* 6**,** 1339-52.
DENT, J. R., FLETCHER, D. K. & MCGUIGAN, M. R. 2012. Evidence for a Non-Genomic Action of Testosterone in Skeletal Muscle Which may Improve Athletic Performance: Implications for the Female Athlete. *J Sports Sci Med,* 11**,** 363-70.
DESCHENES, M. R., GAERTNER, J. R. & O'REILLY, S. 2013. The effects of sarcopenia on muscles with different recruitment patterns and myofiber profiles. *Curr Aging Sci,* 6**,** 266-72.
DRUMMOND, G. B. 2009. Reporting ethical matters in the Journal of Physiology: standards and advice. *J Physiol,* 587**,** 713-9.
DUBOIS, V., LAURENT, M., BOONEN, S., VANDERSCHUEREN, D. & CLAESSENS, F. 2012. Androgens and skeletal muscle: cellular and molecular action mechanisms underlying the anabolic actions. *Cell Mol Life Sci,* 69**,** 1651-67.
ERIKSSON, A., KADI, F., MALM, C. & THORNELL, L. E. 2005. Skeletal muscle morphology in power-lifters with and without anabolic steroids. *Histochem Cell Biol,* 124**,** 167-75.

EVANS, K., NASIM, Z., BROWN, J., CLAPP, E., AMIN, A., YANG, B., HERBERT, T. P. & BEVINGTON, A. 2008. Inhibition of SNAT2 by metabolic acidosis enhances proteolysis in skeletal muscle. *J Am Soc Nephrol,* 19**,** 2119-29.

EXNER, G. U., STAUDTE, H. W. & PETTE, D. 1973. Isometric training of rats--effects upon fast and slow muscle and modification by an anabolic hormone (nandrolone decanoate). I. Female rats. *Pflugers Arch,* 345**,** 1-14.

FELDMAN, H. A., LONGCOPE, C., DERBY, C. A., JOHANNES, C. B., ARAUJO, A. B., COVIELLO, A. D., BREMNER, W. J. & MCKINLAY, J. B. 2002. Age trends in the level of serum testosterone and other hormones in middle-aged men: longitudinal results from the Massachusetts male aging study. *J Clin Endocrinol Metab,* 87**,** 589-98.

FERRANDO, A. A., SHEFFIELD-MOORE, M., YECKEL, C. W., GILKISON, C., JIANG, J., ACHACOSA, A., LIEBERMAN, S. A., TIPTON, K., WOLFE, R. R. & URBAN, R. J. 2002. Testosterone administration to older men improves muscle function: molecular and physiological mechanisms. *Am J Physiol Endocrinol Metab,* 282**,** E601-7.

FINK, H. A., EWING, S. K., ENSRUD, K. E., BARRETT-CONNOR, E., TAYLOR, B. C., CAULEY, J. A. & ORWOLL, E. S. 2006. Association of testosterone and estradiol deficiency with osteoporosis and rapid bone loss in older men. *J Clin Endocrinol Metab,* 91**,** 3908-15.

FORADORI, C. D., WEISER, M. J. & HANDA, R. J. 2008. Non-genomic actions of androgens. *Front Neuroendocrinol,* 29**,** 169-81.

FRANCHI-GAZZOLA, R., DALL'ASTA, V., SALA, R., VISIGALLI, R., BEVILACQUA, E., GACCIOLI, F., GAZZOLA, G. C. & BUSSOLATI, O. 2006. The role of the neutral amino acid transporter SNAT2 in cell volume regulation. *Acta Physiol (Oxf),* 187**,** 273-83.

FREEMAN, T. L., THIELE, G. M., KLASSEN, L. W., KLASSEN, B. T. & MAILLIARD, M. E. 2004. N-(methylamino)isobutyric acid inhibits proliferation of CFSC-2C hepatic stellate cells. *Biochem Pharmacol,* 68**,** 223-30.

FRONTERA, W. R., HUGHES, V. A., LUTZ, K. J. & EVANS, W. J. 1991. A cross-sectional study of muscle strength and mass in 45- to 78-yr-old men and women. *J Appl Physiol (1985),* 71**,** 644-50.

FUCHS, B. C. & BODE, B. P. 2005. Amino acid transporters ASCT2 and LAT1 in cancer: partners in crime? *Semin Cancer Biol,* 15**,** 254-66.

GACCIOLI, F., HUANG, C. C., WANG, C., BEVILACQUA, E., FRANCHI-GAZZOLA, R., GAZZOLA, G. C., BUSSOLATI, O., SNIDER, M. D. & HATZOGLOU, M. 2006. Amino acid starvation induces the SNAT2 neutral amino acid transporter by a mechanism that involves eukaryotic initiation factor 2alpha phosphorylation and cap-independent translation. *J Biol Chem,* 281**,** 17929-40.

GANNON, J., DORAN, P., KIRWAN, A. & OHLENDIECK, K. 2009. Drastic increase of myosin light chain MLC-2 in senescent skeletal muscle indicates fast-to-slow fibre transition in sarcopenia of old age. *Eur J Cell Biol,* 88**,** 685-700.

GAZZOLA, R. F., SALA, R., BUSSOLATI, O., VISIGALLI, R., DALL'ASTA, V., GANAPATHY, V. & GAZZOLA, G. C. 2001. The adaptive regulation of amino acid transport system A is associated to changes in ATA2 expression. *FEBS Lett,* 490**,** 11-4.

GELMANN, E. P. 2002. Molecular biology of the androgen receptor. *J Clin Oncol,* 20**,** 3001-15.

GLASER, R. & DIMITRAKAKIS, C. 2015. Testosterone and breast cancer prevention. *Maturitas,* 82**,** 291-5.

GORCZYNSKA, E. & HANDELSMAN, D. J. 1995. Androgens rapidly increase the cytosolic calcium concentration in Sertoli cells. *Endocrinology,* 136**,** 2052-9.

GRINO, P. B., GRIFFIN, J. E. & WILSON, J. D. 1990. Testosterone at high concentrations interacts with the human androgen receptor similarly to dihydrotestosterone. *Endocrinology,* 126**,** 1165-72.

GRUENEWALD, D. A. & MATSUMOTO, A. M. 2003. Testosterone supplementation therapy for older men: potential benefits and risks. *J Am Geriatr Soc,* 51**,** 101-15; discussion 115.

GRUNFELD, C., KOTLER, D. P., DOBS, A., GLESBY, M. & BHASIN, S. 2006. Oxandrolone in the treatment of HIV-associated weight loss in men: a randomized, double-blind, placebo-controlled study. *J Acquir Immune Defic Syndr,* 41**,** 304-14.

HAMDI, M. M. & MUTUNGI, G. 2010. Dihydrotestosterone activates the MAPK pathway and modulates maximum isometric force through the EGF receptor in isolated intact mouse skeletal muscle fibres. *J Physiol,* 588**,** 511-25.

HAMDI, M. M. & MUTUNGI, G. 2011. Dihydrotestosterone stimulates amino acid uptake and the expression of LAT2 in mouse skeletal muscle fibres through an ERK1/2-dependent mechanism. *J Physiol,* 589**,** 3623-40.

HARMAN, S. M., METTER, E. J., TOBIN, J. D., PEARSON, J., BLACKMAN, M. R. & BALTIMORE LONGITUDINAL STUDY OF, A. 2001. Longitudinal effects of aging on serum total and free testosterone levels in healthy men. Baltimore Longitudinal Study of Aging. *J Clin Endocrinol Metab,* 86**,** 724-31.

HATAKEYAMA, H. & KANZAKI, M. 2011. Molecular basis of insulin-responsive GLUT4 trafficking systems revealed by single molecule imaging. *Traffic,* 12**,** 1805-20.

HATANAKA, T., HUANG, W., LING, R., PRASAD, P. D., SUGAWARA, M., LEIBACH, F. H. & GANAPATHY, V. 2001. Evidence for the transport of neutral as well as cationic amino acids by ATA3, a novel and liver-specific subtype of amino acid transport system A. *Biochim Biophys Acta,* 1510**,** 10-7.

HEW, K. E., MILLER, P. C., EL-ASHRY, D., SUN, J., BESSER, A. H., INCE, T. A., GU, M., WEI, Z., ZHANG, G., BRAFFORD, P., GAO, W., LU, Y., MILLS, G. B., SLINGERLAND, J. M. & SIMPKINS, F. 2016. MAPK Activation Predicts Poor Outcome and the MEK Inhibitor, Selumetinib, Reverses Antiestrogen Resistance in ER-Positive High-Grade Serous Ovarian Cancer. *Clin Cancer Res,* 22**,** 935-47.

HIKIDA, R. S. 2011. Aging changes in satellite cells and their functions. *Curr Aging Sci,* 4**,** 279-97.

HORII, N., SATO, K., MESAKI, N. & IEMITSU, M. 2016. Increased Muscular 5alpha-Dihydrotestosterone in Response to Resistance Training Relates to Skeletal Muscle Mass and Glucose Metabolism in Type 2 Diabetic Rats. *PLoS One,* 11**,** e0165689.

HUANG, S. & CZECH, M. P. 2007. The GLUT4 glucose transporter. *Cell Metab,* 5**,** 237-52.

HULMI, J. J., AHTIAINEN, J. P., SELANNE, H., VOLEK, J. S., HAKKINEN, K., KOVANEN, V. & MERO, A. A. 2008. Androgen receptors and testosterone in men--effects of protein ingestion, resistance exercise and fiber type. *J Steroid Biochem Mol Biol,* 110**,** 130-7.

HUNDAL, H. S., BILAN, P. J., TSAKIRIDIS, T., MARETTE, A. & KLIP, A. 1994. Structural disruption of the trans-Golgi network does not interfere with the acute stimulation of glucose and amino acid uptake by insulin-like growth factor I in muscle cells. *Biochem J,* 297 (Pt 2)**,** 289-95.

HUNDAL, H. S. & TAYLOR, P. M. 2009. Amino acid transceptors: gate keepers of nutrient exchange and regulators of nutrient signaling. *Am J Physiol Endocrinol Metab,* 296**,** E603-13.

HUXLEY, A. F. & NIEDERGERKE, R. 1954. Structural changes in muscle during contraction; interference microscopy of living muscle fibres. *Nature,* 173**,** 971-3.

HYDE, R., CHRISTIE, G. R., LITHERLAND, G. J., HAJDUCH, E., TAYLOR, P. M. & HUNDAL, H. S. 2001. Subcellular localization and adaptive up-regulation of the System A (SAT2) amino acid transporter in skeletal-muscle cells and adipocytes. *Biochem J,* 355**,** 563-8.

HYDE, R., CWIKLINSKI, E. L., MACAULAY, K., TAYLOR, P. M. & HUNDAL, H. S. 2007. Distinct sensor pathways in the hierarchical control of SNAT2, a putative amino acid transceptor, by amino acid availability. *J Biol Chem,* 282**,** 19788-98.

HYDE, R., PEYROLLIER, K. & HUNDAL, H. S. 2002. Insulin promotes the cell surface recruitment of the SAT2/ATA2 system A amino acid transporter from an endosomal compartment in skeletal muscle cells. *J Biol Chem,* 277**,** 13628-34.

HYDE, R., TAYLOR, P. M. & HUNDAL, H. S. 2003. Amino acid transporters: roles in amino acid sensing and signalling in animal cells. *Biochem J,* 373**,** 1-18.

IKOTUN, O. F., MARQUEZ, B. V., HUANG, C., MASUKO, K., DAIJI, M., MASUKO, T., MCCONATHY, J. & LAPI, S. E. 2013. Imaging the L-type amino acid transporter-1 (LAT1) with Zr-89 immunoPET. *PLoS One,* 8**,** e77476.

JANPIPATKUL, K., SUKSEN, K., BORWORNPINYO, S., JEARAWIRIYAPAISARN, N., HONGENG, S., PIYACHATURAWAT, P. & CHAIROUNGDUA, A. 2014. Downregulation of LAT1 expression suppresses cholangiocarcinoma cell invasion and migration. *Cell Signal,* 26**,** 1668-79.

JOANISSE, S., NEDERVEEN, J. P., SNIJDERS, T., MCKAY, B. R. & PARISE, G. 2017. Skeletal Muscle Regeneration, Repair and Remodelling in Aging: The Importance of Muscle Stem Cells and Vascularization. *Gerontology,* 63**,** 91-100.

JUNG, J., GENAU, H. M. & BEHRENDS, C. 2015. Amino Acid-Dependent mTORC1 Regulation by the Lysosomal Membrane Protein SLC38A9. *Mol Cell Biol,* 35**,** 2479-94.

KADI, F., CHARIFI, N., DENIS, C., LEXELL, J., ANDERSEN, J. L., SCHJERLING, P., OLSEN, S. & KJAER, M. 2005. The behaviour of satellite cells in response to exercise: what have we learned from human studies? *Pflugers Arch,* 451**,** 319-27.

KADI, F., SCHJERLING, P., ANDERSEN, L. L., CHARIFI, N., MADSEN, J. L., CHRISTENSEN, L. R. & ANDERSEN, J. L. 2004. The effects of heavy resistance training and detraining on satellite cells in human skeletal muscles. *J Physiol,* 558**,** 1005-12.

KASHIWAGI, H., YAMAZAKI, K., TAKEKUMA, Y., GANAPATHY, V. & SUGAWARA, M. 2009. Regulatory mechanisms of SNAT2, an amino acid transporter, in L6 rat skeletal muscle cells by insulin, osmotic shock and amino acid deprivation. *Amino Acids,* 36**,** 219-30.

KORZENIEWSKI, B. 1998. Is it possible to predict any properties of oxidative phosphorylation in a theoretical way? *Mol Cell Biochem,* 184**,** 345-58.

KRIEL, J., HAESENDONCKX, S., RUBIO-TEXEIRA, M., VAN ZEEBROECK, G. & THEVELEIN, J. M. 2011. From transporter to transceptor: signaling from transporters provokes re-evaluation of complex trafficking and regulatory controls: endocytic internalization and intracellular trafficking of nutrient transceptors may, at least in part, be governed by their signaling function. *Bioessays,* 33**,** 870-9.

LAURITZEN, H. P., GALBO, H., BRANDAUER, J., GOODYEAR, L. J. & PLOUG, T. 2008. Large GLUT4 vesicles are stationary while locally and reversibly depleted during transient insulin stimulation of skeletal muscle of living mice: imaging analysis of GLUT4-enhanced green fluorescent protein vesicle dynamics. *Diabetes,* 57**,** 315-24.

LAWSON, M. A. & PURSLOW, P. P. 2000. Differentiation of myoblasts in serum-free media: effects of modified media are cell line-specific. *Cells Tissues Organs,* 167**,** 130-7.

LE GRAND, F. & RUDNICKI, M. A. 2007. Skeletal muscle satellite cells and adult myogenesis. *Curr Opin Cell Biol,* 19**,** 628-33.

LEE, D. C., SHOOK, R. P., DRENOWATZ, C. & BLAIR, S. N. 2016a. Physical activity and sarcopenic obesity: definition, assessment, prevalence and mechanism. *Future Sci OA,* 2**,** FSO127.

LEE, E. S. & PARK, H. M. 2015. Prevalence of Sarcopenia in Healthy Korean Elderly Women. *J Bone Metab,* 22**,** 191-5.

LEE, J., HONG, Y. P., SHIN, H. J. & LEE, W. 2016b. Associations of Sarcopenia and Sarcopenic Obesity With Metabolic Syndrome Considering Both Muscle Mass and Muscle Strength. *J Prev Med Public Health,* 49**,** 35-44.

LEE, M. K., SMITH, S. M., MURRAY, S., PHAM, L. D., MINOO, P. & NIELSEN, H. C. 2014. Dihydrotestosterone potentiates EGF-induced ERK activation by inducing SRC in fetal lung fibroblasts. *Am J Respir Cell Mol Biol,* 51**,** 114-24.

LETERRIER, C., BONNARD, D., CARREL, D., ROSSIER, J. & LENKEI, Z. 2004. Constitutive endocytic cycle of the CB1 cannabinoid receptor. *J Biol Chem,* 279**,** 36013-21.

LETO, D. & SALTIEL, A. R. 2012. Regulation of glucose transport by insulin: traffic control of GLUT4. *Nat Rev Mol Cell Biol,* 13**,** 383-96.
LEXELL, J., TAYLOR, C. C. & SJOSTROM, M. 1988. What is the cause of the ageing atrophy? Total number, size and proportion of different fiber types studied in whole vastus lateralis muscle from 15- to 83-year-old men. *J Neurol Sci,* 84**,** 275-94.
LIEBERHERR, M., GROSSE, B., KACHKACHE, M. & BALSAN, S. 1993. Cell signaling and estrogens in female rat osteoblasts: a possible involvement of unconventional nonnuclear receptors. *J Bone Miner Res,* 8**,** 1365-76.
LING, R., BRIDGES, C. C., SUGAWARA, M., FUJITA, T., LEIBACH, F. H., PRASAD, P. D. & GANAPATHY, V. 2001. Involvement of transporter recruitment as well as gene expression in the substrate-induced adaptive regulation of amino acid transport system A. *Biochim Biophys Acta,* 1512**,** 15-21.
LINGREL, J. B. & KUNTZWEILER, T. 1994. Na+,K(+)-ATPase. *J Biol Chem,* 269**,** 19659-62.
LINGREL, J. B., VAN HUYSSE, J., O'BRIEN, W., JEWELL-MOTZ, E., ASKEW, R. & SCHULTHEIS, P. 1994. Structure-function studies of the Na,K-ATPase. *Kidney Int Suppl,* 44**,** S32-9.
LOPEZ-FONTANALS, M., RODRIGUEZ-MULERO, S., CASADO, F. J., DERIJARD, B. & PASTOR-ANGLADA, M. 2003. The osmoregulatory and the amino acid-regulated responses of system A are mediated by different signal transduction pathways. *J Gen Physiol,* 122**,** 5-16.
LOPEZ, A., TORRES, N., ORTIZ, V., ALEMAN, G., HERNANDEZ-PANDO, R. & TOVAR, A. R. 2006. Characterization and regulation of the gene expression of amino acid transport system A (SNAT2) in rat mammary gland. *Am J Physiol Endocrinol Metab,* 291**,** E1059-66.
LOSEL, R. & WEHLING, M. 2003. Nongenomic actions of steroid hormones. *Nat Rev Mol Cell Biol,* 4**,** 46-56.
MACKENZIE, B. & ERICKSON, J. D. 2004. Sodium-coupled neutral amino acid (System N/A) transporters of the SLC38 gene family. *Pflugers Arch,* 447**,** 784-95.
MACKEY, A. L., KARLSEN, A., COUPPE, C., MIKKELSEN, U. R., NIELSEN, R. H., MAGNUSSON, S. P. & KJAER, M. 2014. Differential satellite cell density of type I and II fibres with lifelong endurance running in old men. *Acta Physiol (Oxf),* 210**,** 612-27.
MATSUMOTO, A. M. 2002. Andropause: clinical implications of the decline in serum testosterone levels with aging in men. *J Gerontol A Biol Sci Med Sci,* 57**,** M76-99.
MCCUBREY, J. A., STEELMAN, L. S., CHAPPELL, W. H., ABRAMS, S. L., WONG, E. W., CHANG, F., LEHMANN, B., TERRIAN, D. M., MILELLA, M., TAFURI, A., STIVALA, F., LIBRA, M., BASECKE, J., EVANGELISTI, C., MARTELLI, A. M. & FRANKLIN, R. A. 2007. Roles of the Raf/MEK/ERK pathway in cell growth, malignant transformation and drug resistance. *Biochim Biophys Acta,* 1773**,** 1263-84.
MCCULLOUGH, A. R., KHERA, M., GOLDSTEIN, I., HELLSTROM, W. J., MORGENTALER, A. & LEVINE, L. A. 2012. A multi-institutional observational study of testosterone levels after testosterone pellet (Testopel((R))) insertion. *J Sex Med,* 9**,** 594-601.
MCGIVAN, J. D. & PASTOR-ANGLADA, M. 1994. Regulatory and molecular aspects of mammalian amino acid transport. *Biochem J,* 299 (Pt 2)**,** 321-34.
MEIER, C., RISTIC, Z., KLAUSER, S. & VERREY, F. 2002. Activation of system L heterodimeric amino acid exchangers by intracellular substrates. *EMBO J,* 21**,** 580-9.
MICHIHARA, A., TODA, K., KUBO, T., FUJIWARA, Y., AKASAKI, K. & TSUJI, H. 2005. Disruptive effect of chloroquine on lysosomes in cultured rat hepatocytes. *Biol Pharm Bull,* 28**,** 947-51.
MIDZAK, A. S., CHEN, H., PAPADOPOULOS, V. & ZIRKIN, B. R. 2009. Leydig cell aging and the mechanisms of reduced testosterone synthesis. *Mol Cell Endocrinol,* 299**,** 23-31.
MOORADIAN, A. D. & KORENMAN, S. G. 2006. Management of the cardinal features of andropause. *Am J Ther,* 13**,** 145-60.

MORGAN, J. E. & PARTRIDGE, T. A. 2003. Muscle satellite cells. *Int J Biochem Cell Biol,* 35**,** 1151-6.

MORI, R., SHAMOTO, H., MAEDA, K. & WAKABAYASHI, H. 2016. Sarcopenia Is a Possible Independent Risk Factor of Cognitive Decline in Community-Dwelling Older People. *J Am Med Dir Assoc,* 17**,** 559-60.

MORLEY, J. E., BAUMGARTNER, R. N., ROUBENOFF, R., MAYER, J. & NAIR, K. S. 2001. Sarcopenia. *J Lab Clin Med,* 137**,** 231-43.

MUKHERJEE, B. & MAYER, D. 2008. Dihydrotestosterone interacts with EGFR/MAPK signalling and modulates EGFR levels in androgen receptor-positive LNCaP prostate cancer cells. *Int J Oncol,* 33**,** 623-9.

MUNOZ, P., GUMA, A., CAMPS, M., FURRIOLS, M., TESTAR, X., PALACIN, M. & ZORZANO, A. 1992. Vanadate stimulates system A amino acid transport activity in skeletal muscle. Evidence for the involvement of intracellular pH as a mediator of vanadate action. *J Biol Chem,* 267**,** 10381-8.

MURETTA, J. M., ROMENSKAIA, I. & MASTICK, C. C. 2008. Insulin releases Glut4 from static storage compartments into cycling endosomes and increases the rate constant for Glut4 exocytosis. *J Biol Chem,* 283**,** 311-23.

NARDI, F., HOFFMANN, T. M., STRETTON, C., CWIKLINSKI, E., TAYLOR, P. M. & HUNDAL, H. S. 2015. Proteasomal modulation of cellular SNAT2 (SLC38A2) abundance and function by unsaturated fatty acid availability. *J Biol Chem,* 290**,** 8173-84.

NAWASHIRO, H., OTANI, N., SHINOMIYA, N., FUKUI, S., OOIGAWA, H., SHIMA, K., MATSUO, H., KANAI, Y. & ENDOU, H. 2006. L-type amino acid transporter 1 as a potential molecular target in human astrocytic tumors. *Int J Cancer,* 119**,** 484-92.

NEUNHAUSERER, D., ZEBEDIN, M., OBERMOSER, M., MOSER, G., TAUBER, M., NIEBAUER, J., RESCH, H. & GALLER, S. 2011. Human skeletal muscle: transition between fast and slow fibre types. *Pflugers Arch,* 461**,** 537-43.

OHLSSON, C., WALLASCHOFSKI, H., LUNETTA, K. L., STOLK, L., PERRY, J. R., KOSTER, A., PETERSEN, A. K., ERIKSSON, J., LEHTIMAKI, T., HUHTANIEMI, I. T., HAMMOND, G. L., MAGGIO, M., COVIELLO, A. D., GROUP, E. S., FERRUCCI, L., HEIER, M., HOFMAN, A., HOLLIDAY, K. L., JANSSON, J. O., KAHONEN, M., KARASIK, D., KARLSSON, M. K., KIEL, D. P., LIU, Y., LJUNGGREN, O., LORENTZON, M., LYYTIKAINEN, L. P., MEITINGER, T., MELLSTROM, D., MELZER, D., MILJKOVIC, I., NAUCK, M., NILSSON, M., PENNINX, B., PYE, S. R., VASAN, R. S., REINCKE, M., RIVADENEIRA, F., TAJAR, A., TEUMER, A., UITTERLINDEN, A. G., ULLOOR, J., VIIKARI, J., VOLKER, U., VOLZKE, H., WICHMANN, H. E., WU, T. S., ZHUANG, W. V., ZIV, E., WU, F. C., RAITAKARI, O., ERIKSSON, A., BIDLINGMAIER, M., HARRIS, T. B., MURRAY, A., DE JONG, F. H., MURABITO, J. M., BHASIN, S., VANDENPUT, L. & HARING, R. 2011. Genetic determinants of serum testosterone concentrations in men. *PLoS Genet,* 7**,** e1002313.

OKABE, S., KITANO, K., NAGASAWA, M., MOGI, K. & KIKUSUI, T. 2013. Testosterone inhibits facilitating effects of parenting experience on parental behavior and the oxytocin neural system in mice. *Physiol Behav,* 118**,** 159-64.

OLIVER, V. L., POULIOS, K., VENTURA, S. & HAYNES, J. M. 2013. A novel androgen signalling pathway uses dihydrotestosterone, but not testosterone, to activate the EGF receptor signalling cascade in prostate stromal cells. *Br J Pharmacol,* 170**,** 592-601.

PALACIN, M., ESTEVEZ, R., BERTRAN, J. & ZORZANO, A. 1998. Molecular biology of mammalian plasma membrane amino acid transporters. *Physiol Rev,* 78**,** 969-1054.

PERCY, D. H. & JONAS, A. M. 1971. Incidence of spontaneous tumors in CD (R) -1 HaM-ICR mice. *J Natl Cancer Inst,* 46**,** 1045-65.

PEREZ, M. H., CORMACK, J., MALLINSON, D. & MUTUNGI, G. 2013. A membrane glucocorticoid receptor mediates the rapid/non-genomic actions of glucocorticoids in mammalian skeletal muscle fibres. *J Physiol,* 591**,** 5171-85.

PETTE, D. & STARON, R. S. 2000. Myosin isoforms, muscle fiber types, and transitions. *Microsc Res Tech,* 50**,** 500-9.
PINEDA, M., FERNANDEZ, E., TORRENTS, D., ESTEVEZ, R., LOPEZ, C., CAMPS, M., LLOBERAS, J., ZORZANO, A. & PALACIN, M. 1999. Identification of a membrane protein, LAT-2, that Co-expresses with 4F2 heavy chain, an L-type amino acid transport activity with broad specificity for small and large zwitterionic amino acids. *J Biol Chem,* 274**,** 19738-44.
PINILLA, J., ALEDO, J. C., CWIKLINSKI, E., HYDE, R., TAYLOR, P. M. & HUNDAL, H. S. 2011. SNAT2 transceptor signalling via mTOR: a role in cell growth and proliferation? *Front Biosci (Elite Ed),* 3**,** 1289-99.
PIROG, E. C. & COLLINS, D. C. 1999. Metabolism of dihydrotestosterone in human liver: importance of 3alpha- and 3beta-hydroxysteroid dehydrogenase. *J Clin Endocrinol Metab,* 84**,** 3217-21.
POCHINI, L., SCALISE, M., GALLUCCIO, M. & INDIVERI, C. 2014. Membrane transporters for the special amino acid glutamine: structure/function relationships and relevance to human health. *Front Chem,* 2**,** 61.
PRATT, R. L. & KINCH, M. S. 2003. Ligand binding up-regulates EphA2 messenger RNA through the mitogen-activated protein/extracellular signal-regulated kinase pathway. *Mol Cancer Res,* 1**,** 1070-6.
PRATT, W. B. & TOFT, D. O. 2003. Regulation of signaling protein function and trafficking by the hsp90/hsp70-based chaperone machinery. *Exp Biol Med (Maywood),* 228**,** 111-33.
PUERTOLLANO, R. & ALONSO, M. A. 1999. MAL, an integral element of the apical sorting machinery, is an itinerant protein that cycles between the trans-Golgi network and the plasma membrane. *Mol Biol Cell,* 10**,** 3435-47.
RAMADAN, T., CAMARGO, S. M., HERZOG, B., BORDIN, M., POS, K. M. & VERREY, F. 2007. Recycling of aromatic amino acids via TAT1 allows efflux of neutral amino acids via LAT2-4F2hc exchanger. *Pflugers Arch,* 454**,** 507-16.
RAMM, G. A., POWELL, L. W. & HALLIDAY, J. W. 1994. Pathways of intracellular trafficking and release of ferritin by the liver in vivo: the effect of chloroquine and cytochalasin D. *Hepatology,* 19**,** 504-13.
RANDALL, D., BURGGREN, W. & FRENCH, K. 1997. *Eckert animal*

physiology: mechanisms and adaptations, New York, W.H. Freeman

and Company.
REBSAMEN, M. & SUPERTI-FURGA, G. 2016. SLC38A9: A lysosomal amino acid transporter at the core of the amino acid-sensing machinery that controls MTORC1. *Autophagy,* 12**,** 1061-2.
REGINSTER, J. Y., COOPER, C., RIZZOLI, R., KANIS, J. A., APPELBOOM, G., BAUTMANS, I., BISCHOFF-FERRARI, H. A., BOERS, M., BRANDI, M. L., BRUYERE, O., CHERUBINI, A., FLAMION, B., FIELDING, R. A., GASPARIK, A. I., VAN LOON, L., MCCLOSKEY, E., MITLAK, B. H., PILOTTO, A., REITER-NIESERT, S., ROLLAND, Y., TSOUDEROS, Y., VISSER, M. & CRUZ-JENTOFT, A. J. 2016. Recommendations for the conduct of clinical trials for drugs to treat or prevent sarcopenia. *Aging Clin Exp Res,* 28**,** 47-58.
ROCHETTE-EGLY, C. 2003. Nuclear receptors: integration of multiple signalling pathways through phosphorylation. *Cell Signal,* 15**,** 355-66.
ROMANEK, R., SARGEANT, R., PAQUET, M. R., GLUCK, S., KLIP, A. & GRINSTEIN, S. 1993. Chloroquine inhibits glucose-transporter recruitment induced by insulin in rat adipocytes independently of its action on endomembrane pH. *Biochem J,* 296 (Pt 2)**,** 321-7.
RONGO, C. 2011. Epidermal growth factor and aging: a signaling molecule reveals a new eye opening function. *Aging (Albany NY),* 3**,** 896-905.

ROOYACKERS, O. E., ADEY, D. B., ADES, P. A. & NAIR, K. S. 1996. Effect of age on in vivo rates of mitochondrial protein synthesis in human skeletal muscle. *Proc Natl Acad Sci U S A,* 93**,** 15364-9.

ROOYACKERS, O. E. & NAIR, K. S. 1997. Hormonal regulation of human muscle protein metabolism. *Annu Rev Nutr,* 17**,** 457-85.

RYALL, J. G., SCHERTZER, J. D. & LYNCH, G. S. 2008. Cellular and molecular mechanisms underlying age-related skeletal muscle wasting and weakness. *Biogerontology,* 9**,** 213-28.

SAARTOK, T., DAHLBERG, E. & GUSTAFSSON, J. A. 1984. Relative binding affinity of anabolic-androgenic steroids: comparison of the binding to the androgen receptors in skeletal muscle and in prostate, as well as to sex hormone-binding globulin. *Endocrinology,* 114**,** 2100-6.

SADACCA, L. A., BRUNO, J., WEN, J., XIONG, W. & MCGRAW, T. E. 2013. Specialized sorting of GLUT4 and its recruitment to the cell surface are independently regulated by distinct Rabs. *Mol Biol Cell,* 24**,** 2544-57.

SAKATA, T., FERDOUS, G., TSURUTA, T., SATOH, T., BABA, S., MUTO, T., UENO, A., KANAI, Y., ENDOU, H. & OKAYASU, I. 2009. L-type amino-acid transporter 1 as a novel biomarker for high-grade malignancy in prostate cancer. *Pathol Int,* 59**,** 7-18.

SAKUMA, K. & YAMAGUCHI, A. 2012. Sarcopenia and age-related endocrine function. *Int J Endocrinol,* 2012**,** 127362.

SANO, H., EGUEZ, L., TERUEL, M. N., FUKUDA, M., CHUANG, T. D., CHAVEZ, J. A., LIENHARD, G. E. & MCGRAW, T. E. 2007. Rab10, a target of the AS160 Rab GAP, is required for insulin-stimulated translocation of GLUT4 to the adipocyte plasma membrane. *Cell Metab,* 5**,** 293-303.

SARRABAY, A., HILMI, C., TINWELL, H., SCHORSCH, F., PALLARDY, M., BARS, R. & ROUQUIE, D. 2015. Low dose evaluation of the antiandrogen flutamide following a Mode of Action approach. *Toxicol Appl Pharmacol,* 289**,** 515-24.

SEALE, P., POLESSKAYA, A. & RUDNICKI, M. A. 2003. Adult stem cell specification by Wnt signaling in muscle regeneration. *Cell Cycle,* 2**,** 418-9.

SEBOLT-LEOPOLD, J. S. 2008. Advances in the development of cancer therapeutics directed against the RAS-mitogen-activated protein kinase pathway. *Clin Cancer Res,* 14**,** 3651-6.

SINHA-HIKIM, I., TAYLOR, W. E., GONZALEZ-CADAVID, N. F., ZHENG, W. & BHASIN, S. 2004. Androgen receptor in human skeletal muscle and cultured muscle satellite cells: up-regulation by androgen treatment. *J Clin Endocrinol Metab,* 89**,** 5245-55.

STANWORTH, R. D. & JONES, T. H. 2008. Testosterone for the aging male; current evidence and recommended practice. *Clin Interv Aging,* 3**,** 25-44.

STEPHENSON, G. M. 2001. Hybrid skeletal muscle fibres: a rare or common phenomenon? *Clin Exp Pharmacol Physiol,* 28**,** 692-702.

SUH, J. H., CHATTOPADHYAY, A., SIEGLAFF, D. H., STORER SAMANIEGO, C., COX, M. B. & WEBB, P. 2015. Similarities and Distinctions in Actions of Surface-Directed and Classic Androgen Receptor Antagonists. *PLoS One,* 10**,** e0137103.

SURYAWAN, A. & DAVIS, T. A. 2011. Regulation of protein synthesis by amino acids in muscle of neonates. *Front Biosci (Landmark Ed),* 16**,** 1445-60.

TOTH, M. J., MATTHEWS, D. E., TRACY, R. P. & PREVIS, M. J. 2005. Age-related differences in skeletal muscle protein synthesis: relation to markers of immune activation. *Am J Physiol Endocrinol Metab,* 288**,** E883-91.

VAN ZEEBROECK, G., RUBIO-TEXEIRA, M., SCHOTHORST, J. & THEVELEIN, J. M. 2014. Specific analogues uncouple transport, signalling, oligo-ubiquitination and endocytosis in the yeast Gap1 amino acid transceptor. *Mol Microbiol,* 93**,** 213-33.

VERMEULEN, A., RUBENS, R. & VERDONCK, L. 1971. Testosterone secretion and metabolism in old age. *Acta Endocrinol Suppl (Copenh),* 152**,** 23.

VERREY, F. 2003. System L: heteromeric exchangers of large, neutral amino acids involved in directional transport. *Pflugers Arch,* 445**,** 529-33.

VOLPI, E., MITTENDORFER, B., WOLF, S. E. & WOLFE, R. R. 1999. Oral amino acids stimulate muscle protein anabolism in the elderly despite higher first-pass splanchnic extraction. *Am J Physiol,* 277**,** E513-20.

VOLPI, E., SHEFFIELD-MOORE, M., RASMUSSEN, B. B. & WOLFE, R. R. 2001. Basal muscle amino acid kinetics and protein synthesis in healthy young and older men. *JAMA,* 286**,** 1206-12.

WAGNER, C. A., LANG, F. & BRÖER, S. 2001. *Function and structure of heterodimeric amino acid transporters*.

WAKABAYASHI, H. & SAKUMA, K. 2014. Comprehensive approach to sarcopenia treatment. *Curr Clin Pharmacol,* 9**,** 171-80.

WANG, H., LISTRAT, A., MEUNIER, B., GUEUGNEAU, M., COUDY-GANDILHON, C., COMBARET, L., TAILLANDIER, D., POLGE, C., ATTAIX, D., LETHIAS, C., LEE, K., GOH, K. L. & BECHET, D. 2014. Apoptosis in capillary endothelial cells in ageing skeletal muscle. *Aging Cell,* 13**,** 254-62.

WELLE, S., THORNTON, C., JOZEFOWICZ, R. & STATT, M. 1993. Myofibrillar protein synthesis in young and old men. *Am J Physiol,* 264**,** E693-8.

WENDOWSKI, O., REDSHAW, Z. & MUTUNGI, G. 2016. Dihydrotestosterone treatment rescues the decline in protein synthesis as a result of sarcopenia in isolated mouse skeletal muscle fibres. *J Cachexia Sarcopenia Muscle*.

WENG, Y., XIE, F., XU, L., ZAGOREVSKI, D., SPINK, D. C. & DING, X. 2010. Analysis of testosterone and dihydrotestosterone in mouse tissues by liquid chromatography-electrospray ionization-tandem mass spectrometry. *Anal Biochem,* 402**,** 121-8.

WILSON, J. M. & KING, B. F. 1986. Sorting and transepithelial transport of adsorbed protein tracers: effects of temperature. *Anat Rec,* 216**,** 33-9.

XING, B., XIN, T., HUNTER, R. L. & BING, G. 2008. Pioglitazone inhibition of lipopolysaccharide-induced nitric oxide synthase is associated with altered activity of p38 MAP kinase and PI3K/Akt. *J Neuroinflammation,* 5**,** 4.

YAFFE, D. & SAXEL, O. 1977. A myogenic cell line with altered serum requirements for differentiation. *Differentiation,* 7**,** 159-66.

YAO, D., MACKENZIE, B., MING, H., VAROQUI, H., ZHU, H., HEDIGER, M. A. & ERICKSON, J. D. 2000. A novel system A isoform mediating Na+/neutral amino acid cotransport. *J Biol Chem,* 275**,** 22790-7.

YU, J. G., BONNERUD, P., ERIKSSON, A., STAL, P. S., TEGNER, Y. & MALM, C. 2014. Effects of long term supplementation of anabolic androgen steroids on human skeletal muscle. *PLoS One,* 9**,** e105330.

ZHANG, Z. & GREWER, C. 2007. The sodium-coupled neutral amino acid transporter SNAT2 mediates an anion leak conductance that is differentially inhibited by transported substrates. *Biophys J,* 92**,** 2621-32.

ZHANG, Z., ZANDER, C. B. & GREWER, C. 2011. The C-terminal domain of the neutral amino acid transporter SNAT2 regulates transport activity through voltage-dependent processes. *Biochem J,* 434**,** 287-96.

ZHOU, Y. Y., LI, Y., JIANG, W. Q. & ZHOU, L. F. 2015a. MAPK/JNK signalling: a potential autophagy regulation pathway. *Biosci Rep,* 35.

ZHOU, Z. Y., LI, F., CHENG, S. P., HUANG, H., PENG, B. W., WANG, J., LIU, C. M., XING, C., SUN, Y. L., BSOUL, N., PAN, H., YI, C. J., LIU, R. H. & ZHONG, G. J. 2015b. Short hairpin ribonucleic acid constructs targeting insulin-like growth factor binding protein-3

rehabilitated decreased testosterone concentrations in diabetic rats. *Med Sci Monit,* 21**,** 94-9.

ZOICO, E., DI FRANCESCO, V., GURALNIK, J. M., MAZZALI, G., BORTOLANI, A., GUARIENTO, S., SERGI, G., BOSELLO, O. & ZAMBONI, M. 2004. Physical disability and muscular strength in relation to obesity and different body composition indexes in a sample of healthy elderly women. *Int J Obes Relat Metab Disord,* 28**,** 234-41.

Acknowledgements

In the rare event that anyone will find themselves reading this page, I want to thank my friends and family for their understanding during the many hours I gave up spending with them to work on this thesis. A big thank you to my supervisor Tom Wileman and to Penny Powell for helping me along the way through unforeseen circumstances. I'm especially grateful for the help of my amazing fiancé Thuria for all her help and support, I would not have done this without her. I love you darling!

Appendix

A2 SNAT2 Plasmid Backbone